# TEMPORAL AND SPATIAL VARIATION OF GROUNDWATER LEVEL NORTH OF LAKE NAIVASHA, KENYA

**ANALYSED USING MODFLOW**

Sekela R.U. Kibona
April, 2000

# TEMPORAL AND SPATIAL VARIATION OF GROUNDWATER LEVEL NORTH OF LAKE NAIVASHA, KENYA. ANALYSED USING MODFLOW

By

Sekela Rodrick Kibona

Thesis submitted to the International Institute for Aerospace Survey and Earth Sciences in partial fulfilment of the requirements for the degree of Master of Science in Water Resources and Environmental Management.

Board of Examiners

| | |
|---|---|
| Prof. Dr. A.M.J. Meijerink (Chairman) | - ITC, Enschede |
| Dr. E. Seyhan (External Examiner) | - Free University of Amsterdam |
| Drs.D. Kovacs (Director of Studies) | - ITC, Enschede |
| Drs.R.Becht (Supervisor) | - ITC, Enschede |
| Dr.Ir. M. Lubczynski | - ITC, Enschede |
| Dr. A. S. M. Gieske | - ITC, Enschede |


**INTERNATIONAL INSTITUTE FOR AEROSPACE SURVEY AND EARTH SCIENCES ENSCHEDE, THE NETHERLANDS**

*for the memory of my husband Beda, my brother Morrison, and my sister Aswe*

*&*

*to my daughter Nakiete, my father Rodrick and my mother Lena*

*ABSTRACT*

*Numerical model of the groundwater flow system in northern Naivasha, was used to find the conceptual understanding of the flow system, estimate the effect of past and future human-caused changes to groundwater levels, and the amount of groundwater abstraction by acacia xanthophloea trees. A three-dimensional modular model (MODFLOW) was used to simulate the groundwater flow. The model covers an area of 185 km$^2$*

*Two models were developed for this purpose, two and three-layer. The two-layer model modelled the lake as a constant head. The three-layer model modelled the lake the way it fluctuates.*

*All models were calibrated in steady-state by using historical data from 1930s to 1970s. Transmissivity and recharge were adjusted until a reasonable fit was obtained between simulated and observed heads. In general, simulated heads satisfactorily match observed heads. Model results indicate that;*

*Final transmissivity in the clays, diatomite, silts and fine-grained sands units was not more than 10 m$^2$/day and in the second aquifer (reworked volcanics or weathered contacts between different lithological units), ranged from 10 to 1500 m$^2$/day. The root mean square error was 1.17 m and 0.93 m for two and three layer models respectively.*

*Simulated recharge was 25 mm/year and 52 mm/year in thin (thickness < 10 m) and thick sediments respectively. Most of the groundwater flux through the aquifer system occurred within the second aquifer.*

*One condition for future groundwater withdraws was simulated in transient model on the basis of steady-state model to test the effects of pumping. Pumpage estimates in this condition were based on the amount they were pumping for the year 1999 of about 14,000 m$^3$/day. After 40 years the model showed water level declines were as much as 8 m in the aquifer and 1 m in the lake, the equilibrium was reached after 17 years. The same amount was abstracted from the lake, the water level in the aquifer as well as in the lake went down by 1 m ,equilibrium was reached after 15 years.*

*By modelling the lake as a constant head may not provide reliable estimates of groundwater fluxes and lake level fluctuations as it was done in two-layer model. For this reason the study concludes that, a three-layer model is reliable than two-layer model, because three-layer model incorporates evaporation from the lake surface, inflow from runoff and rivers. These flow components affect lake levels and changes in these components lead to lake level fluctuations. Therefore future improvement in the model is recommended.*

*The rate of groundwater abstraction by acacia trees is not known exactly, therefore a study to find the amount the trees abstract is necessary.*

*More data collection through groundwater level monitoring and periodic updating of well discharge would facilitate future improvement in the model developed in this study.*

ACKNOWLEDGEMENT

I thank God through my Lord and saviour Jesus Christ. Through Him this work has been possible " I can do all things through Christ who strengthens me" Philippians 4:13.

Thank you my father and mother for sending me to school.

I would like to extend my thanks to the Ministry of Water for allowing me to pursue the course in Water Resources Survey (WRS) at ITC. I am grateful to the Netherlands Government for providing me the financial support under the Netherlands Fellowships Programme without which my participation in the course would be impossible.

My thanks also to Dr I. M. Marobhe of University of Dar-es-salaam, P.B. Mabuba of British Council and W.E.N Lyimo of Ministry of Water for recommending me to pursue this course.

Special thanks go to my Supervisor Drs. Robert Becht for his professional guidance, constructive comments and criticisms that made the quality of this report scientifically acceptable. I am grateful to the Head of WREM Prof. A. M. F. Maijerink, directors of studies Drs. D. Kovacs and Dr C. Mannaerts for their smooth academic co-ordination and supervision throughout the study period. My gratitude goes to all staff members of the WREM Division and the entire ITC community who in one way or another made my study period enjoyable and fruitful.

My fieldwork could have been difficult without the assistance of employees of Ministry of Water, Nakuru District; Mr Lidonde, Mr Tanui, Mr Opiyo, Mr M. Wachira and Mr Mwangi, without forgetting Mr Kimiri, Mr James and Mr George of Naivasha town thank you. I appreciate also the assistance of Sara Haggins of LNROA and the owners of farms and wells.

I would like to thank all my Fellow MSc. students Jolicoeur (Haiti), Owor (Uganda), Mai (Vietnam), Obed (Botswana), Merka (Zimbabwe), Patricia and Carlos (Bolivia), Worku and Mogesie (Ethiopia), Gotah (Ghana) and Maango (Zambia), for their support both academically and socially. Special thanks go to My Fellow Tanzanian students at ITC for their company, encouragement and social support.

My heartfelt thanks go to the ITC Christian Revival Believers Fellowship and to Pastor Henk Bentveld and brethren of the 'Evangelische Gemeente Pniël de Rots' church for both their moral support and spiritual encouragement during my stay at Enschede. Also to brethren of Moravian and Tanzania Assemblies of God back home, thank you so much for your prayers.

I am Indebted to my sister Tuntwa and her family for taking care of my daughter Nakiete. Special thanks to my daughter for her encouraging letters. Also I thank my brothers Tully, Gabriely, Ambokile and Nuru, my brother in-laws Bruno and Pius, for their moral and spiritual support

Thanks to Sam (Liberia) and his wife Faith and their son Martin for their encouragement and making me feel at home.

My family friends back home Kisaro's, Chiboko's and Shilinde's family I really appreciate your support. All my relatives, friends, neighbours and work mates your support is highly appreciated.

GOD BLESS YOU SO MUCH.

Sekela R.U. Kibona
Enschede, 2000

# TABLE OF CONTENTS

# LIST OF FIGURES

# LIST OF TABLES

# LIST OF ACRONYMS

| | |
|---|---|
| a.m.s.l | Above mean sea level |
| D.O | District Office |
| RMS | Root Mean Square |
| TM | Thematic mapper |
| UTM | Universal Transversal Mercator |
| W.D.D | Water Development Department |
| ILWIS | Integrated Land and Water Information System |
| K.C.C | Kenya Creamery Corporation |
| KWS | Kenya Wildlife Services |
| LNROA | Lake Riparian Owners |
| PMWIN | Processing Modflow for Windows |
| T | Transmissivity |
| WRAP | Water Resources Assessment Project |
| WREM | Water Resources and Environmental Management |

# 1 CHAPTER ONE

## 1.1 INTRODUCTION

### 1.1.1 Groundwater, an overview

The term water is usually reserved for the subsurface water that occurs beneath the water table in soils and geology formation that are fully saturated Freeze and Cherry (1979). Groundwater is the safest and most reliable source of available freshwater. Unlike water in lakes, rivers, streams, and ponds, groundwater is not subjected to floods. Therefore, groundwater is a more stable and reliable source than rivers and lakes. Most groundwater is found in underground layers of rock, sand and gravel called aquifers.

Underground water is in motion most of the time, flowing slowly from recharge areas until it discharges into a spring, stream, lake, wetlands or ocean. Groundwater often follows the course of rivers or lies underneath marshes and swamps, keeping rivers from drying up and protecting vegetation when rain is scarce. The upward and downward movement of water through the ground has also a filtering effect, accounting for the generally good quality of groundwater.

Groundwater is one of the most valuable natural resources possessed by many developing nations. Groundwater has many advantages over surface water for water supply:

- It is reliable in dry seasons or droughts because of the large storage.
- It is cheaper to develop, since, unpolluted, it requires little treatment.
- It can often be tapped where it is needed, on a stage-by-stage basis.
- It is less affected by catastrophic events (e.g floods).

As a result groundwater has become immensely important for human water supply in urban and rural areas in developed and developing nations alike. Countless large towns and many cities derive much of their domestic and industrial water supply from aquifers, both through municipal wellfields and through very many private boreholes.

Annually huge amounts of groundwater are abstracted from the renewable and fossil resources available in the aquifers. These abstractions and return flow by irrigation create several problems due to change in groundwater flow systems and aquifer conditions.

Falling groundwater tables, waterlogging, land subsidence, desiccation and deterioration of groundwater quality are frequently observed phenomena in areas with intensive groundwater abstraction.

More and more farmers all over the world are using groundwater to irrigate their crops during the dry season. In the more arid areas, where rainfall is low and less predictable, groundwater may be the only source of supply for all types of agricultural activity, including watering livestock.

### 1.1.2 Problem Definition

The groundwater system is set up with a natural recharge system, (hydrologic cycle) that replenishes and refurnishes the water table. If water is withdrawn faster than it can be replenished, it means lowering the water table in the area and causing shallow wells to go dry. Water that took thousands of years to accumulate is being used up in a matter of only a few years. The only problem is that our increased population has caused a need for more water. We can not speed up natures recharge system. This causes a problem of over-drawing of the water table.

In the study area, groundwater is extensively used for irrigation such that the water table has gone down. The situation can be evidenced by a number of shallow dry well observed during fieldwork and from water static level data.

Apart from human activities, *Acacia trees*, gregarious in high ground water areas, contribute to the lowering of groundwater table in the area.

### 1.1.3 Objectives

#### 1.1.3.1 Main Objective

To find how deep the water table has been lowered by extensive irrigation in the study area.

#### 1.1.3.2 Other Objectives

- To construct the natural and present piezometric surface of the area, by using both historic and recent well data

- To estimate groundwater abstraction by phreatophytic plants (acacia trees).

### 1.1.4 Research Methodology

#### 1.1.4.1 Pre-field work

- Literature review:

Study of published reports, theses, other relevant study material in order to have a general overview of the study area.

- Input data

Study and interpretation of aerial photographs of the area, satellite images, geological maps, topographical maps and boreholes point maps of the study area as input data.

#### 1.1.4.2 Field Work

The fieldwork commenced in Naivasha in 2nd to 22 nd October 1999 to obtain better perspectives of the study area as well as data collection, which involved the following tasks:

- Locating existing wells.
- Pumping test was conducted in order to determine the parameters transmissivity (T) and storativity (S) for the aquifer
- Measurement of water rest level in the wells.
- Measurement of water electrical conductivity.
- Collection and analysis of existing data so as to construct a historical and present groundwater level.
- Identification of landuse and landcover types.
- Augering along Malewa river to estimate the hydraulic conductivity of the soil beneath the riverbed so as to estimate the amount of water that seeps to the aquifer.
- Augering close to acacia trees to find the depth of the rooting zone in order to findout if these trees tap water from shallow groundwater.

#### 1.1.4.3 Post-field Work

- Analysis of the data collected during fieldwork and existing data.
- Groundwater modelling.
- Discussion of results.

## Methodology flow diagram

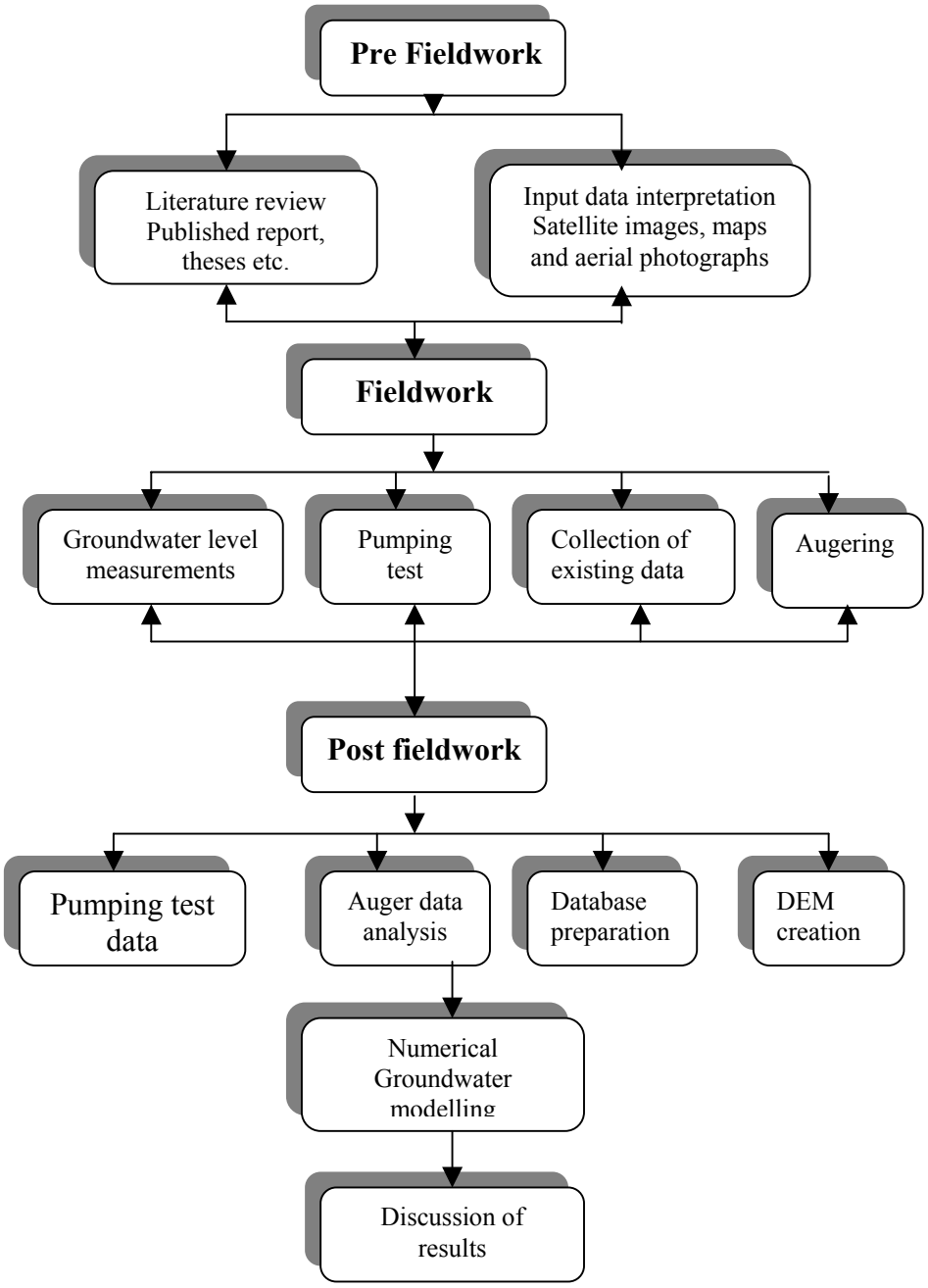


**Figure 1-1** ***Methodology flow diagram***

### 1.1.5 Previous Studies

Exploration of the Naivasha area began as early as the 1880's by European explorers. Numerous studies have been conducted.

In geology of the Naivasha area report by Thompson (1963), a detailed geology of the areas embraces the two flanks of the Gregory Rift Valley, with the Kinangop plateau on the east and the Mau escarpment on the west. Concerning groundwater they pointed out that water table is controlled by lake Naivasha drops sharply on the southern side beyond the limits of the Gamblian deposits and, if there is connection between it and lake Elementeita likewise on the northern side.

McCann (1974) in the report hydrogeologic investigation of the Rift Valley catchment, he pointed out that "in the Naivasha catchment groundwater generally flows towards the lake from the Mau and Aberdare escarpments, although it is diverted locally by the presence of faults that either form barriers or conduits"

The report Groundwater investigation by Wiberg (1976), he used quantitative methods for non-steady state conditions to assess the hydraulic properties of a confined leaky aquifer. Which enabled a prediction of the response of the groundwater level for various abstraction rates.

Geological, volcanological and hydrogeological controls on the occurrence of the geothermal activity in the area surrounding Lake Naivasha, Kenya by Clarke et.al (1990) provide information on geology, volcanology, petrology, geothermal sources, physical and chemical hydrogeology. The study indicates that the permeability of the volcanic rocks underlying the Rift valley is generally low although there is local variation. Aquifers are normally found in fractured or reworked volcanics, or along the weathered contacts between different lithological units.

In the final report of monitoring lakes in Kenya: An environmental Analysis Methodology for Developing Countries (1995), the authors developed a methodology to model and monitor lake level changes on three Rift valley lakes in Kenya (Naivasha, Nakuru and Elementeita. In one of the appendices a conceptual hydrogeology model of the study area was constructed so as to define groundwater circulation and estimate the relations between the groundwater and the lake levels. They concluded that groundwater circulation in the rift floor plain points out that Lake Naivasha has two floor directions: towards southeast to Suswa volcanic complex and North which cross the Eburru volcanic complex, interact with lakes Elementaita and Nakuru, flow west of Menengai complex and proceeds northwards.

Ojiambo (1996) in his thesis Characterization of Subsurface Outflow from a Closed-basin Freshwater Tropical Lake, Rift Valley, Kenya, he pointed out that groundwater level to the north of the lake have dropped below the lake level compared to what they were in 1972 when studied by McCann. The drop in water levels in northern wells around Manera may not be wholly explained by the drop in the lake level, but may be largely explained due to increasing pumping from the aquifer.

A list of maps used is as follows:

| | Sheet | Title | Date | Map Scale | Source |
|---|---|---|---|---|---|
| Topographic map | 133/2 | Naivasha | 1975 | 1:50,000 | UK Ordinance Survey Overseas Survey Departments maps |
| Topographic map | 134/2 | Kinangop | 1975 | 1:50,000 | UK Ordinance Survey Overseas Survey Departments maps |
| Geological map | | Geological Map of Longonot Volcano, The Greater Olkaria and Eburru Volcanic Complexes, and Adjacent Areas | 1988 | 1:100,000 | Government of Kenya Ministry of Energy Geothermal Section |
| Topographic map | | Naivasha Water Supply Project | 1974 | 1:10,000 | Ministry of Agriculture Water Department |
| Topographic map | | Lake Naivasha Contour Survey | 1957 | 1:10,000 | Hydraulic Engineer Ministry of Works |

**Table 1-1** ***List of input maps***

Other materials used include;

Satellite image TM of 21st January 1995.

Aerial photographs

Panchromantic hardcopy, scale 1:12,500 of 1984.
Panchromatic hardcopy and coloured digital photographed in 1998.

# 2 CHAPTER TWO

## 2.1 BACKGROUND INFORMATION

### 2.1.1 Location of the study area

#### 2.1.1.1 Regional Setting

The Lake Naivasha area is situated in the Kenya Rift Valley, 70 km north-west of Nairobi, lies within the highest central portion of the East African section of the Rift Valley (a complex graben that runs from Ethiopia to Tanzania). Within UTM zone 37 and coordinates 194000 m E, 9932000 m N and 215000 m E, 9908000 m N. The Rift valley width in this region is between 45 and 70 km. Administratively, it is situated in the Naivasha division of Nakuru district, in Rift Valley province of Kenya (Figure 2-1).

#### 2.1.1.2 Local Setting

The study area is the northern part of Lake Naivasha (Figure 2-3) between Universal Transverse Mercator (UTM) coordinates $X_{minimum}$ 197220, $Y_{minimum}$ 1917760 and $X_{maximum}$ 215250, $Y_{maximum}$ 9949980. Which is part of Ilkek plains. The Ilkek plains extend up to 23 km north of Lake Naivasha and they range in width from a maximum of 13 km to the south, near Naivasha Town, to a minimum of 4 km in the extreme north near Giligil Town (Clarke et. al. 1990). The detail map of the study area is shown in (Figure 2-3)

### 2.1.2 Physiography

Lake Naivasha and its surroundings are located within the wide floor of the Gregory Rift Valley. The bottom of the Rift is diverse in its structures and topography. It is made up of numerous volcanic cones and craters, scarps and lakes. On the western and south-western showers of the Lake Naivasha numerous volcanic craters, some are faulted, are built up of acid and basaltic ashes. Lake Naivasha is confined by the Mau escarpment to the west (exceeding 3,000 m) and the Kinangop Plateau on the east, which forms a broad step between Nyandarua range (formally known as Aberdare) (elevated to over 3,960 m) and the valley floor Stuttard et.al (1995). To the south there is Longonot Mountain. The area is drained by three major rivers: Malewa, Giligil and Karati (Figure 2-2).

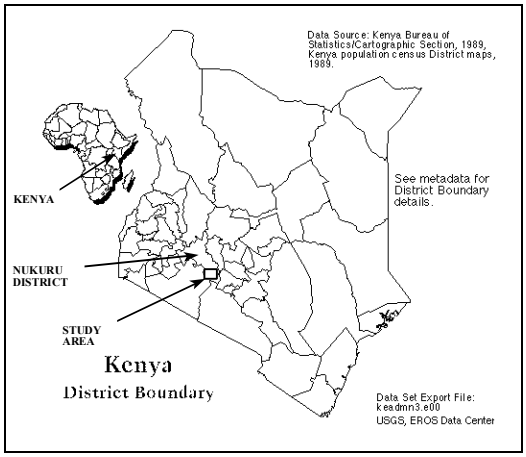


Source: USAID

**Figure 2-1** ***Location map of the study area***

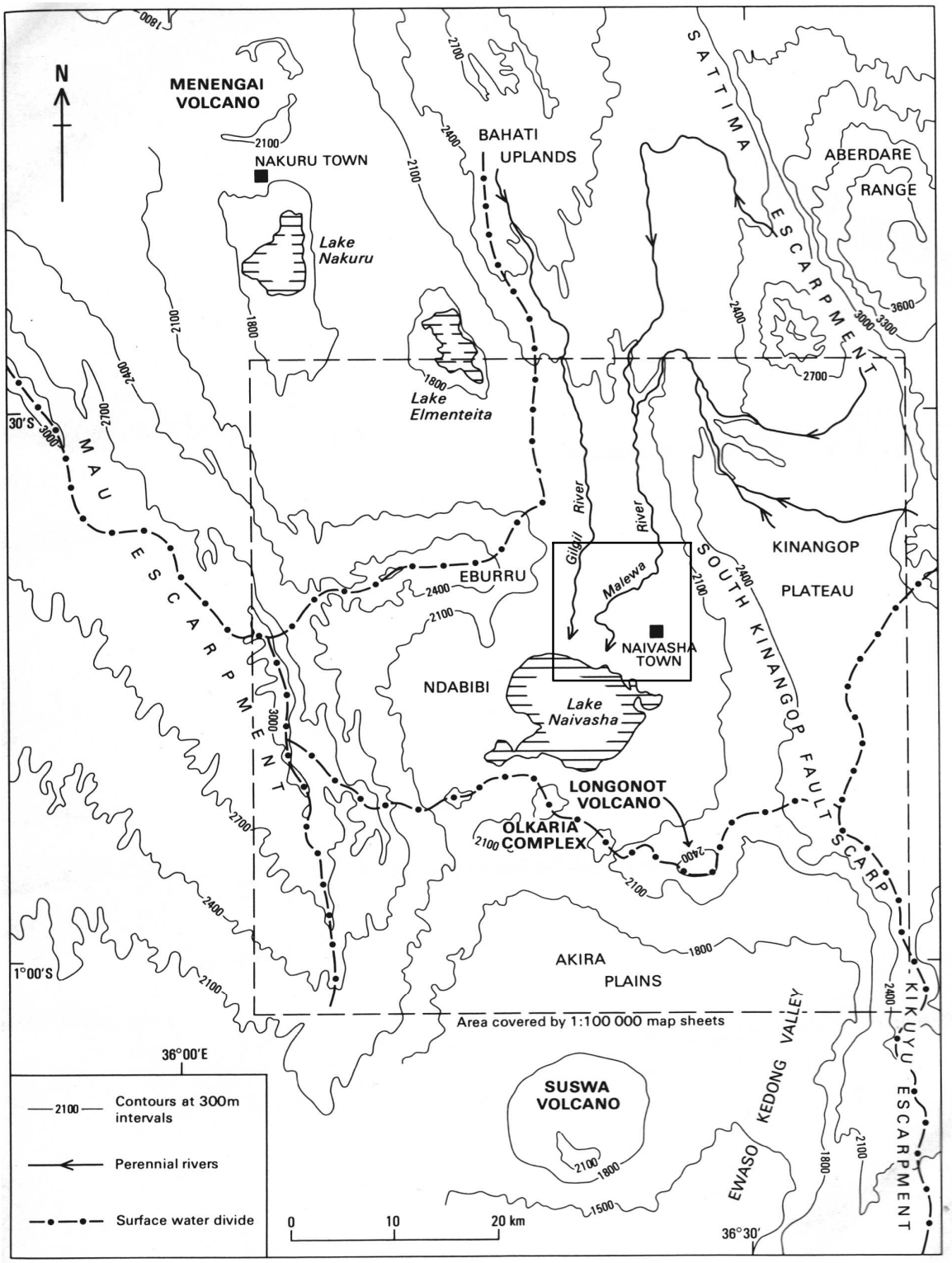


**Figure 2-2** ***Study area and physiography of the central rift valley (After Clarke.et.al 1990)***

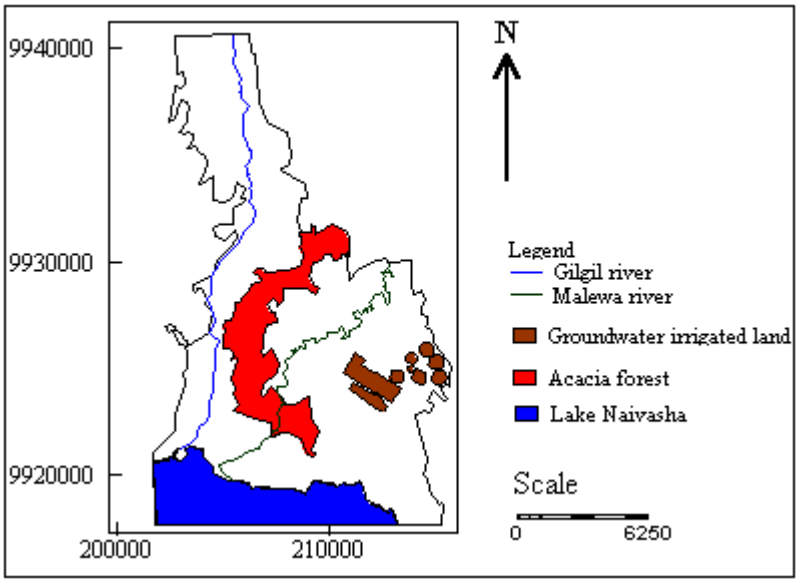


**Figure 2-3** ***Detailed map of the study area***

### 2.1.3 Climate

Climatic conditions in the study area are quite diverse. The Naivasha area is marked by cool temperature and semi-arid climate.

#### 2.1.3.1 Rainfall

Precipitation is one of the most important sources of groundwater recharge. Rain and snow falls to the earth. It will then runoff to a surface water body, evaporate, be taken in by plants, or soak through the ground to the water table. The amount of precipitation that falls in an area and the rate at which it falls has a strong influence on groundwater levels.

The rainfall regime within the lake Naivasha catchment is influenced by the rainshadow from the surrounding highlands of the Nyandarua range to the east, and the Mau Escarpment to the west. It is greatest along the Mau and Nyandarua escarpments where it averages from 1250 to 1500 mm annually in valley areas where it averages about 650 mm at Lake Naivasha (McCann 1974). Some precipitation occurs during each month of the year, although the are two main rainy seasons per year, “the long rains” occurring in March, April and May and the “short rains” in October and November (Stuttard et. al 1995).

Seven selected stations in the study area are shown in (Figure 2-4). The mean monthly rainfall data are in **appendix 2-A**. The general pattern of rainfall for long-term average monthly is presented in figure 2-5 and figure 2-6. It is observed that rainfall pattern in general follow the typical trend of two rainy seasons. However this pattern only merge when the average of many years of rainfall are taken and in any given year the actual pattern and quantity of rainfall may differ significantly from the long term average.

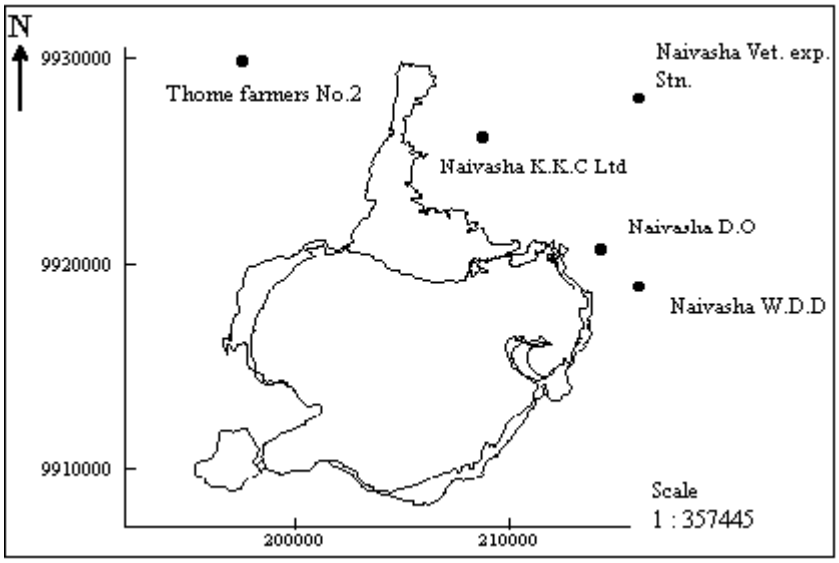


**Figure 2-4** ***Locations of selected rainfall station in the study area***

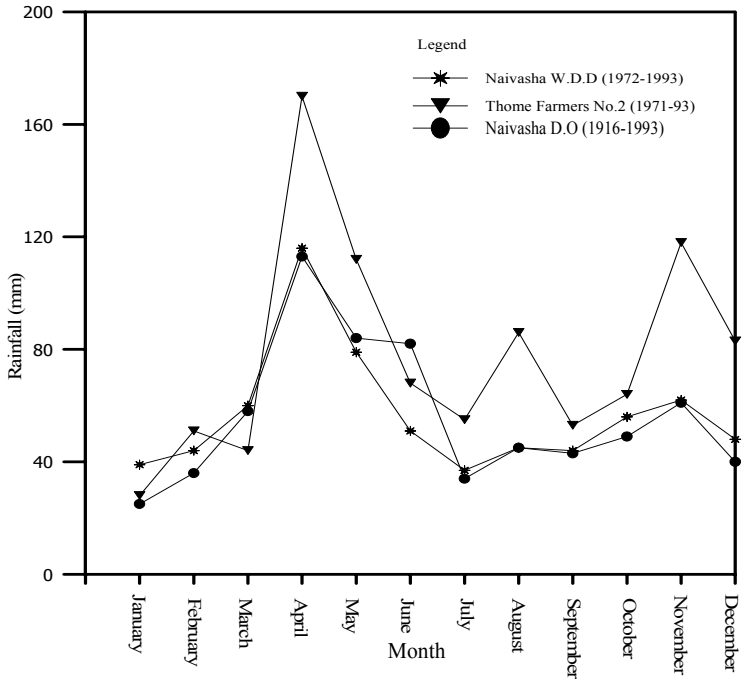


**Figure 2-5** ***Graph of long-term mean monthly rainfall for Naivasha W.D.D, Thome Farmers No.2 and Naivasha D.O.***

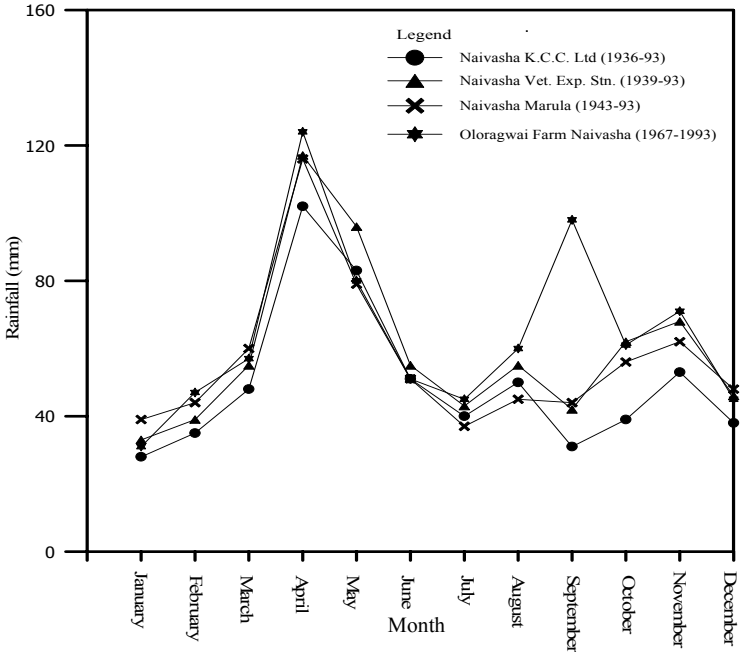


**Figure 2-6** ***Graph of long-term mean monthly rainfall for Naivasha K.C.C Ltd, Naivasha Vet. Exp. Stn, Naivasha Marula and Olarogwai Farm Naivasha.***

### 2.1.4 Geology of the study area

The Rift floor is covered with the sediments that accumulated during the Gamblian stage of the Pleistocene period. Despite their extensive distribution the Gamblian lakebeds are not thick and rarely exceed 30 m (Thompson et. al., 1963). Beneath, within and above the Gamblian beds are unconformities (Figure 2-7). A geology of the Naivasha area is described in detail in Thompson and Dodson (1963) and Clarke et. al (1990). The following formations are predominately occupy the study area;

#### 2.1.4.1 Lake sediments

Lake sediments form a large part of the floor of the Naivasha basin and are exposed in gullies, road section and small quarries in the vicinity of the Naivasha Town. Mainly composed of re-worked volcanic material or sub-aqueously deposited pyroclastics. Is the pumiceous granule made up of pebble gravel, coarse sand, gravelly sand, silt and clay, where it is exposed reaches maximum thickness of 15 m. Is underlain by Akiria basalts, Eburru pantellerites and, Kedong valley tuffs.

#### 2.1.4.2 Alluvial Deposits

Composed of silt, fine sand, some ferruginous coarse sand and locally boulder gravel. Formed due to gully floor and basin (small) deposits, latter possibly interbedded with lake sediments, alluvial fan eg Ndabibi plains. Alluvial deposits associated with Malewa river are dominated by greyish brown silt and fine sand within which there are intervals of reddish brown ferruginous coarse sand and gravel, and pale grey clay (Clarke et.al 1990). A photograph showing such succession was taken in Malewa River, during fieldwork 1999 (Figure 2-8).

**Figure 2-7** ***Unconformity as seen in Karati river***

**Figure 2-8** ***Malewa River succession of greyish brown silt and fine sand***

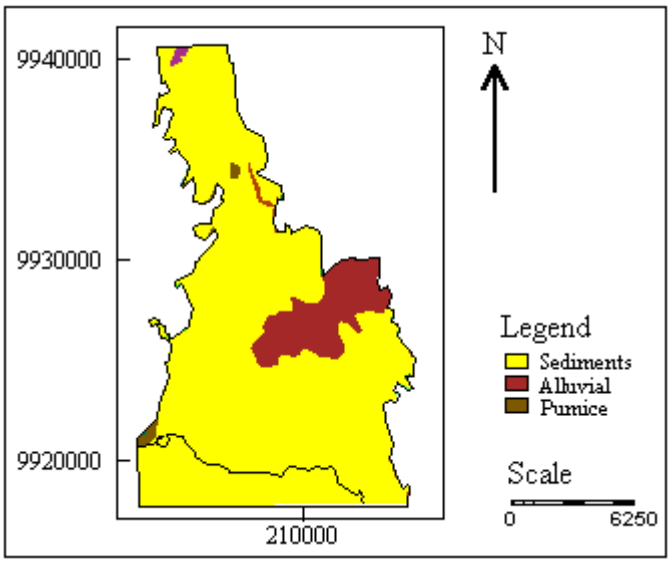


**Figure 2-9** ***Simplified geology map of the study area (Source: Government of Kenya, Ministry of Energy 1988)***

### 2.1.5 Surface Water Hydrology

#### 2.1.5.1 Lake Naivasha

The wetland system lies in the high altitude trough of the Eastern Rift valley in Kenya at approximately 1,886 m.a.s.l, (Abiya 1996). It is comprised of a shallow, freshwater lake, a deep Crater Lake, a partially separated sodic extension and a separate sodic Crater Lake. One of the few freshwater lakes in the country (and eastern Africa) making it valuable to people as a source and store of water. There are no known outlets, yet the water remains fresh, thus leading to suggestions of possible unique and intricate hydro-geological mechanisms involving underground seepage in this part of the Rift Valley, which account Lake's freshness. Naivasha's wetlands receive inflow

from two perennial and several ephemeral streams. The catchment area is approximately 3,000 km$^2$. The floodplains of the two largest rivers, the Malewa and Gilgil, have a delta, which enters the lake from the north. The main lake has an average depth of four metres and a maximum depth of 16m at the submerged crater. The lake water level can however vary significantly from time to time

#### 2.1.5.2 Drainage network

The morphology of the rift valley has affected surface drainage. Most of the surface drainage occurs within the rift valley. There are number of rivers around the lake but only two of these have substantial flows into the lake. These are Malewa River, which is by far the most important, and the Gilgil River, which together account for 90 percent of the rive flows to the lake (Abiya 1996). Malewa river rises on the western slopes of the Nyandarua range at an altitude of 3000 to 4000 m. The small streams flow westwards and develop into four main tributaries; the Mugyutu, the Turasha, Kitiri, and Makungi. All four flow from north-south before turning west and joining the Malewa. Giligil river's headwaters are situated in the Bahati forest where it drains a long narrow basin. The river raises at 2740 m in an area where rainfall is high at 1300 mm per annum. There are few tributaries. Karati River flows from the north and rises on the Kinangop plateau at an altitude of 2620 m where there is a mean annual rainfall of 800 mm.

### 2.1.6 General Hydrogeological Setting

#### 2.1.6.1 Groundwater Occurrence

In the Rift Valley several water-bearing strata appear. The floor of the Rift Valley is covered with younger volcanic and lake sediments. These vulcano-lacustrine series are referred to as the Upper Pleistocene Gamblian Stage or more easily as the lake sediments. These sediments constitute a continuous aquifer in contrary to the discontinuous and perched aquifers, which may prevail in the older volcanic formations. The lake sediments consists of layers of pyroclastics, and waterlain sediments originating from erosion of the volcanics (ITC-WRAP Phase V, 1996).

A cross-section along some of the boreholes in the study area, which indicate different types of aquifers in the area, was done by (Wiberg 1975, VIAK). **Appendix 2-B** shows the boreholes and the cross section. The profile is given in **Appendix 2-C.** It can be seen that the aquifers in the study area are complex, this is due to sedimentation, which took place concurrently with the tectonic history and associated volcanism.

The permeability of the rocks underlying the Rift Valley is generally low, although there is considerable variation. Aquifers are normally in fractured or reworked volcanics, or along the weathered contacts between different lithological units. These aquifers are often confined or semi-confined and storage coefficients are likely to be low.

The water tables are considerably higher on the often steep and markedly elevated boundary escarpments to the east and west. In the vicinity of the Lake Naivasha, the groundwater table is generally between 1880 and 1890 m a.m.s.l, i.e. similar to the lake level (Groundwater Survey (Kenya), 1998)

#### 2.1.6.2 Old Land Surface

The old land surfaces between lava flows occur in Tertiary volcanic rocks of the area in which ground water is stored in old weathered zones and older formation as well as between successive flows. Aquifers with relatively high permeabilities are found in sediments covering parts of the Rift floor (particularly around Lake Naivasha). Such aquifers are often unconfined and will have relatively high specific yields. The highest values of permeability are found in the reworked volcanics composing the sediments of the Naivasha area, where the specific capacities of the wells often exceed 3 l/s/m and where estimated hydraulic conductivities of greater than 10 m/d are common (Clarke et. Al.1990).

#### 2.1.6.3 Recharge and Groundwater Movement

Groundwater movement from recharge area to discharge area depends on the available recharge, the aquifer characteristics and the mode of recharge. Recharge in the area is mainly from local precipitation, and this recharge is affected by climatic conditions, landuse, vegetation cover and soil characteristics.

The floor of Rift Valley has its highest elevation in the area of Lake Naivasha, generally falling to the north and south. There is thus potential hydraulic gradient within the Rift in these axial, directions (Clarke et. Al.1990). The water tables are considerably higher on the often steep markedly elevated boundary escarpments to the east and west. The highlands support well-developed tropical rain forest, which partially covers the Nyandarua, Mau, Kikuyu and Kinangop escarpments. Precipitation in the higher areas is significantly higher than within the Rift, where the vegetation is of the semi-arid character.

Meteorological records confirm this difference: the escarpments experience an annual rainfall of 1000 to 1500 mm, with similar potential evapotranspiration losses (i.e a semi humid to humid climate). The considerable lower rainfall within the Rift is exceeded by potential evapotranspiration rates that are often many times higher than the precipitation (i.e. semi-arid to arid character) (McCann 1974).
The direction of groundwater flow is generally west, northwest and southwest from Nyandarua Range and east from Mau escarpment into the Naivasha basin.

Examination of boreholes records shows that the piezometric surface generally follows the surface contours, i.e., underground movement of water is occurring both AXIALLY along the Rift, and LATERALLY from the bounding highlands into the Rift. The data supports out flow both north and south from Naivasha, with a steeper fall to the south (Clarke et. Al.1990).

Infiltration capacities in Nyandarua and Mau escarpments are high due to the forest cover and the relatively course underlying rocks and permeable soils. Direct recharge also occurs where Quaternary alluvial deposits do not contain beds of fine-grained volcanic ash and clay silts, which would inhibit deep infiltration (McCann 1974).

### 2.1.7 Geothermal Water

The most active thermal areas are associated with volcanic complexes at Ebburu, Olkaria, Longonot and Suswa (not in the study area). In these areas fumaroles, often controlled by linear or ring fractures, are common, although thermal springs are rare. This is in part because the volcanoes occupy high ground and are therefore in hydrological recharge areas (Clarke et al. 1999). Rarely, hot springs associated with these areas are found in topographically lower regions such as to the north of Ebburru and in Njorowa Gorge within the Olkaria Complex. The complexes strongly affect groundwater flow.
Deep geothermal drillings are carried mainly in the Ebburu and Olkaria geothermal fields, in some cases these drillings reached depths in excess of 1000m (Stuttard et.al 1995).

### 2.1.8 Landuse types

Major landuse units in the study area are:

Agriculture (Irrigated and rainfed)
Settlements
Game sanctuaries
Rangeland (dairy) and meat.
Natural vegetation

Below a brief description of irrigated agriculture by groundwater is given.

#### 2.1.8.1 Groundwater irrigation

Three Point Ostriche and Delamere Estate farms get their irrigation water from groundwater. They have drilled a number of boreholes, which are electrically driven. As for October 1999 Three Point Ostriche Farm was using Center-Pivot which is an automated sprinkler irrigation achieved by automatically rotating the sprinkler pipe, supplying water to the sprinkler heads or nozzles, as a radius from the center of the field to be irrigated. Water is delivered to the center or pivot point of the system. The pipe is supported above the crop by towers at fixed spacings and propelled by electric power on wheels in fixed circular paths at uniform angular speeds (Figure 2-10). Single units ranges from about 175 m to 375 m long and irrigate minimum about a 96250 $m^2$ circular area, by that time there were 8 centre pivot. From the air, a scene is so dramatic as the prevalence of center-pivot irrigation circles along the farms. The field, round because the irrigation sprinklers pivot about a central point (Figure 2-11). The fields are by and large maintained with groundwater pumped from the pivot point, water that is contributing to the depletion of groundwater.

Dalamere farm had one centre-pivot, the rest of irrigation was done by using parallel pipes which are moved by hand from one position to another.

**Figure 2-10** ***Centre pivot irrigation in Three Point Ostriche***

**Figure 2-11** ***Centre pivot irrigation from the air***

# 3 CHAPTER THREE

## 3.1 METHODOLOGY AND DATA ANALYSIS

### 3.1.1 Database Preparation

#### 3.1.1.1 Purpose of the database

Is to store surface and groundwater measurements in Naivasha basin (station number, position, altitude, depth et cetera) in a single repository and to allow the generation of tabular overviews from selected stations for some time duration in a synchronised way.

#### 3.1.1.2 Structure of the database

There are two important tables, namely **STATION** and **MDATA**. The first contains a single tuple (row) for each measuring station, indicating its type plus some extra information. It also has an attribute [Include?] that can be set to either YES or NO, and indicates whether measurements for that station will be included in the synchronisation analysis. The station identifier (attribute STATION) is unique.
The **MDATA** table is far bigger and includes all measurements for all stations. To this end, it has a station identifier, a timestamp and a value for each measurement. The combination of attributes STATION, RTIME (for recording time) are unique.

#### 3.1.1.3 Using the database

There are two main phases for using the database, namely **data preparation** and **data extraction**. Data preparation is performed to add base data (station names, measurements) to the database; data extraction is the phase in which one or more tabular overviews are extracted from the base data in the database.

#### 3.1.1.4 Data preparation

During data preparation station information and measurements were added to the database. First a tuple was added to **STATION** for each station for which measurements will be included in the database. Then, measurements for the now included stations were entered in the **MDATA** table. Some data were prepared in excel spreadsheet and imported in database for a matter of simplicity. Any data can be added in a database, the only rule to be aware of is to have a station tuple in the STATION before including measurements for that station.

#### 3.1.1.5 Data extraction

The database includes also a number of predefined queries that can be run on the data, and that will lead to production of the tabular overviews required.

The query definitions are a little bit involved. When run, they generate a data set that will be eventually being included in an Excel spreadsheet. This intermediate data set is stored in a temporary table. The spreadsheet is then fed from that temporary table.

The simplest way to obtain a synchronised tabular overview of measurements for the stations selected is to run the query **MDATA Plain Crosstab**. It simply generates a chronological list of measurements with a column for each station, interpreting the recording time of a measurement as a discrete time event. The query will prompt you for the **Start time** and **End time**, defining the time window of measurements to be included. Values for these prompts can be valid Windows DateTime values, as in Excel spreadsheets. This means you can input "1/1/1999" or "1/23/1999 20:06" as values.

Measurements from different stations occurring at the same discrete time event are combined in a single row of the output. Like other tabular results created, this output may have fields with no value (or 'null' value). This means there was no value available, or a value could not be computed from the input (Rolf de By, 1999)

By using this database it was easy to retrieve information needed at a particular defined period. All wells in the database are given in **appendix 3-A**

### 3.1.2 Pumping test

#### 3.1.2.1 Basic Principle

Pumping tests are generally conducted in order to determine the parameters Transmissivity (T) and Storativity (S) for the aquifer. The magnitude of these parameters influence the yield of the well and the shape and size of the cone of depression. These are not the only important parameters that can be determined from this test. The principle of pumping test is that if we pump water from a well and measure the discharge of the well and the drawdown in the well and in piezometers at known distance from the well, we can substitute these measurements into an appropriate well-flow equation and can calculate the hydraulic characteristics of the aquifer (Kruseman and Ridder 1994).

#### 3.1.2.2 Pumping Test Three Point Ostrich farm

Pumping test was conducted in wells at Three Point Ostrich farm. The night before the tests were performed, the pump was shut down for at least twelve hours. Before pumping started the initial water level was taken. The drawdown was measured in observation well and in the pumped well at frequent intervals during the pumping. During the pumping test, discharge rates measurement were constant the pumped water was used for irrigation by pivot.

Well BH D was pumped and BH C that is 65 m from BH D was used as an observation well. The time-drawdown data were then interpreted to yield the transmissivity and storativity of the aquifer. Aquifer Test for windows was used to analyse the data.

Aquifer Test contains a complete set of analytical solutions for estimating the transmissivity, hydraulic conductivity, and storage properties for confined, unconfined and fractured rock aquifers. The slug test analysis methods include the popular Hvorslev and Bouwer-Rice methods while the pumping test analysis methods

include; Theis; Cooper-Jacob; Neuman; Hantush; Moench (unconfined); Moench (fracture flow); Well Performance Tests; Step-Test Analysis; and Recovery Analysis (Theis-Jacob).
The aquifer parameters are obtained by matching type curves or by fitting straight lines to the drawdown data points. Automatic curve matching and manual curve matching capabilities are provided.

The following methods were used:

Jacob straight-line method using the equation:

$$KD = \frac{2.30Q}{4\pi\Delta s} \qquad \textbf{Equation 3-1}$$

Where

$KD$ is the Transmissivity ($m^2$/day)
$Q$ is discharge ($m^3$/day)
$\Delta s$ is the drawdown per log cycle of distance (m).

Hantush method (leakey, no aquitard storage) using the equation

$$S = \frac{Q}{4\pi T} W\left(u, \frac{r}{L}\right) \qquad \textbf{Equation 3-2}$$

T is the Transmissivity ($m^2$/day)
$Q$ is discharge ($m^3$/day)
$\Delta s$ is the drawdown (m)
$W(u, r/L)$ is the leaky artesian well function

The pumping test results are enclosed in **appendix 3-B**. The aquifer test plots for well BHC are shown in the **appendix 3-C**

Summary of the obtained transmissivity

| Method | Transmisivity ($m^2$/day) | Storativity |
|---|---|---|
| Hantush method(leakey, no aquitard storage) | 462 | $3.95 \times 10^{-3}$ |
| Cooper and Jacob straight-line | 1150 | $1.46 \times 10^{-3}$ |

**Table 3-1** ***Transmissivity from BH C at Three Point Ostrich farm***

### 3.1.2.3 Reported Transmissivity

Different researchers have calculated groundwater transmissivity around Lake Naivasha and from their data it shows clearly that transmissivity varies locally within the area as indicated in the table 3-2

| Borehole Name | Place | Coordinates | | Transmissivity | Source of data |
|---|---|---|---|---|---|
| | | x | y | $M^2$/day | |
| BH 1 | Naivasha water supply | 212921 | 9923339 | 233.28 | VIAK |
| BH 3 | Naivasha water supply | 212995 | 9923310 | 224.64 | VIAK |
| BH 4 | Naivasha water supply | 212936 | 9923318 | 198.72 | VIAK |
| BH A | 3 Point Ostriche | 213712 | 9925550 | 1020 | Ramirez (Msc 1999) |
| BH C | 3 Point Ostriche | 213459 | 9924929 | 1150 | Kibona (Msc 2000) |
| BH 9 | Manera farm | 211434 | 9921380 | 670 | Ramirez (Msc 1999) |
| BH | Marula farm | 207698 | 9925728 | 220 | Ramirez (Msc 1999) |
| KCC | Milk factory | 209037 | 9925717 | 75 | Ramirez (Msc 1999) |
| C1482 | | 214316 | 9917024 | 1330 | McCann |
| C1063 | | 197600 | 9929926 | 38.9 | McCann |

**Table 3-2** ***Transmissivity calculated by different researchers in the study area.***

The map below shows the spatial distribution of the transmissivity.

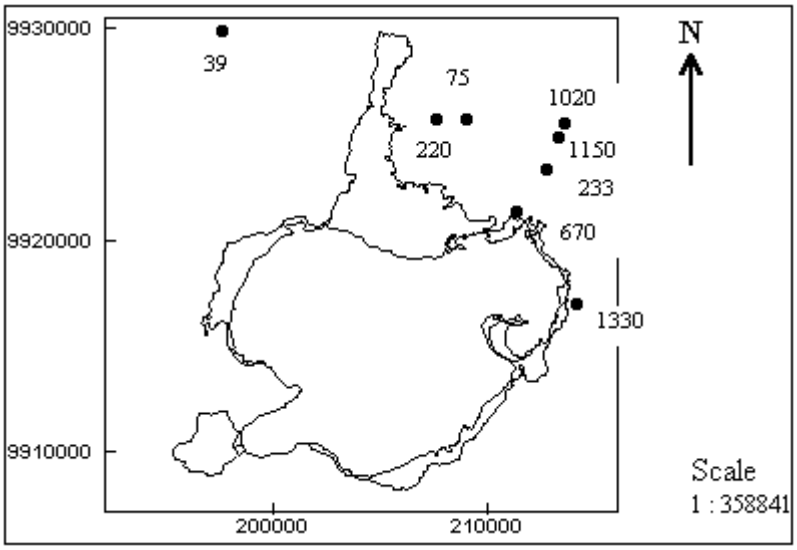


**Figure 3-1** ***Spatial distribution of the calculated transmissivity***

Transmissivity calculated by Clarke et al 1990 for the whole of Lake Naivasha from different boreholes is given in the table 3-3.

| Area | Lithology | Geometric mean estimated Transmissivity $m^2$/day | Geometric mean estimated permeability m/day | Total number of boreholes |
|---|---|---|---|---|
| NE Naivasha | Sediment & volcanics | 307 (1170) | 12 (33) | 35 |
| SE Naivasha | Sediment & volcanics | 502 (3082) | 20 (114) | 22 |
| SW Naivasha | Sediment & volcanics | 297 (940) | 63 (196) | 17 |
| NW Naivasha | Sediment & volcanics | 1601 (5308) | 148 (818) | 26 |

**Table 3-3** ***Average aquifer characteristics of the selected areas and lithologies from borehole data (Figures in brackets are arithmetic means).***

High transmissivity in some of the boreholes is related to fractured and fissured zones also from the coarser pyroclastics and weathered zones. The coarser pyroclastics beneath the Kinangop plateau have high transmissity, indicating that they were deposited in a high-energy environment (the escarpments).

### 3.1.3 Hydraulic Conductivity Measurement along Malewa River

There is seepage of water from Malewa River to the groundwater, since water level in Malewa River is higher than in the aquifer (Behar 1999). Measurements were done in connection of estimating how much water from the river seeps to the aquifer; therefore augering was done along the river to achieve the purpose. Two methods were used auger-hole and inverse auger-hole method.

#### 3.1.3.1 The auger-hole method

A hole was bored into the soil to a certain depth below the water table. When equilibrium was reached with the surrounding groundwater, a volume of water was removed from the hole and the surrounding groundwater was allowed to seep in to replace it. The rate at which water was rising in the hole was measured and then converted by a suitable formula to the hydraulic conductivity (k) for the soil. Care was taken to complete the measurements before 25 percent of the volume of water removed from the hole has been replaced by inflowing groundwater. For after that, a funnel-shaped water table develops around the top of the hole. Which increases resistance to the flow around and into the hole. This effect is not accounted for in the formula or flow charts developed for the auger-hole method.

The profiles of the auqer-hole are dominated by greyish brown silt and fine sand. As the material is almost homogeneous it was considered as one layer. The water level in the auger holes was lower than in the river, the water level was measured by using electric dipper.

Calculation for the single-layer situation

Landon (1991) explains that, Ernest (1950) found that the relation between the hydraulic conductivity of the soil and the flow of water into the auger hole depends on the boundary conditions; this relation derived numerically, is given as:

**k = C*dh/dt** **Equation 3-3**

Where

k = hydraulic conductivity (m/day)

C = geometric factor which is the function of (*h,* H, r, S) see **appendix 3-D**

dh/dt = rate of rise of water-level in the auger hole (cm/s)

After the reading have been taken, the reliability of the measurements was checked. The (dh) value of each measurement was computed to see whether the consecutive readings are reasonably consistent.

Results of auger-hole method are enclosed in **Appendix 3-E.**

Summary of calculated hydraulic conductivity

| Identification | Distance from Malewa river | Depth of the hole | Coordinates | | Hydraulic Conductivity (k) |
|---|---|---|---|---|---|
| | | | X | Y | |
| Auger-hole A | 110 cm | 186.5 cm | 211900 | 9927739 | 0.1 m/d |
| Auger-hole B | 110 cm | 174 cm | 211900 | 9927739 | 0.42 m/d |

**Table 3-4** ***Hydraulic conductivity calculated from auger-hole method***

3.1.3.1.1 Limitation of the method

The use of this method is limited:

1. To areas where a high groundwater table occurs (at least during party of the year)
2. To soil where a boring of known shape can be maintained throughout the test.
3. The method is unsuitable for use in very stone or coarse soils where artesian conditions occur, or in soils containing small sand lenses within less permeable material.

3.1.3.2 The inverse auger-hole method

A hole was bored at a certain depth above water table and filled with water and the rate of fall of water was measured. The measurement was done along the river where by the soil was wet, therefore there was no need of prewetting.

3.1.3.2.1 Basic principles

For the cylindrical auger hole and its flat base

$A(ti) = 2\pi rh(ti) + \pi r^2$

Where

A(ti) = area through which water passes into the soil at time ti ($cm^2$)

r = radius of the auger hole (cm)

h(ti) = water-level in the hole at time ti (cm)

Supposing that the hydraulic gradient is approximately one, then according to Darcy's Law the volume rate of flow is given by:

$Q(ti) = kA(ti) = 2k\pi r(h(ti) + r/2)$

Where Q(ti) = volume rate of flow at time ti ($cm^3s^{-1}$)

If during the time interval (dt) the water-level falls over a distance (dh), the volume rate of flow into the soil equals:

$Q(ti) = -\pi r^2 dh/dt$

Combining the last two equations gives:
$2k\pi r(h(ti) = r/2) = -\pi r^2 dh/dt$

Integration between the limits

ti = t1, h(ti) = h(t1) and
ti = tn, h(ti) = h(tn)

gives:

$2k/r(tn-t1) = 1n(h(t1) + r/2) – 1n(h(tn) + r/2)$
changing to common logarithms and rearranging gives:

$k = 1.15r[\log (h(t1) – \log(h(tn) + r/2)]/ tn – t1$

$k = 1.15r \tan \alpha$ (cm/day)

By plotting ((hti) + r/2) against ti on semi-logarithmic paper, a straight line with a slope $\alpha$ is obtained.

**$k = 1.15* 864*r*\text{Tan } \alpha$ (m/day)** **Equation 3-4**

Where:
r is the radius of the auger-hole
$\alpha$ is the slope of the line

The results obtained from inverse auger-hole method were plotted on the semi-logarithmic paper and the hydraulic conductivity was calculated in metres per day (m/d).

Field measurements are in **appendix 3-F.** Graphs and their respective calculated hydraulic conductivity for all the inverse auger-hole are as follows:

**POINT C**

The auger hole is 330 cm from Malewa River
Position: (212717,9928025)
Depth of the hole: 330 cm
Radius of the Hole: 5 cm

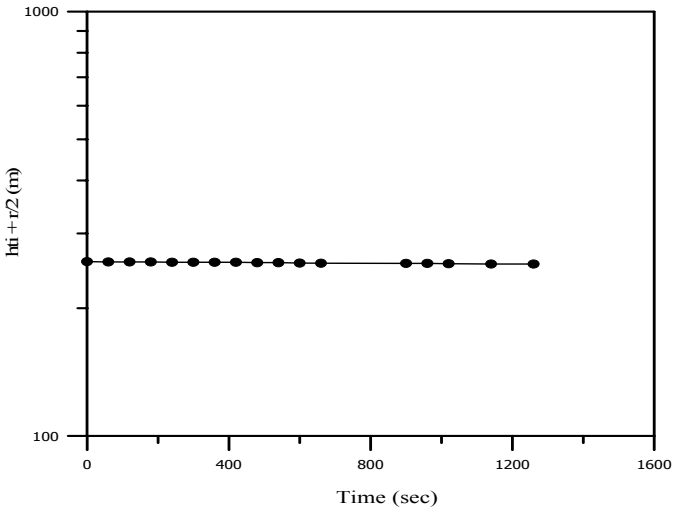


**Figure 3-2** ***Inverse auger hole graph for point C***

Equation:
Y = -0.00274462 * X + 257.356

Tan 0.0027 = 0.00004712
**k = 0.23 m/day**

POINT D

The auger-hole is 100 cm from Malewa River
Position:(212717,992805)
Depth of the hole: 110 cm
Radius of the Hole: 5 cm

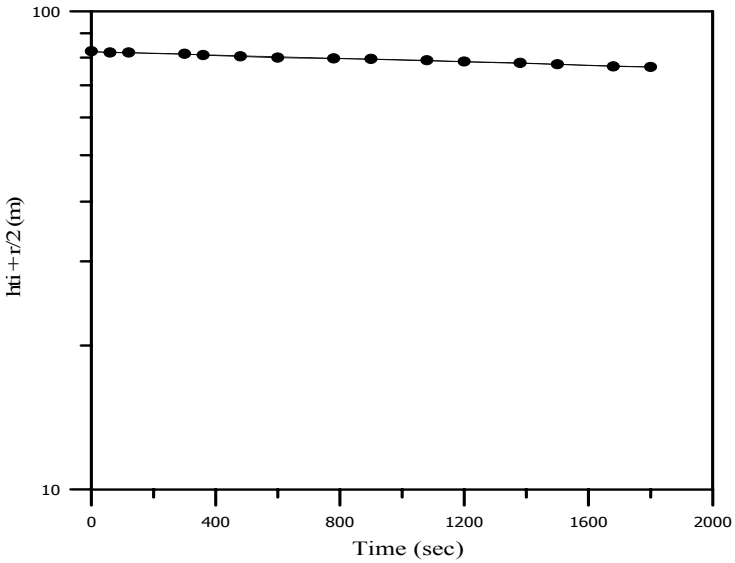


**Figure 3-3** ***Inverse auger hole graph for point D***

Equation:
Y = -0.00321668 * X + 82.2848
Tan 0.0032 = 0.00005585
**k = 0.277 m/day**

**POINT E**

The auger-hole is 270 cm from the Malewa River
Position: (211489, 9927104)
Depth of the hole: 71 cm
Radius of the Hole: 4 cm

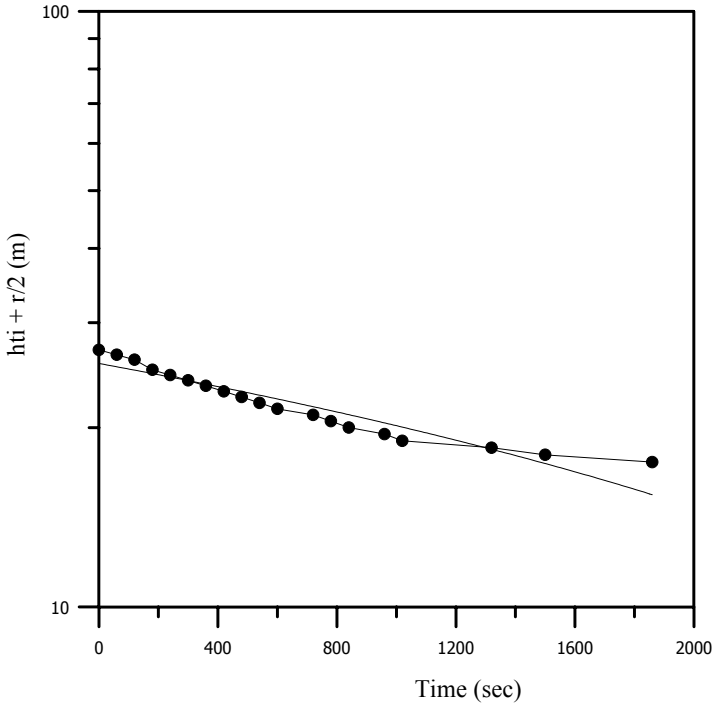


**Figure 3-4** ***Inverse auger hole graph for point*** **E**

Equation:
Y = -0.0054823 * X + 25.628

Tan 0.0055 = 0.00009599
k = 0.38 m/day

Summary of calculated hydraulic conductivity

| Identification | Distance from Malewa river | Depth of the hole | Coordinates | | Hydraulic Conductivity |
|---|---|---|---|---|---|
| | | | X | Y | |
| Inverse auger-hole C | 330 cm | 330 cm | 212717 | 9928025 | 0.23 m/d |
| Inverse auger-hole D | 100 cm | 110 cm | 212717 | 9928025 | 0.28 m/d |
| Inverse auger-hole E | 270 cm | 71 cm | 211489 | 9927104 | 0.38 m/d |

**Table 3-5** ***Hydraulic conductivity values for inverse auger-hole method***

3.1.3.2.2 Limitation of the method

- Due to swelling properties of soil, a k value obtained by this method may differ from one obtained if the soil is saturated. If this change of structure is significant, it has to be taken into consideration when measured k is evaluated.

- The test should not be done on a dry soil but only after saturating the test site.

### 3.1.4 Conclusion

♦ Six other holes were augered along the Malewa river, but were discarded (Table 3-6), because the profile were dominated by gravel and course sand, making difficult to remove the water from the auger holes due to rapid inflow of water as a result of high transmissivity. Therefore it looks like locally the river is underlain by former river channel.

♦ The results of auger holes could have been affected by slightly smearing of the holes.

♦ Finding places for augering was also difficult because the river is deeply incised.

| Identification | Distance from Malewa river | Depth of the hole | Coordinates | |
|---|---|---|---|---|
| | | | X | Y |
| Auger-hole F | 200 cm | 200 cm | 209097 | 9926338 |
| Auger-hole G | 350 cm | 100 cm | 209003 | 9926399 |
| Auger-hole H | 200 cm | 163 cm | 209160 | 9926356 |
| Auger-hole I | 150 cm | 141 cm | 209160 | 9926356 |
| Auger-hole J | 270 cm | 71 cm | 211489 | 9927104 |
| Auger-hole K | 255 cm | 103 cm | 211489 | 9927104 |

**Table 3-6** ***Auger holes which were discarded***

### 3.1.5 Water Level

Groundwater levels are affected by many variables (e.g. precipitation, pumping, river flow, and aquifer characteristics). The depth of the water reflects a balance between the rate of recharge and the rate of discharge at rivers and springs or pumped water wells. The water table remains at constant when rain falls frequently enough to balance the river, spring, and well outflow. Any imbalance, typically by seasonal fluctuation of rainfall, raises or lowers the water table. Accurate location and elevation of groundwater measuring points are important data to be known in the area. Groundwater levels data is valuable because:

♦ Provides current information against which future water levels can be compared;
♦ Helps to determine naturally occurring seasonal variations in groundwater levels (due to changes in precipitation); and
♦ Provides data that can be used to develop a groundwater flow model

In the study area the groundwater levels in the upper aquifer are governed by the lake level, precipitation and the water abstractions).

Discharge from the aquifer is by natural or artificial. Where the water table is shallow, evapotranspiration of water from saturated zone occurs naturally, and where the water table is intersected by the land surface, natural seepage of water to streams and spring occurs.

Artificial discharge from the Naivasha basin is due to water being pumped from wells, with most of the water used for irrigation and other agricultural purposes. Other uses include domestic, livestock. Water-level changes reflect the amount of water that is pumped from the aquifer, precipitation and groundwater flow.

#### 3.1.5.1 Measurement of water rest level of the wells.

A day before taking water level at selected wells, the owner was requested to shut down the pump in the evening for at least twelve hours before the measurements were taken the following day. This period was reasonable adequate because wells in the study area recover for a short period even after long aquifer pumping tests (Ramirez 1999). The waterlevel was taken by lowering the electric dipper in the well. When contact was made the electric deeper made a continuos sound, then the depth of water was recorded the process was repeated three times to make sure that the correct water depth has been recorded. The level was read to within 0.5 cm. It was not possible to measure some of the wells water level due to luck of access hole and other wells although they have access holes the electric wire blocked the deeper (the water level and other well data are shown in **appendix 3-G**).

#### 3.1.5.2 Groundwater table decline

In the north of Lake Naivasha the rate of groundwater withdrawal exceeds recharge. Groundwater level is decreasing gradually. This can be evidenced by deepening of some wells that have become dry or those are yielding less amount of water than it was during their construction. Also new deeper wells have been drilled near those, which have become dry.

#### 3.1.5.3 Reported groundwater decline

Ojiambo 1995, reported a drop in water level of 6.8 m in wells C3366 and a drop of 3.5 in C3675 in 1995, from the time they were drilled. Well C3366 was drilled in 1964 and well C3675 in 1970.

The table below shows local water table decline in some of the boreholes:

| ITC No. | Borehole No. & name | Year | Rest Water Level (m) | Decline (m) |
|---|---|---|---|---|
| ITC002 | BH A | 1998 | 28.54 | |
| | | 1999 | 30.385 | 1.845 |
| ITC001 | C11527 | 1997 | 26.05 | |
| | | 1999 | 28.10 | 2.05 |
| ITC014 | C54 | 1939 | 15 | |
| | | 1998 | 17.8 | |
| | | 1999 | 18.69 | 3.69 |
| ITC016 | C4161 | 1976 | 16.71 | |
| | | 1999 | 18.91 | 2.20 |
| ITC009 | BH 9(M2) | 1998 | 4.63 | |
| | | 1999 | 5.75 | 1.12 |

**Table 3-7** ***Observed water level declines in some wells***

Construction and 1999 levels for the wells are also presented in detail in (table 3-8) and (figure 3-5)

| ITC Number | Borehole No. & name | UTM_X | UTM_Y | Construction Level | Level 1999 |
|---|---|---|---|---|---|
| ITC002 | BH A | 213735 | 9925528 | 1886.46 | 1884.615 |
| ITC001 | C11527 | 213518 | 9924527 | 1883.95 | 1881.9 |
| ITC014 | C54 | 209462 | 9928455 | 1908 | 1904.31 |
| ITC016 | C4161 | 212958 | 9923304 | 1884.29 | 1882.09 |
| ITC009 | BH 9(M2) | 211437 | 9921386 | 1886.37 | 1885.25 |

**Table 3-8** ***Position and Construction and 1999 levels in m.a.s.l.***

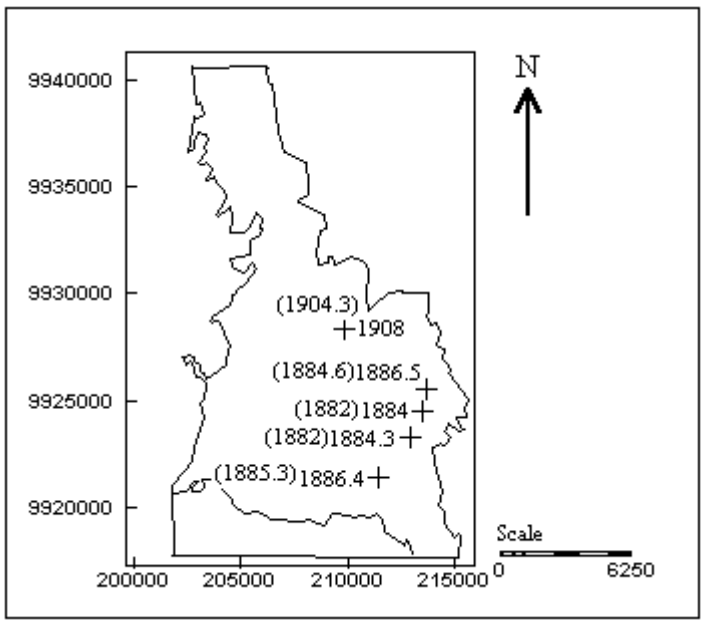


**Figure 3-5** ***Head declines in wells, numbers not in brackets are construction level and numbers in brackets are levels as for 1999***

### 3.1.6 Position and Elevation of wells

Understanding the spatial distribution of existing wells is clearly an important first step in developing a well siting strategy; a preliminary screening of productive versus dry wells can provide a valuable initial assessment of groundwater flow conditions. Furthermore, without accurate locational (and elevation) data for these wells (borehole), other data collected during drilling is not much useful.

Position of wells was measured by using a Germin G.P.S and plotted on a 1:50,000 topographical map of Naivasha and Longonot. Due to the flat slopes of water table in the Rift floor precise levelling of the wells was done by differential **Differential G.P.S.** procedure. Where by from the reference observations differences are computed either between the actual position and the known position or between the actually observed pseudoranges and the ranges derived from the satellite coordinates are transmitted to the moving platform and are used as corrections to the navigation solution (Seeber, 1993). Prior to the GPS survey, all wells to be surveyed were plotted in a topographical map.

The GPS (Global Positioning System) is a satellite positioning and navigation system. The fundamental principle is based on the measurement of the so-called pseudo ranges between the user and four satellites. Starting from the known satellite coordinates in a suitable reference frame the coordinates of the user antenna can be determined.

In this study, two Leica GPS receivers (tripod-mounted) were used to determine the eastings (x), northings (y) and heights (z) of the data points. One of the receivers was used as a base, which means a reference station. It was placed and left at a known control point with known coordinates. The other receiver was used as a rover, meaning it was moved through new points whose coordinates were to be determined. With this set-up all the required points were measured in terms of their easting (x), northings (y) and heights (z) (Seeber, 1993). The wells were levelled with reference to the access hole (Figure 3-6)


**Figure 3-6** ***GPS levelling, A indicates an access hole from which the reference was made.***

### 3.1.7 Creation of Digital Elevation Model (DEM)

A DEM of the study area was created in ILWIS program. Segment map containing contour lines digitized from three topographic maps were used, contour map for the lake unofficial blue print which was drawn by Ministry of Works 1957 (1:20,000 scale) in feet. Furthermore contour lines from Naivasha and Longonot sheet (1:50,000 scale) in metres and contour lines drawn by VIAK 1975 (1:10,000 scale) in metres.

Due to difference in the datum used the contour lines from Naivasha and Longonot sheet were below that of the lake by 3.5 m and those drawn by VIAK were lower by 2 m, therefore the correction were made before creating the DEM. Then the three contour maps were glued together and converted to raster map. GPS determined survey points were used to create point map of altitude of wells (Figure 3-7) from the table in **(Appendix 3-H)** and converted into raster map too. Finally a raster contour map and raster point map were combined. Interpolation method was applied to transform the contour data into a DEM. The selected cell size was 50 m. In the table containing all the wells in the study area, the altitude of the wells that were not measured in the field was obtained, by using map calculation operation;

**Value = MAPVALUE(dem,COORD(X,Y))** .

Whereby

Value is the altitude
Coord is coordinate
Dem is the name of the map

The groundwater levels were obtained by subtracting water level measured below ground surface from the altitude of the well. The results were used to obtain historical (Figure 3-11) and present well water levels (Figure 3-8). However due to errors caused by wrong position of non-existing wells, most of the wells in the database were not used in the modelling.

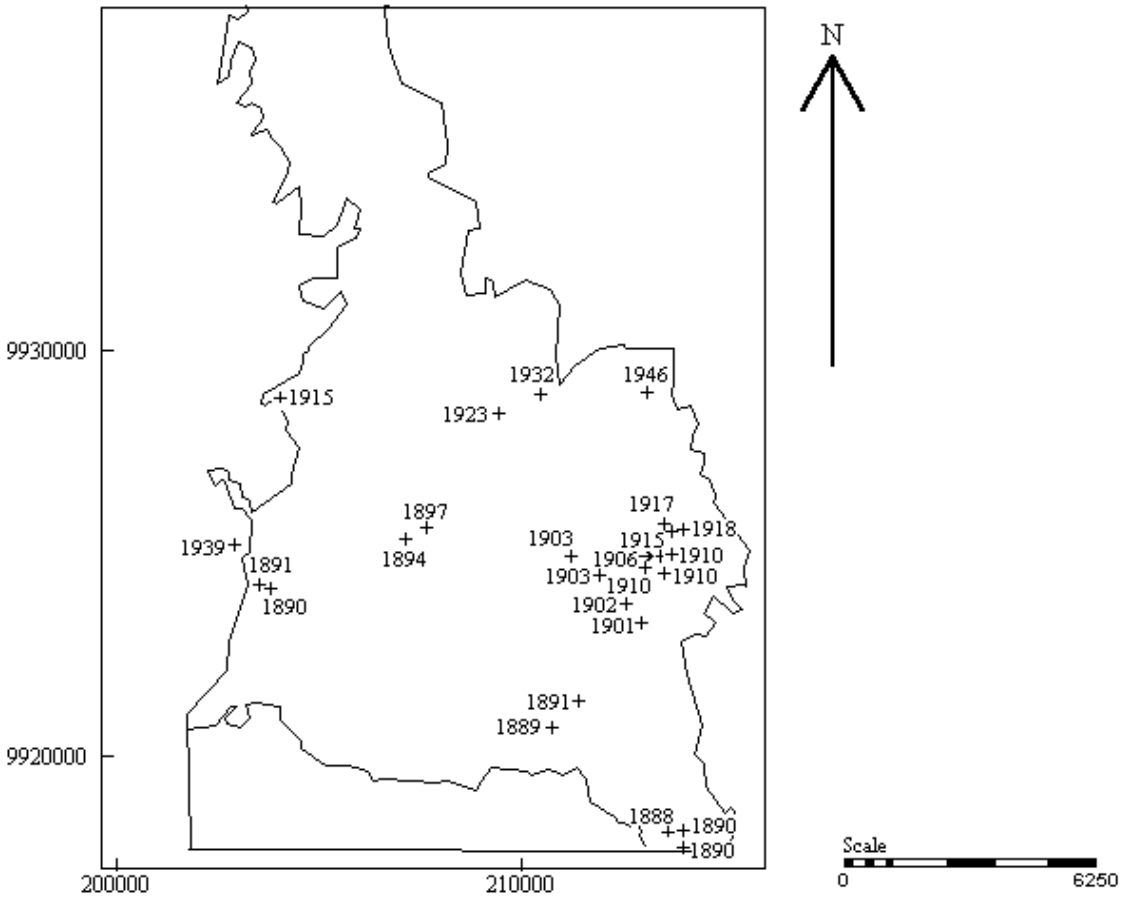


**Figure 3-7** ***Map showing points used to create a DEM (Number indicate topographic level in m.a.s.l)***

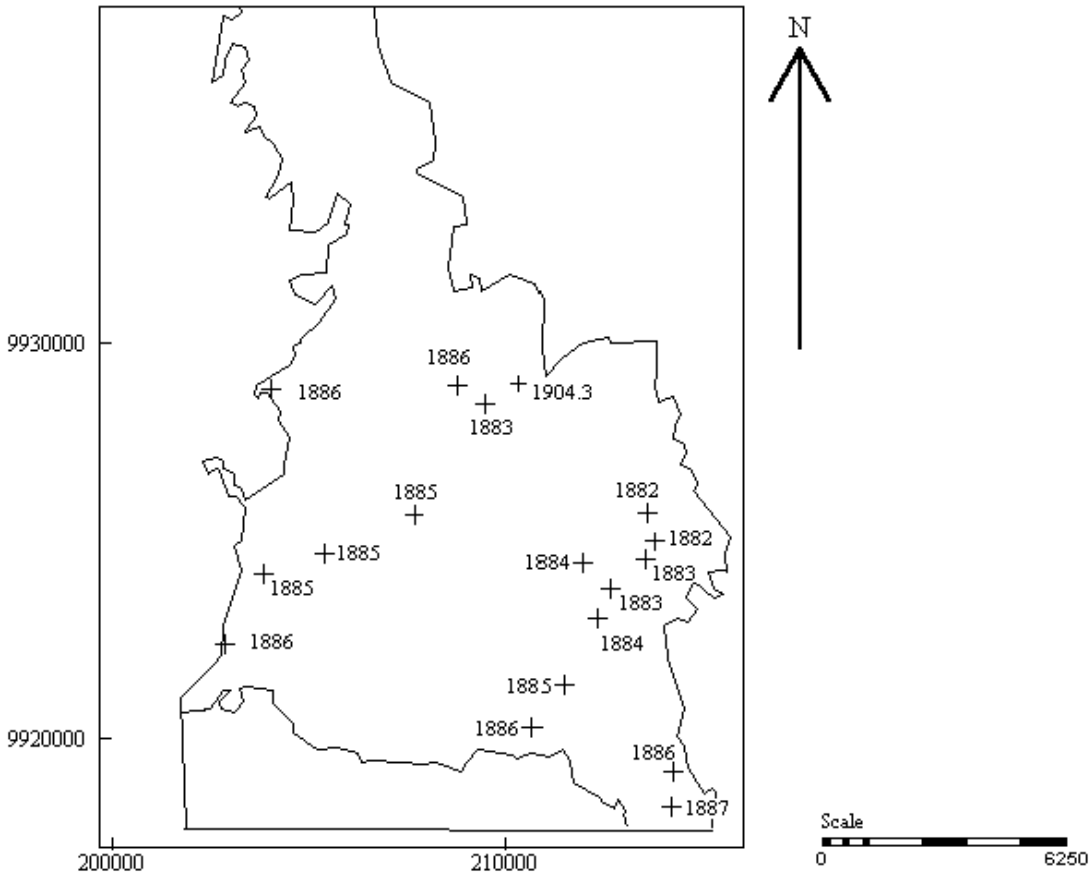


**Figure 3-8** ***Observed heads in the study area in m.a.s.l., as for October 1999.***

### 3.1.8 Historical Water Levels

#### 3.1.8.1 Lake level fluctuations

The lake has been subjected to wide fluctuations in water-levels over time and said to become almost dried some 150 years ago (Abiya 1996). It rises and falls in the natural cycle over a tremendous volume, which translates, into a very large acreage of land covered and uncovered at different stages of the cycle. The changes in level generally reflect periods of drought versus excessive rainfall. Because of shallowness of the lake basin, relatively small changes in Lake level result in large changes in open-water surface area. Historic lake level is shown in figure 3-9

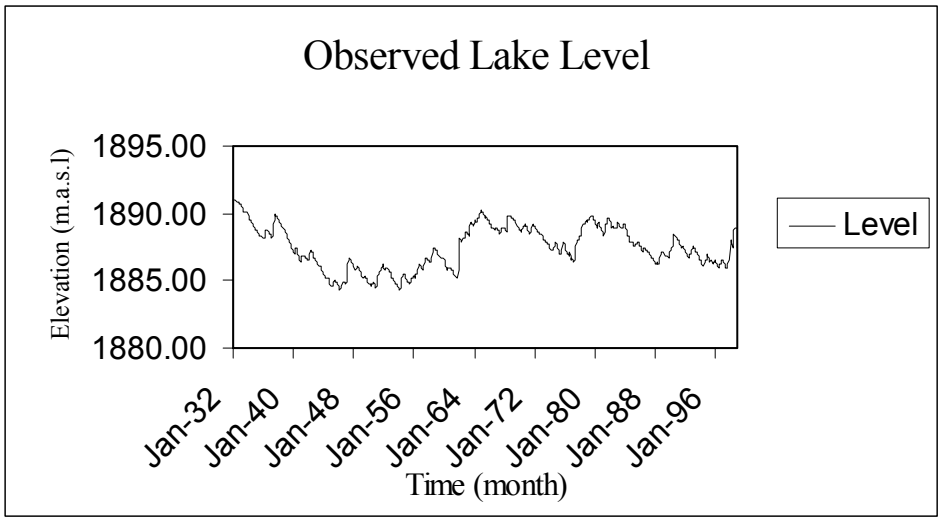


**Figure 3-9** ***Observed lake level (1932 to 1997) adopted from Mmbui 1999.***

### 3.1.8.2 Monthly Variation

Lake levels also vary monthly, the level normally drops during the beginning of the year, until the long rains start in April. However, water level normally continues to rise even during June, July and August and the maximum occurs in September. During the short rains water level normally drops, figure 3-10 (Ase et.al 1985)

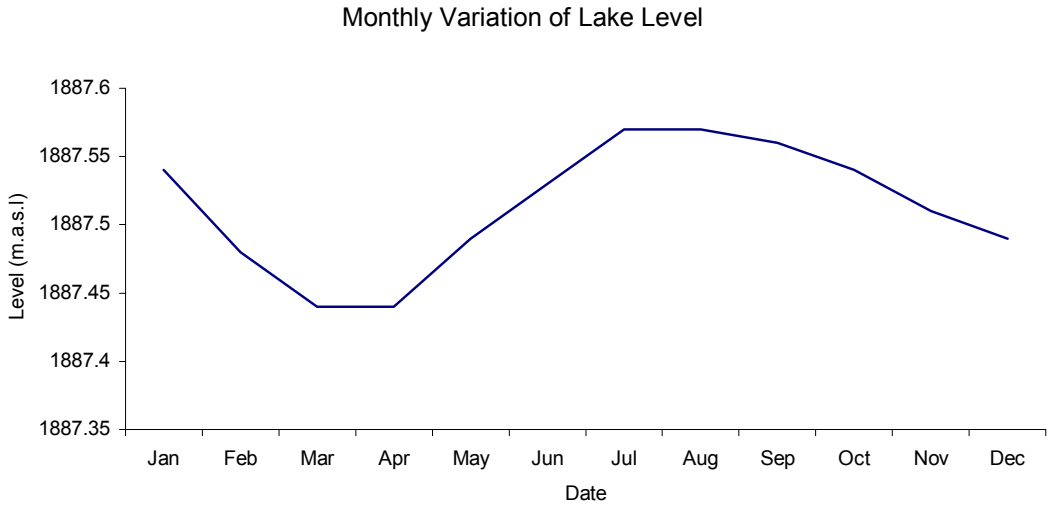


**Figure 3-10** ***Monthly variations of water level in Lake Naivasha***

### 3.1.8.3 Groundwater Level

The records of the well data were obtained from the Groundwater database of the Ministry of water resources. From this data it was possible to obtain the lithological logs, yield, depth and the water level of the wells during the time they were drilled.

The data assisted in the construction of historical and present groundwater level. The groundwater levels in the study area were obtained after subtracting the water level measured below ground surface recorded during construction from the well altitude.

The water-level data used to produce the map come from records of the earliest wells drilled in the region. Because the data are more numerous in the northeast and south of the area, the map accuracy is much better in those areas than in areas where there are only a few scattered measurements. Another factor limiting map accuracy is that the data used to assemble the map are not all from the same time period. Many of the water-level measurements were taken in wells that were installed in the 1930s through the 1970s. This is because development of water resources in Naivasha basin began at different times in different places. To limit the amount of introduced error, only the earliest measurements taken in any one area were used to generate the piezometric map.

The points used to create the pizometric map are in figure 3-11. The Naivasha historic piezometric map in Figure 3-12 shows that the hydraulic head in the Naivasha aquifer is higher in the scarps. The piezometric map indicates water flows out of the area through north towards Ebburu and Lake Elementaita, and south to Olkaria.

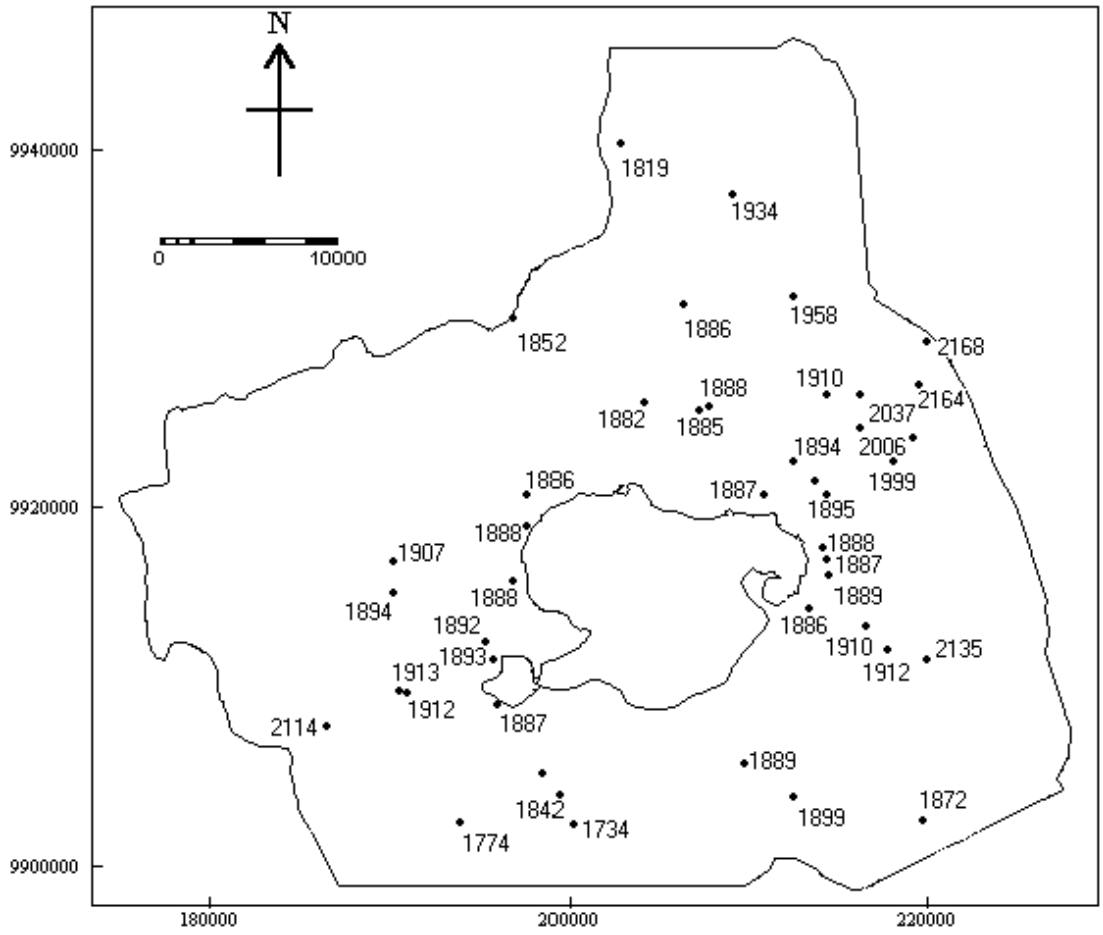


**Figure 3-11** ***Points used to create the historic piezometric map.***

The historic piezometric level for the whole Naivasha basin is represented in the figure 3-12 and table for the data used is in **appendix 3-I**

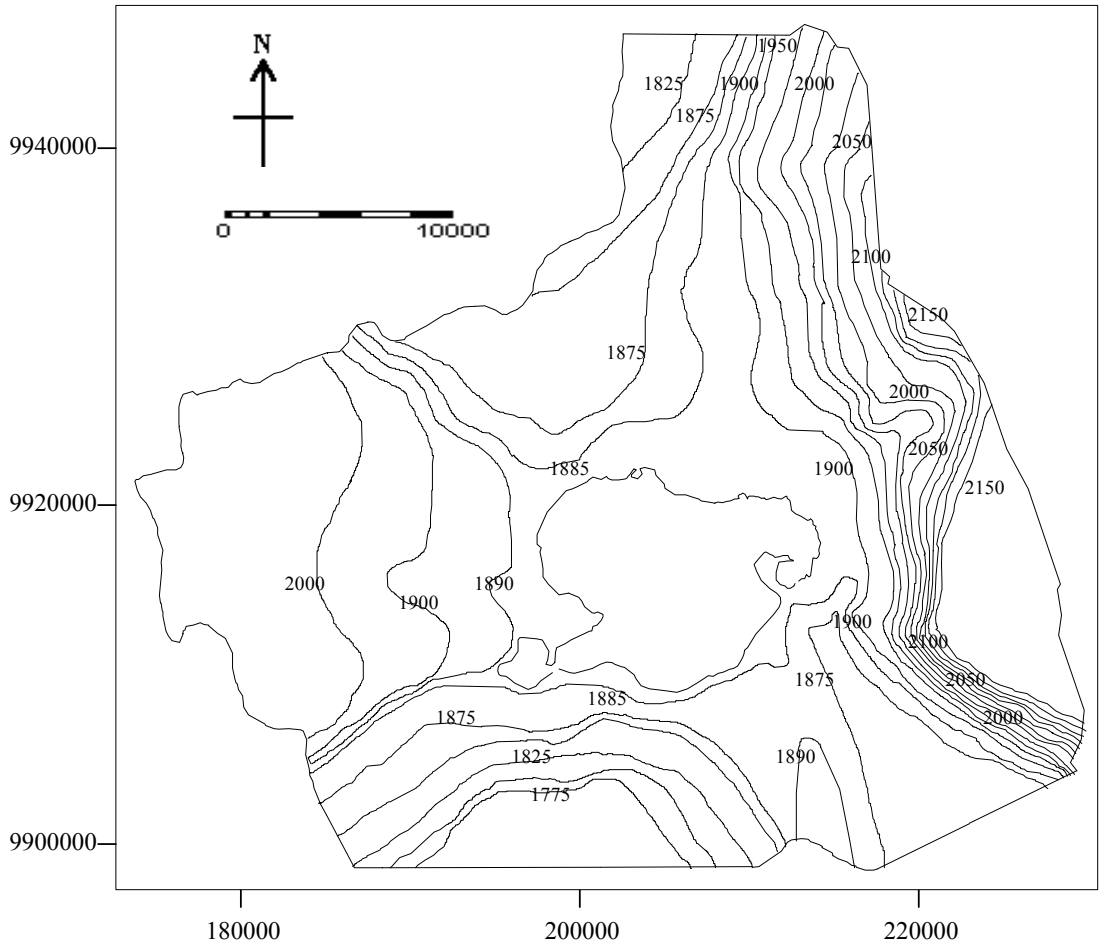


**Figure 3-12** ***Historic piezometric level (m.a.s.l) of Naivasha area (Manual interpolation).***

### 3.1.8.4 Lake-groundwater Fluctuation

Lake Levels since February 1932 to November 1998 were also obtained from (Mmbui 1999). In the well database it was possible to retrieve water level in the wells and lake by synchronising different time duration. By drawing lake and groundwater level it was possible to see the relationship between the two at a particular period. Trottman, 1998 modelled and found that wells close to the lake (a radius of about 2,000 m) fluctuate in the same manner as the lake level. Behar (1999) analysed the lake and groundwater interaction, whereby he found that the groundwater level around the lake mimics the lake level (tables 3-9 and 3-10, and figure 3-13 and 3-14). The water level of the wells close to the lake depends on the lake level at that time. That is why you can find two very close wells with different construction level or a well can have higher present level than that observed during construction, due to the rise or fall of lake level.

| Well | Coordinates | | Altitude (m.a.s.l) | Record years (years) |
|---|---|---|---|---|
| | X | Y | | |
| W15 | 203634 | 9925042 | 1891 | 1957-1969 |
| W16 | 207935 | 9925786 | 1896.6 | 1957-1963 |
| W17 | 207165 | 9925364 | 1894 | 1957-1965 |
| W19 | 210769 | 9920726 | 1889 | 1957-1969 |

**Table 3-9** ***Location, distance and altitude of the wells***

| Date | Lake | w15 | w16 | w17 | w19 |
|---|---|---|---|---|---|
| 1957 | 1886.57 | 1884.98 | 1885.59 | 1885.4 | 1885.43 |
| 1958 | 1886.98 | 1885.39 | 1886.93 | 1885.69 | 1886 |
| 1959 | 1886.83 | 1885.57 | 1887.55 | 1885.7 | 1886.25 |
| 1960 | 1886.01 | 1885.07 | 1886.56 | 1885.02 | 1885.42 |
| 1961 | 1885.61 | 1884.61 | 1886.46 | 1884.61 | 1884.91 |
| 1962 | 1888.17 | 1886.88 | 1889.78 | 1887.12 | 1888.06 |
| 1963 | 1888.88 | 1887.81 | 1889.11 | 1887.36 | 1888.77 |
| 1964 | 1889.66 | 1888.96 | 1889.62 | | 1888.57 |
| 1965 | 1889.75 | 1889.4 | 1889.49 | | 1888.38 |
| 1966 | 1888.96 | 1888.8 | | | 1887.11 |
| 1967 | 1888.77 | 1888.74 | | | 1887.68 |
| 1968 | 1889.43 | 1889.38 | | | 1888.77 |
| 1969 | 1889.3 | 1889.42 | | | 1888.7 |

**Table 3-10** ***Lake and wells water levels***

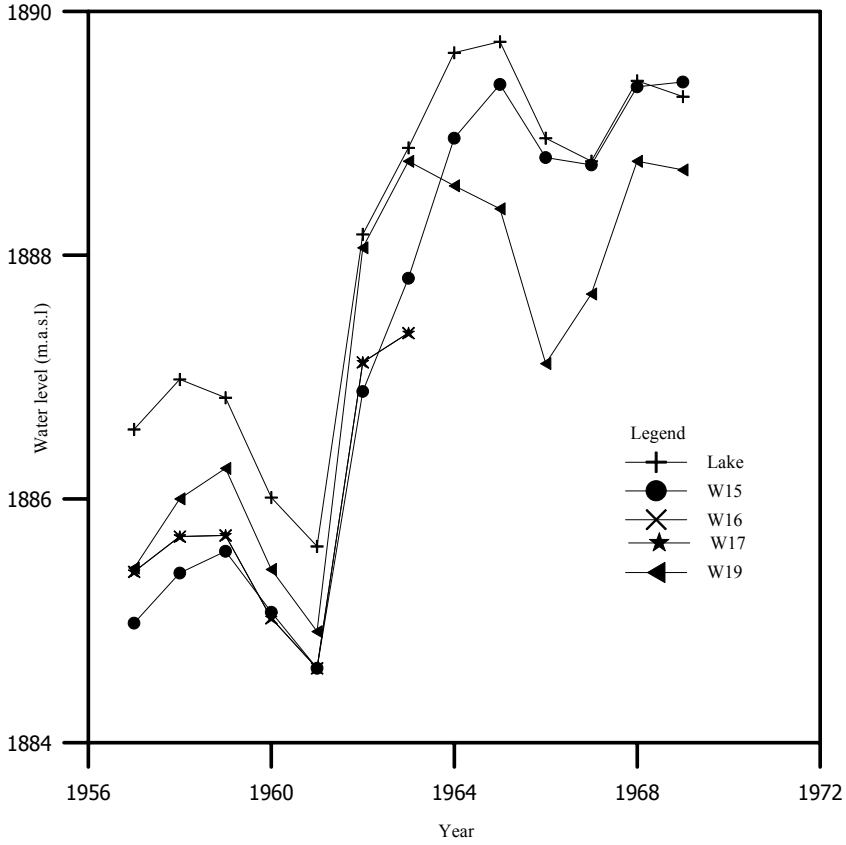


**Figure 3-13** ***Lake level and groundwater level fluctuations***

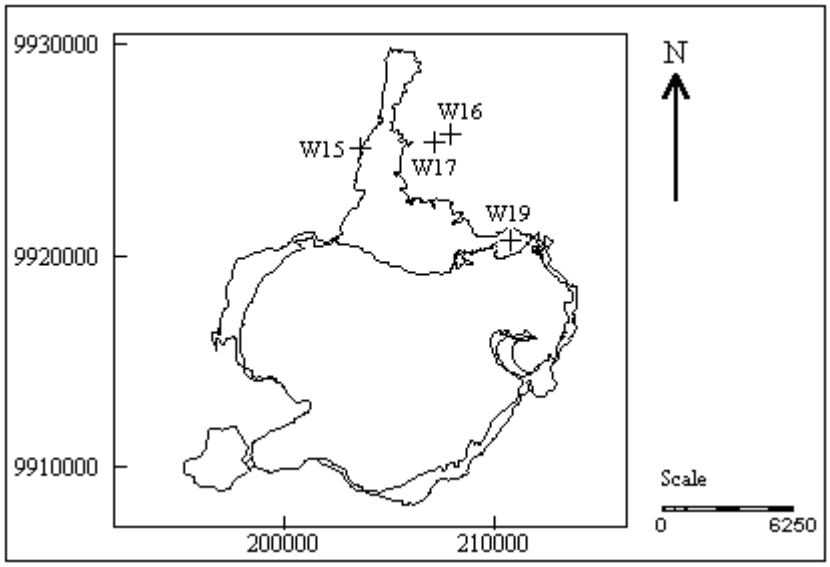


**Figure 3-14** ***Map showing position of the wells***

### 3.1.9 Acacia Forest

*Acacia xanthophloea* Benth., commonly known as Fever Tree or Naivasha Thorn, is a large tree reaching about 25 m height, gregarious in high ground water areas, between 600 to 2000 m often in black cotton soil. Acacia forest occupies big area in the north of the lake (figure 2-3). The faster growing properties of the acacia trees in the study area can be attributed to the shallower groundwater table from which the rooting system can find a shorter and easiest way of extracting the water necessary for the growth.

| Type | Coverage (%) | Theoretical water consumption(mm/d) | Remarks |
|---|---|---|---|
| Acacia | 50 | 6.3 | Can go up 15 m height |
| Xantho Pholea | 15 | 1.5 | Smaller than acacia |
| Eurphobia | 10 | 1.5 | |
| Eucalyptus | 10 | 4.0 | |
| Non-wood | 15 | 1.0 | |

**Table 3-11** ***Tree types in the Naivasha catchment with their coverage and theoretical water consumption (source: Naivasha Forestry Department and (Calder, 1996) adopted from Salah 1999***

In the study area (Rift floor) where semi arid condition exist, rainfall is low but the acacia trees are green throughout the year therefore the only source of water that makes the trees to survive is groundwater. A number of soil profiles was done during the fieldwork to find the depth of the acacia roots. The acacia roots were found up to12 m depth. The water table ranges from 3 to 12 m(**Appendix 3-J)**

#### 3.1.9.1 Evapotranspiration from acacia forest

The average evapotranspiration for the forest calculated by (Mekonnen1999) was 4.0 mm/day. Evapotranspiration value for acacia forest, calculated by (Farah 1999) was 5.0 mm/day. Therefore the amount of evapotranspiration was estimated by using this data.

### 3.1.10 Groundwater Abstraction

Groundwater abstraction for irrigation was determined both by TM image, aerial photographs and fieldwork. Water is abstracted for the irrigation of vegetables, flowers, maize and grass, also for domestic use, industry and cattle. Groundwater abstractions for domestic purposes are minor comparing to that abstracted for irrigation. By using ILWIS program the area under irrigation, which is visible in a False Colour Composite of TM image was digitized and the area that was mapped during fieldwork was also included in a digitized map. Area-numbering operation was used to obtain the area, by using Histogram operation, total area irrigated as for October 1999 was calculated and found to be 5 $km^2$.

The rate of depth of irrigation was estimated to be 1000 mm/year.

Therefore amount of abstraction was calculated using the formula;

**Abstraction rate ($m^3$/day) = area of irrigated land * depth of irrigation.**

# 4 CHAPTER FOUR

## 4.1 GROUNDWATER FLOW MODELLING

### 4.1.1 Introduction

A model is any device that represents an approximation of a field situation (Anderson & Woessner 1992). In recent years groundwater modelling has become a major part of many projects dealing with groundwater exploitation, protection, and remediation. There are two areas of hydrogeology where we need to rely upon models of real hydrogeologic system: to understand why a flow is behaving in a particular observed manner and to predict how a flow system will behave in future (Fetter 1994).

### 4.1.2 Numerical model

Numerical model is the most commonly used form of groundwater water modelling analysis. The model describe the entire field of interest at the same time, providing solutions for as many as data points as specified by the user. The area of interest is subdivided into many small areas (cells or elements) and a basic groundwater flow equation is solved for each cell usually considering its water balance (water inputs and outputs). The solution of a numerical model is the distribution of hydraulic heads at points representing individual cells. The basic differential flow equation for each cell is replaced (approximated) by an algebraic equation so that the entire flow field is represented by x equations with x unknowns where x is the number of cells.

Numerical models are often selected for application in a detailed modelling study because they can simulate a more realistic and detailed picture of the site. The predicted results are correspondingly more specific and reliable (Spitz et. al 1996)

The steps taken to prepare a realistic site –specific model are shown in figure 1-4

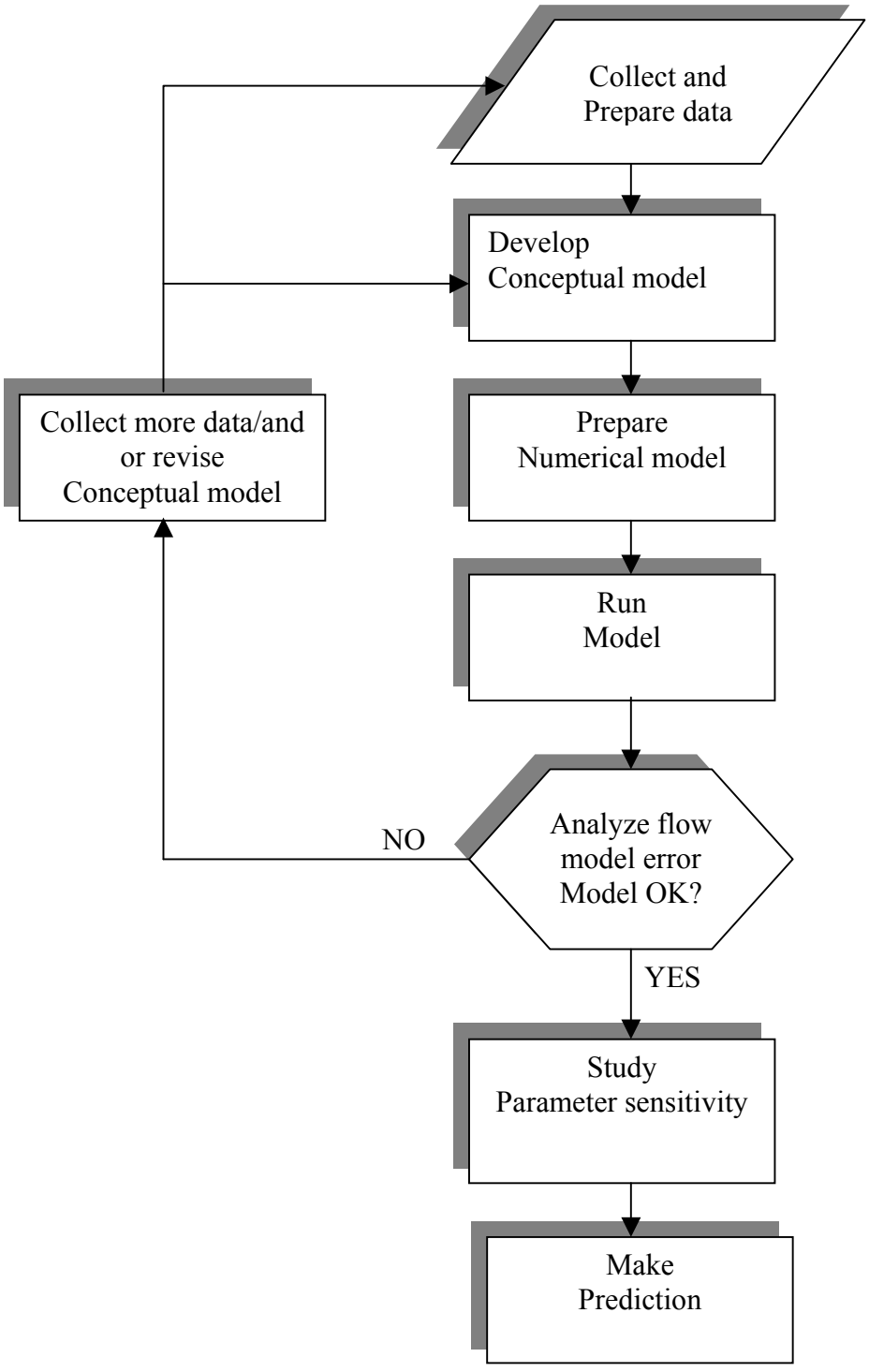


**Figure 4-1** ***The groundwater modelling process.***

### 4.1.3 Compiling Data

The first step of a model study consists of collecting and evaluating relevant data on the flow system under investigation. Typical model data input are:

#### 4.1.3.1 Physical framework

| | |
|---|---|
| Aquifer type | Topography |
| | Geology |
| | Stratigraphy |
| | Aquifer geometry |
| | Lithological variation within the aquifer |
| Aquifer characteristic | hydraulic conductivity/anisotropy |
| | Porosity |
| | Specific yield |
| | Specific storage |
| Aquifer boundaries | Location |
| | Constant head boundary |
| | Constant flow boundary |
| | Semipermeable boundary (Leakage factor, head in adjacent system) |

### 4.1.4 Model design

#### 4.1.4.1 Conceptual model

A conceptual model is a pictorial representation of the groundwater flow system, frequently in the form of a block diagram or a cross section (Anderson & Woessner 1992). Conceptual models are static. They describe the present condition of system (Fetter 1994). The nature of the conceptual model will determine the dimensions of the numerical model and design of the grid. The purpose of building a conceptual model is to simplify the field problem and organize the associated field data so that the systems can be analyzed more readily.

Key elements of the conceptual model are defining the model boundaries, simplifying the aquifer system, and determining the required model dimension to produce meaningful conclusion.

#### 4.1.4.2 Selecting model boundaries

A model boundary is the interface between the model calculation domain and the surrounding environment. Boundaries occur at the edges of the model domain and at the points where external influences are represented, such as rivers, wells and so forth.

### 4.1.5 Selection of the Model and Discretization

#### 4.1.5.1 Computer code

A Processing Modflow for Windows (PMWIN*)* was used. Is *a* simulation system for modelling groundwater and transport processes with modular three-dimensional finite-difference ground-water flow model developed by the U.S. Geological Survey (USGS) is a computer program for simulating common features in ground-water systems (McDonald and Harbaugh, 1988; Harbaugh and McDonald, 1996*)*. Is considered by many to be the most reliable, verified and utilized groundwater flow model available (Kresic 1997).

#### 4.1.5.2 Governing equation

The flow of fluids through media is governed by the laws of physics. As such it can be described by differential equations. Since the flow is a function of several variables, it is usually described by partial differential equations in which the spatial coordinates, $x$, $y$, $z$, and $t$, are the independent variables. In deriving the equations, the law of conservation for mass and energy are employed. Based upon these principles and Darcy's law, the main equations of groundwater flow have been derived.

MODFLOW utilizes a numerical solution for the governing groundwater flow

through porous media:

$$\frac{\partial}{\partial_x}\left(k_{xx}\frac{\partial h}{\partial x}\right)+\frac{\partial}{\partial_y}\left(k_{yy}\frac{\partial h}{\partial y}\right)+\frac{\partial}{\partial z}\left(k_{zz}\frac{\partial h}{\partial z}\right)-w=s_s\frac{\partial h}{\partial t} \qquad \textbf{Equation 4-1}$$

Where $K_{xx}$, $K_{yy}$, and $K_{zz}$ are values of hydraulic conductivity along the $x$, $y$, and $z$ coordinate axes, which are assumed to be parallel to the major axes of the hydraulic conductivity ($Lt^{-1}$):
$h$ is the potentiometric head (L);
$W$ is a volumetric flux per unit volume and represents sources and/or sinks of water ($t^{-1}$):
$S_s$ is the specific storage of the porous material ($L^{-1}$): and
$t$ is time

### 4.1.6 Model geometry

Model geometry defines the size and shape of the model. It consists of model boundaries, both external and internal, and model grid.

#### 4.1.6.1 Initial Conditions

The initial conditions describe the distribution of the heads throughout the model domain at the start of the simulation. Error in initial conditions will propagate through a transient solution, causing unrealistic predictions. The initial conditions for the steady state simulation are important mainly to save computational effort in reaching a solution. However, the initial conditions for a transient problem strongly influence the predicted results.

#### 4.1.6.2 Model Parameter

Model parameter are divided into three groups:

- Time
- Space (layer top and bottom)
- Hydrogeologic characteristics (hydraulic conductivity, transmissivity, storage parameters, and effective porosity)

##### 4.1.6.2.1 Time

Two kinds of time interval are used in models: stress periods (during which boundary conditions are constant and between which boundary conditions vary) and time steps (during which model calculations are made). Time parameters are specified when modelling transient conditions. Factors affecting choice of time step include stability considerations, time variation of boundary conditions and time related modelling

objectives. In general, the smaller the time steps, the more accurate are the predicted results.

### 4.1.7 Model Run

After all model parameters are correctly assigned to each cell, the solving packages (solvers) are chosen, specification of several calculation parameters and models to be saved are also chosen. Common for the solvers are the head change criterion for convergence and the maximum allowed number of iterations. When the maximum absolute value of hydraulic head change in any model cell is less than or equal to the head change criterion, the iteration stops. MODFLOW solvers are the Strongly Implicit Procedure (SIP), the Slice-Successive Overrelaxation method (SSOR), and the Preconditioned Conjugate-Gradient 2 method (PCG2).

### 4.1.8 Calibration

A model is initially calibrated by taking the initial estimates of the model parameters and solving the model to see how well it reproduces some known condition of the aquifer. Model calibration can be performed to steady-steady or transient data sets (Anderson & Woessner 1992). Most models are initially calibrated against the steady state groundwater heads. A water-table or potentialmetric-surface map is required for this type of calibration. As this is almost always known with better accuracy than the distribution of aquifer parameters and /or amount of recharge are varied until the model closely reproduce the known water-table or potentialmetric-surface condition. Input data and comparison of simulated and measured values can be altered either manually (trial and error adjustment) or automatically (inverse or parameter estimation models) which is known as PEST in MODFLOW.

#### 4.1.8.1 Evaluating the Calibration

The results of the calibration should be evaluated both qualitatively and quantitatively. The model evaluation should use as many pieces of information as possible.

#### 4.1.8.2 Traditional Measures of Calibration

Comparison between contour maps of measured and simulated heads provides visual, qualitative measure of similarity between patterns, there by giving some idea of spatial distribution of error calibration. A scatter plot of measured against simulated heads is another way of showing the calibrated fit. Deviation of points from the straight line should be randomly distributed
A listing of measured and simulated heads together with their differences and some type of the differences are common way of reporting calibration results.

### 4.1.9 Sensitivity Analysis

Sensitivity analysis helps to rank the input data in terms of its influence on the model prediction and gives the answer to “what if” questions. Sensivity analysis also allows one to assess unforeseeable groundwater stresses in the future. Sensivity analysis is performed by changing one parameter at a time.

## 4.2 TWO-LAYER STEADY-STATE MODEL

### 4.2.1 Model boundaries

The limit of the area included in the model is shown in (Figure 4-3) and was based on geological consideration as explained below;

#### 4.2.1.1 Constant head boundary

The lake, which covers large part on the south of the model area, forms a natural boundary prescribing the heads.

#### 4.2.1.2 Boundary Flux

##### 4.2.1.2.1 Inflow boundaries

In the south-east, the low permeability volcanic material forms a low flux boundary simulated recharge from the scarp. Water enters the model area through the second aquifer.

##### 4.2.1.2.2 Outflow boundaries

Water flows out of the model area in the western part, simulated abstraction from the aquifer. Water flows out of the model area through the second aquifer.

##### 4.2.1.2.3 No flow boundary

North and northeast were simulated in the model as no-flow boundaries. This was because the transmissivity of volcanic material are several orders of magnitude less than that of sediments.

### 4.2.2 Model geometry

#### 4.2.2.1 Model Description

The model area is about 185 $km^2$. The model uses different grid sizes of 200 m by 200 m, 200 m by 100 m, 200 m by 50 m, 100 m by 100 m, 100 m by 50 m and 50 m by 50 m. Contains 157 columns and 211 rows in two-layer. The irregular shape of the study area reduced the number of active cells in the model. Small grids were chosen for the areas with strong groundwater extraction.

#### 4.2.2.2 Conceptual model

The conceptual model is relatively simple and consists of two hydrostratigraphical units. The model represent the aquifer using two layers with layer one containing a lake and the aquifer of variable thickness (0 to 50 m) deep, where clays, diatomite, silts and fine-grained sands are dominant. The second layer, which is highly permeable (reworked volcanics or weathered contacts between different lithological units), has been given an average thickness of 10 m, both layers were modelled using

confined aquifer hydraulic properties Confining units between aquifers are not included as separate layers. Instead, vertical leakance values are calculated by the model for the cells in each aquifer layer to represent hydraulic connections between adjacent layers. Hence, horizontal flow through the aquifers is represented by flow within each layer, and vertical flow between aquifers is represented by flow between adjacent layers (Figure 4-2).

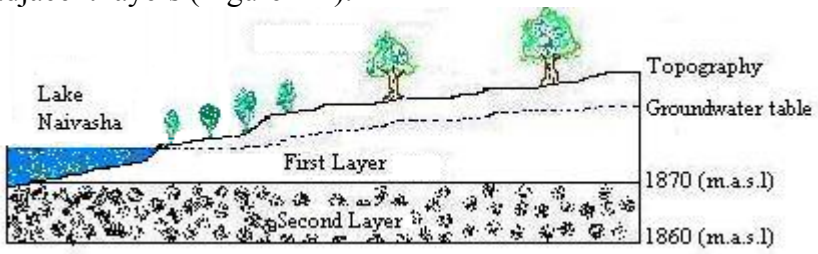


**Figure 4-2** ***Conceptual model of the study area***

### 4.2.3 Selecting Model Input Data

The input data have been selected as follows:

#### 4.2.3.1 Transmissivity

The hydraulic properties of the aquifer were obtained from pumping test and from previous studies. The data indicate the transmissivity for the upper layer is quite low and has been evaluated to be less than 50 $m^2$/ day. The lake has been assigned a transmissivity value of 10,000 $m^2$/d. The second layer has been divided into seven transmissivity zones (figure 4-3) in order to achieve a reasonable fit between observed and simulated heads. The transmissivity values have been assigned according to the pumping test data where possible.

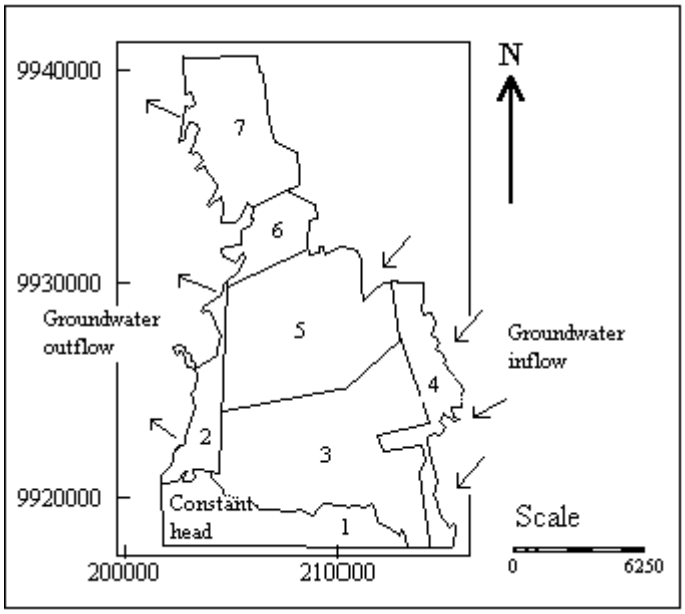


**Figure 4-3** ***Transmissivity zones and boundary conditions.***

#### 4.2.3.2 Vertical Hydraulic Conductivity

The vertical hydraulic conductivity for the first layer has been set two 0.25 m/day, average value from auger hole results. The second layer has been assigned a value of 1 m/day.

#### 4.2.3.3 Recharge

Recharge to the model was applied to the top-most active cell in each vertical column. Uniform recharge over the entire area was first assumed, but it became evident that it was impossible to achieve an acceptable fit. Recharge zones were then considered as a function of the sediment thickness, where by thick sediments were given higher recharge than thin sediments. In the north of the study area sediments thickness is less than ten metres therefore it was considered to have less recharge comparing to the southern part. For that reason half of the amount of recharge in the south was put as recharge value in the north. The area was divided into four-recharge zones. No recharge was put in the acacia forest and lake, because the lake was modelled as constant head.

#### 4.2.3.4 Evapotranspiration

Evapotranspiration was included in a model using recharge package by assigning a negative value. Evapotranspiration for acacia was taken as 5 mm/day, considering an average rainfall of 2 mm/day a value of 3 mm/day was used in a model.

#### 4.2.3.5 Groundwater Inflow and outflow

Inflow into the aquifer was estimated from the percentage of average yearly precipitation. The estimate of the amount of outflow was obtained by calculation according to Darcy's law by using the hydraulic gradient and the transmissivity which are known along the boundary.

Darcy's equation;

$Q = TiL$

where

Q = Subsurface outflow
T = Transmissivity of the aquifer
i = Groundwater table gradient
L = Length of the outflow section, normal to the direction of groundwater outflow.

#### 4.2.3.6 River Package

Rivers Malewa and Gilgil are loosing water to the aquifer. The rate of water loss is a function of the depth of the water and the hydraulic conductivity of the underlying alluvium (Fetter, 1994). The hydraulic conductivity was measured during fieldwork

and was found to be in order of 0.1 to 0.38 m/day. Therefore the river package was used to model the Malewa and Gilgil Rivers.

### 4.2.4 Model Calibration

The groundwater flow model was calibrated by adjusting model-input data and model out put so that model results matched field observations within the acceptable level of accuracy. Parameters changed during the calibration process include transmissivity and recharge rates. After each change in one of the parameters, the simulation was run and simulated groundwater levels were compared to observed groundwater level.

#### 4.2.4.1 Steady –state calibration

The steady-state calibration was performed to simulate heads in the aquifer prior to heavy pumping. The calibration was necessary in order to obtain historical piezometric surface, confirm the conceptual model of groundwater flow, obtain approximate transmissivity and recharge values for transient calibration.

The calibration was carried by trial and error on estimated pre heavy pumping condition of the groundwater system. The collected data prior to 1970 provided an estimate of the head distribution under relatively undisturbed condition (Figure 4-4). Since before 1970 there were few drilled wells which were mainly used for domestic purposes. Heavy groundwater pumping started on early 1970's in the area, the piezometric surface of before 1970's was assumed a reasonable estimate of the average undisturbed piezometric surface prior to heavy pumping. The average lake level was taken as 1888 m.a.s.l. The model was calibrated to reproduce observed heads by varying transmissivity and recharge.

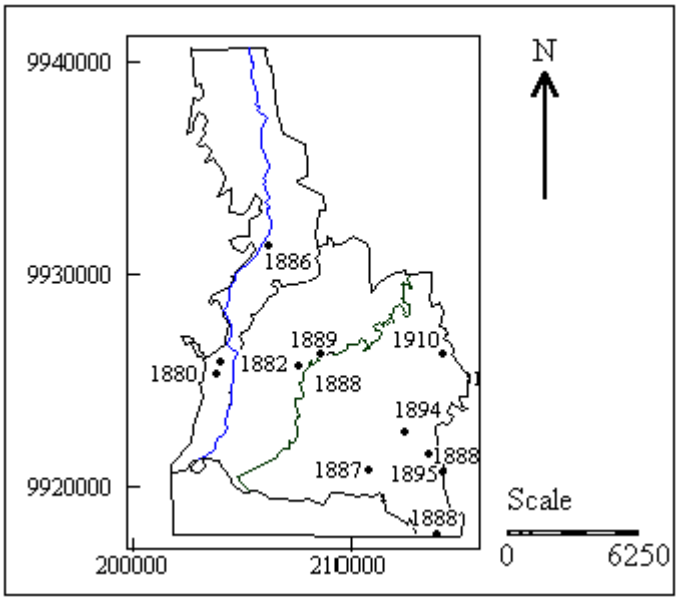


**Figure 4-4** ***Water level points prior 1970 in m.a.s.l.***

### 4.2.5 Model Running

During modelling the effect of 3 mm /day of evapotranspiration from acacia forest on water level was anomalous. In the center of the forest area the simulated water levels were in order of 30 m lower than the observed one (table 4-1). This shows that the evapotranspiration cannot be so high or rather transmissivity value must be high. Therefore the evapotranspiration from acacia forest was removed from the model and replaced by (zero) 0 mm/day recharge, implying that no recharge to groundwater as all precipitation is taken by acacia trees. Considering model results may be acacia trees abstract less than 3 mm/day of water from groundwater.

| ITC_ Number | C_Number | Observed Heads (m.a.s.l) | Observed Heads (m.a.s.l) | Simulated heads (m.a.s.l) | Difference between Observed and simulated heads (m) |
|---|---|---|---|---|---|
| N23 | | 1880 | 1880 | 1854.285 | 25.715 |
| N24 | | 1882 | 1882 | 1851.531 | 30.469 |
| ITC082 | | 1886 | 1886 | 1837.533 | 48.467 |
| ITC027 | | 1888 | 1888 | 1854.134 | 33.866 |
| ITC045 | C54 | 1889 | 1889 | 1854.842 | 34.158 |
| ITC043 | C3292 | 1887 | 1887 | 1880.166 | 6.834 |
| ITC076 | C3929 | 1894 | 1894 | 1877.378 | 16.622 |
| ITC074 | C3929 | 1888 | 1888 | 1881.62 | 6.38 |
| ITC156 | C4155 | 1888 | 1888 | 1886.227 | 1.773 |
| ITC083 | C4157 | 1910 | 1910 | 1882.436 | 27.564 |
| ITC084 | | 1895 | 1895 | 1887.356 | 7.644 |

**Table 4-1** ***Observed and simulated heads calibration with 3mm/day evapotranspiration for acacia forest***

The results were also presented in form of groundwater contours together with observed heads (figure 4-5), it clearly shows that water flows away from the lake, the case which is unrealistic.

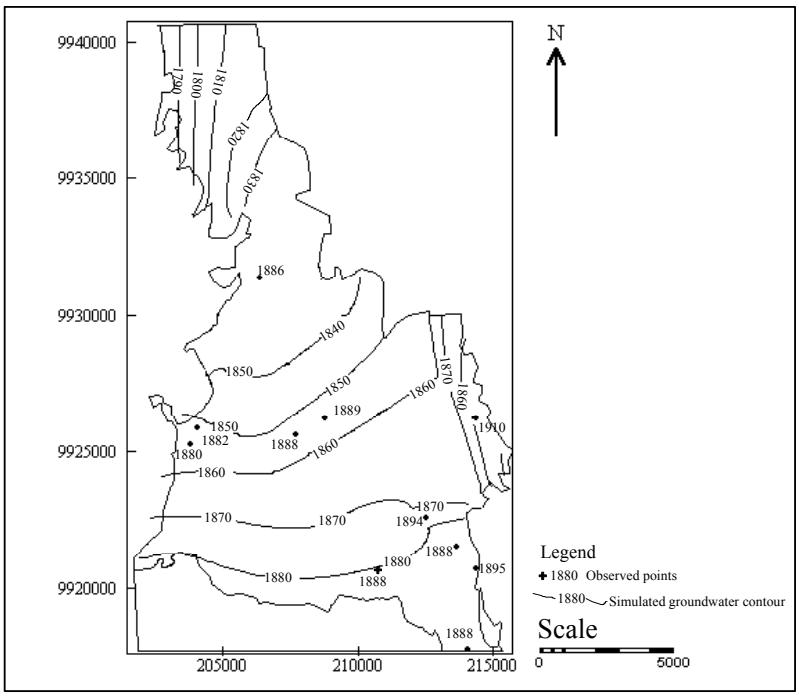


**Figure 4-5 Simulated heads contours calibration with 3mm/day evapotranspiration for acacia forest**

### 4.2.6 Simulation results

#### 4.2.6.1 Transmissivity

The transmissivity values that reproduced reasonable heads were later on found to be 5 $m^2$/day for the first layer and for the second layer the values are as indicated in the map (figure 4-6)

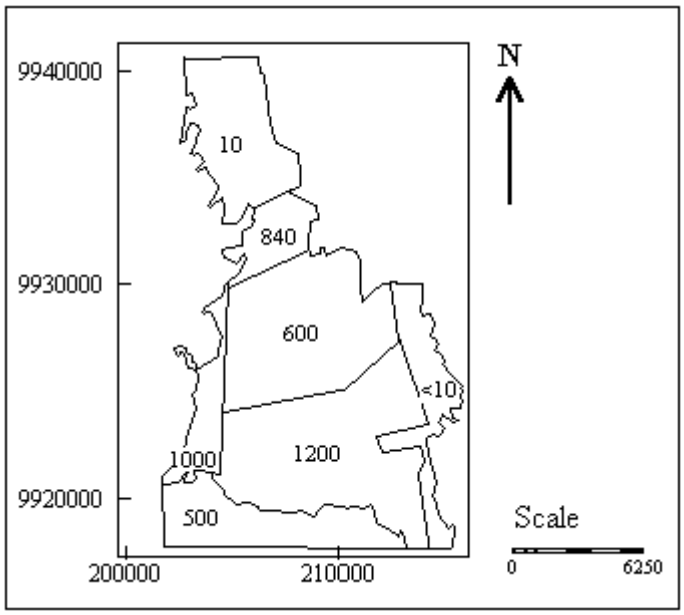


**Figure 4-6** ***Transmissivity zones with their respective transmissity values in $m^2$/day for the second layer.***

### 4.2.6.2 Recharge

Simulated groundwater recharge is 52 mm/year for the thick sediments (thickness > 10 m) and 25 mm/year for the thin sediments, that is 8 percent and 4 percent respectively of the annual precipitation of 650 mm (Figure4-7).

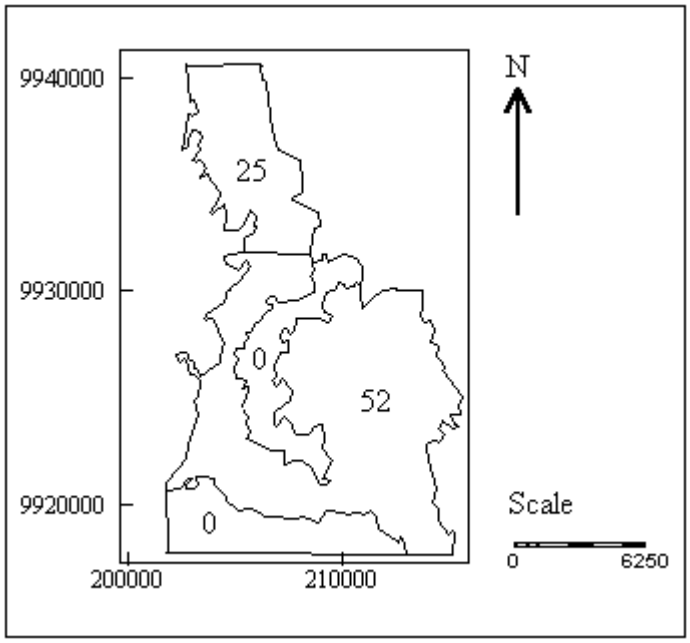


**Figure 4-7** ***Recharge zones with their respective recharge values in mm/year***

#### 4.2.6.3 Groundwater inflow and outflow

The amount of inflow that reasonable fit the observed heads was taken to be 5 percent of average annual rainfall of 650 mm/year. The results for water budget components derived from the calibrated model are presented in (table 4-2)

| Flow Term | In | Out | In-Out |
|---|---|---|---|
| Constant Head | 14968.01 | 12721.01 | 2247.001 |
| Wells | 484.1417 | 21082 | -20597.9 |
| Recharge | 18014.02 | 0 | 18014.02 |
| River Leakage | 337.7216 | 0.018086 | 337.7035 |
| Sum | 33803.88 | 33803.03 | 0.859375 |

**Table 4-2** ***Simulated water balance for the modelled area. Values are in $m^3$/day.***

### 4.2.7 Calibration Evaluation

The results of the calibration were evaluated both qualitatively and quantitatively as follows;

#### 4.2.7.1 Scatter Plot

The model was considered to be calibrated when observed and simulated heads in the scatter plot showed a reasonable fit and points in the straight line were randomly distributed (figure 4-8).

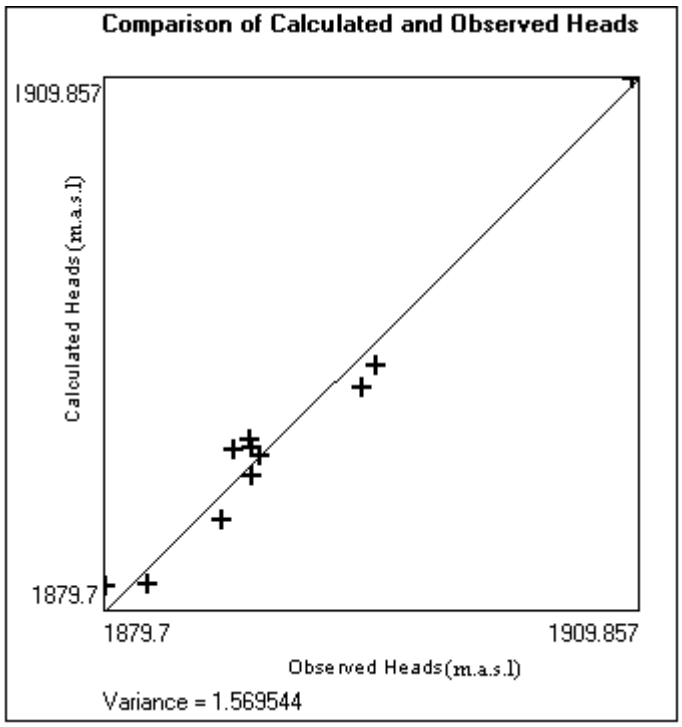


**Figure 4-8** ***A scatter plot of observed and simulated heads (m.a.s.l)***

### 4.2.7.2 Heads

The difference between observe and simulated heads was also evaluated, when the difference between observed and simulated heads was in order of ±2 the model was considered calibrated (Table 4-3).

| ITC_number | C_Number | UTM_X | UTM_Y | Observed Heads (m.a.s.l) | Simulated Heads (m.a.s.l) | Difference Between Observed and simulated (m) |
|---|---|---|---|---|---|---|
| ITC027 | | 207680 | 9925645 | 1888 | 1887.271 | 0.729 |
| ITC043 | | 210769 | 9920726 | 1887 | 1888.836 | -1.836 |
| ITC045 | C54 | 208741 | 9926237 | 1889 | 1888.451 | 0.549 |
| ITC074 | C3292 | 213600 | 9921500 | 1888 | 1889.423 | -1.423 |
| ITC076 | C3299 | 212463 | 9922555 | 1894 | 1892.369 | 1.631 |
| ITC082 | C3929 | 206306 | 9931350 | 1886 | 1884.823 | 1.177 |
| ITC083 | C4155 | 214310 | 9926240 | 1910 | 1909.857 | 0.143 |
| ITC084 | C4157 | 214313 | 9920708 | 1895 | 1893.533 | 1.467 |
| ITC156 | | 214009 | 9917763 | 1888 | 1888.96 | -0.96 |
| N23 | | 203786 | 9925304 | 1880 | 1881.08 | -1.08 |
| N24 | | 204040 | 9925879 | 1882 | 1881.229 | 0.771 |

**Table 4-3** ***A list of observed and simulated heads together with their differences.***

### 4.2.7.3 Map of Observed and simulated heads

The observed and simulated heads were also plotted in the same map so as to see clearly the deviations. The simulated heads are presented in italics.

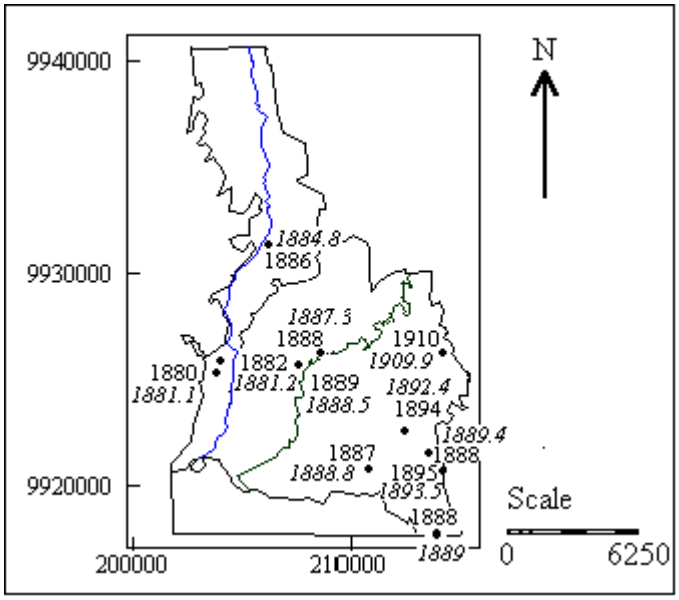


**Figure 4-9** ***Observed and simulated (in Italics) heads in m.a.s.l.***

#### 4.2.7.4 Head residuals

Difference between observed and simulated heads were also represented in the map, positive value means simulated head is lower than observed head. Likewise negative value means simulated head is higher than observed head.

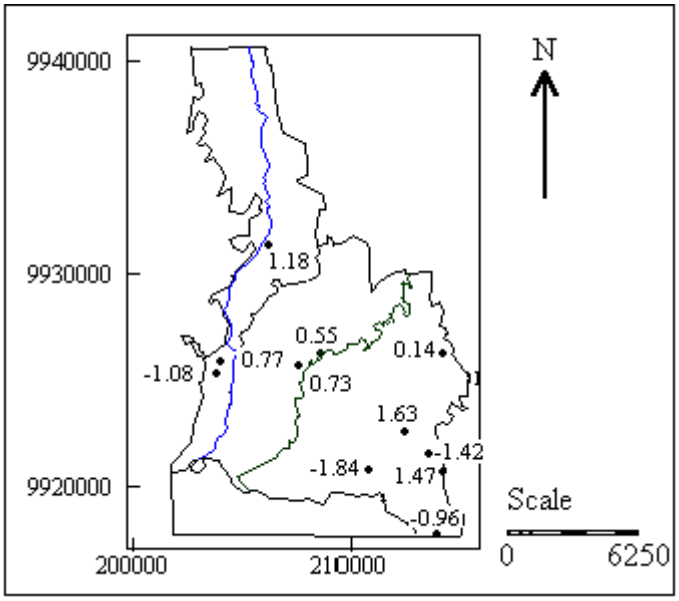


**Figure 4-10** ***Map showing head residuals.***

#### 4.2.7.5 Graphical Representation

Observed and simulated heads were plotted in the same graph to see the relationship between them.

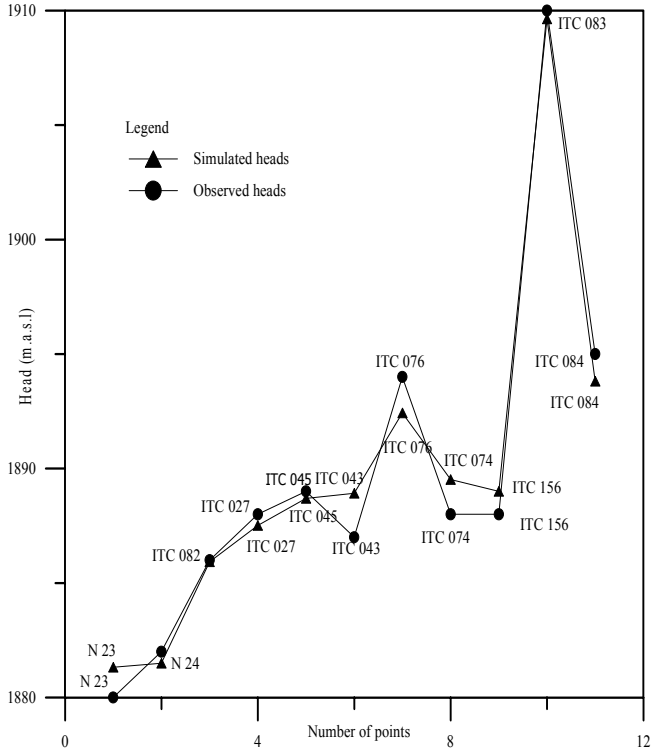


**Figure 4-11** ***Observed versus simulated heads.***

### 4.2.7.6 Contour map of simulated heads

Simulated heads were also Contoured and plotted together with the observed heads (Figure 4-12)

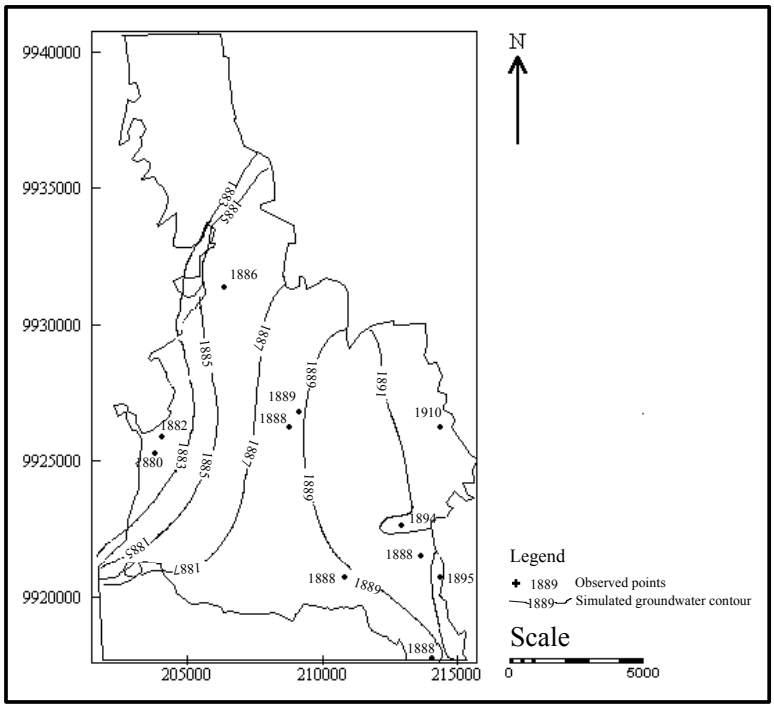


**Figure 4-12 Groundwater contour of simulated heads (m.a.s.l), contour interval 3m.**

#### 4.2.7.7 The root mean squared (RMS)

The average of differences was used to quantify the average error in the calibration. The RMS was used, which is the average of the squared differences in observed and simulated heads.

The model accuracy was calculated using the RMS between observed and model simulated head. Model accuracy is increased by minimizing the RMS errors. The RMS error measures the absolute value of the variation between observed and simulated heads. The RMS of the simulated heads is 1.17 m calculated according to the formula:

$$RMS = \left[ 1/n \sum_{i=1}^{n} (h_m - h_s) i^2 \right]^{0.5}$$ **Equation 4-2**

Where

$h_m$ = observed heads
$h_s$ = simulated heads

## 4.3 THREE-LAYER TEST MODEL

### 4.3.1 Introduction

In two-layer model the lake has been modelled by using a constant head condition to represent the average lake level. However, lake levels often show long and short term transient as explained in section 3.1.7.1. Lake Naivasha contributes water to the groundwater system or drains water from it depending on the head gradient between them. Such water exchange affects lake levels and groundwater heads. Lake level fluctuations result in changes in hydraulic gradient between the lake and groundwater even if groundwater heads remain the same. The changes in hydraulic gradient, in turn, lead to changes in the water exchange between the lake and the groundwater system. Therefore, unless a groundwater flow model incorporates lake level fluctuations it will not predict groundwater heads near a lake accurately. For this reason an attempt was made to model the lake the way it is behaving, by creating a three-layer model.

### 4.3.2 Model Geometry

#### 4.3.2.1 Model Description

A simple three-layer test model was created with uniform grid size of 100 m by 100 m, covers an area of 25 $km^2$. The system was discretized into 50 rows and 50 columns in three layers without inactive cells. First layer represents the lake and two layers represent the aquifers.

#### 4.3.2.2 Conceptual model

The first layer was pseudo (fake) layer, which represents the lake only, its top was set to 2000 m.a.s.l., which is relatively high than the normal topography of the area. The bottom of the lake layer was the topography. The second layer was modelled using unconfined/confined aquifer hydraulic properties of variable thickness (0-50) m deep where clays, diatomite, silts and fine-grained sands are dominant. The bottom of the layer was set to 1870 and the transmissivity was constant. The third layer was modelled as confined aquifer with constant transmissivity and uniform thickness of 10 m, its bottom was set to 1860 (Figure 14-13).

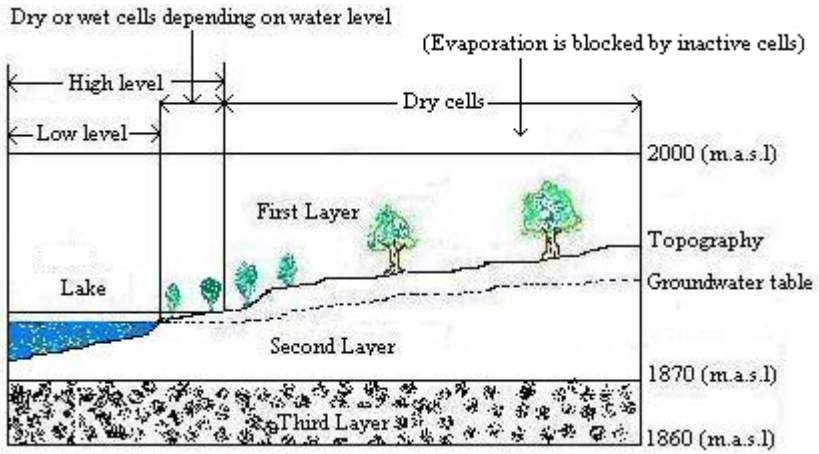


**Figure 4-13** ***The conceptual model of the test model***

### 4.3.3 Selecting Model Input Data

The input data have been selected as follows:

#### 4.3.3.1 Transmissivity

The first layer was given very high transmissivity of $10^6$ $m^2$/day, the second layer was assigned a transmissivity of 0.1 $m^2$/day and the third layer a uniform transmissivity of 1000 $m^2$/day. With high transmissivity in the first layer made all cells that do not belong to the lake to become dry.

#### 4.3.3.2 Horizontal Hydraulic conductivity

The first layer was given hydraulic conductivity of $10^6$ m/day, the second layer was assigned a value of 1 m/day and the third layer a value of 0.1 m/day.

#### 4.3.3.3 Recharge

A recharge value of 0.0001 m/day was applied to the aquifer.

#### 4.3.3.4 Evaporation From the lake

A value of 3 mm /day was used in the model as an average lake evaporation.

#### 4.3.3.5 Inflow into the lake

The amount of inflow was put by using injection wells. In transient mode different reasonable amount of inflows were put in the model, by considering the climatic conditions in the study area.

#### 4.3.3.6 Outflow

Discharge wells were used to simulate outflow from the lake. As the amount of outflow is not constant reasonable values were used, in transient simulation.

### 4.3.4 Model run in steady-state condition

The model was first run in steady state. Due to high transmissivity of first layer all cells which do not belong to Lake went dry and automatically the model considered them as inactive.

#### 4.3.4.1 Wetting Capability Package

The package was used to make sure that the cells that belong to the lake could be turned into wet or dry cells depending on the amount of inflow into the lake, which also determine the lake level. A cell falls dry when the head is below the bottom elevation of the cell. When the cell falls dry MODFLOW turns it to inactive. No water can flow into the cells as the simulation proceeds and the cell remains inactive. To overcome this problem a wetting capability package was used, in which a value THRESH, called wetting threshold is used to decide whether a dry or an inactive cell can be turned into a wet (active) cell.

Therefore the wetting threshold (THRESH) in the first layer was set to >0 so that the cell below a dry cell and the four horizontally adjacent cells can cause the cell to become wet, this was done in order to keep lake cells wet or dry depending on the lake level. The equation used was;

$H = BOT + WETFCT(hn - BOT)$

Where;
hn is the head at the neighbouring cell that causes the dry cell to wet.
WETFCT is a user-specified constant called the wetting factor.

The heads obtained in steady-state were used as initial heads for the transient model.

There was no problem of model converges. The model worked perfectly.

### 4.3.5 Model run in transient condition

After running the model in steady state, it was then switched to transient condition, by applying the heads obtained in steady-state as the initial heads.

#### 4.3.5.1 Storage coefficient

The storage coefficient was set to 0.0001 for second and third layer.

#### 4.3.5.2 Specific yield

The first layer was assigned the value of 1 and the second layer was given the value of 0.25.

### 4.3.6 Discussion

Due to different amount of water flowing into the lake the rise and lowering of the lake level could be observed. When the amount of inflow increased some dry cells became wet and when the amount of inflow decreased they became dry, as indicated in figure 4-13.

The lake level increased when the amount of inflow increased and the lake level decreased when the inflow decreased as shown in figure 4-14. For that matter the lake surface area also changed this was clearly observed in the model.

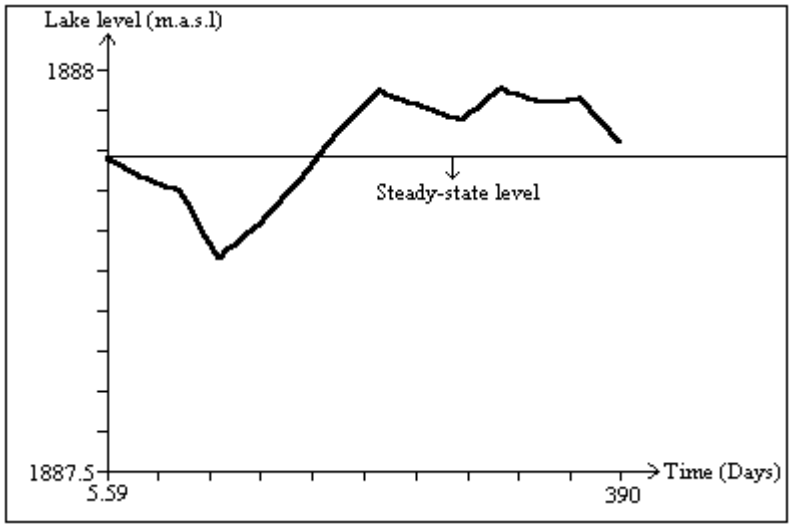


**Figure 4-14** ***The lake level fluctuation as a result of changes in the amount of in and out flow in the lake.***

### 4.3.7 Conclusion

The three-layer model incorporates evaporation from the lake surface, inflow from runoff and rivers. These flow components affect lake levels and changes in these components lead to lake level fluctuations. The three-layer test model worked properly, there was no problem of model convergence. From the basis of this test model the two-layer model of the study area was changed into three-layer model.

## 4.4 THREE-LAYER STEADY STATE MODEL OF THE STUDY AREA

On the basis of the three-layer test model the two-layer model of the study area was changed to a three-layer model as indicated in the figure 4-16.

### 4.4.1 Model Run

During model running the model didn't converge, changing of wetting threshold was done but still the model failed to converge. One reason for convergence failure was probably due to wetting capability package, "convergence problems can occur in MODFOLW even without the wetting capability package but problems are more likely to occur when the wetting capability is used. Symptoms of a problem are slow convergence or divergence combined with the frequent wetting and drying of the same cell" (Chiang and Kinzelbach, 1998). Another reason for the model failing to converge was probably the model size being large. Therefore decision was made to change the grid size of the model so as to reduce number of cells.

A new model was created with square grid of 500 m by 500 m. The model contains 32 columns and 48 rows in three layer Figure 4-15.

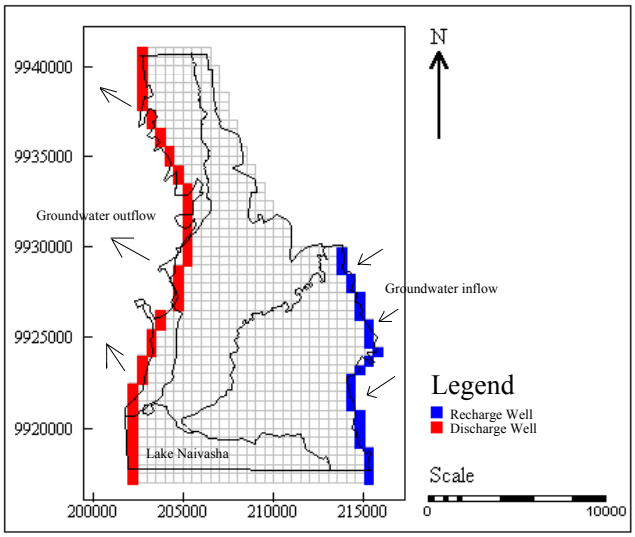


**Figure 4-15** ***Model grid and boundary condition.***

#### 4.4.1.1 Conceptual model

The three-layer conceptual model is as in figure 4-16.

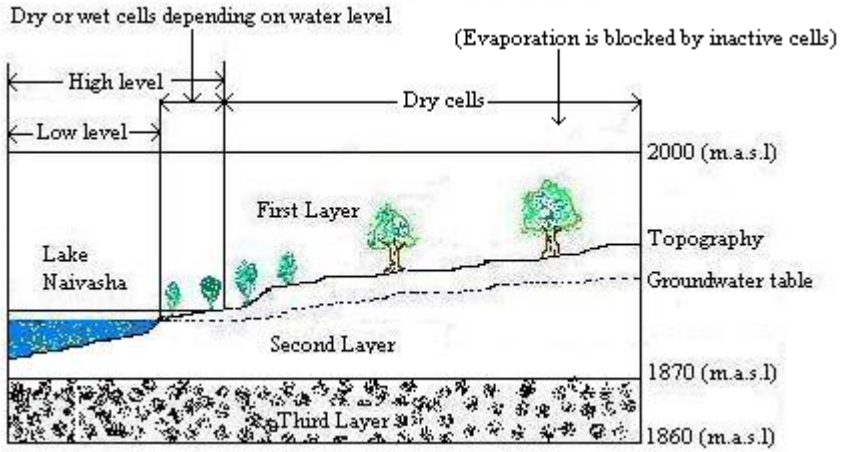


**Figure 4-16** ***Conceptual model of the study area***

### 4.4.2 Selecting Model Input Data

The input data have been selected as follows:

#### 4.4.2.1 Aquifer Parameters

##### 4.4.2.1.1 Transmissivity

The first layer, which represents the lake, has been assigned transmissivity of 1000,000 $m^2$/day.

The second layer was modelled by varying transmissivity making sure that the transmissivity doesn't exceed 50 $m^2$/day

The third layer has been divided into five transmissivity zones (figure 4-17). The transmissivity values have been assigned according to the pumping test data where possible. The zone on the southeast has been omitted in three-layer model in order to model only the aquifers around lake Naivasha. Groundwater levels around the lake are approximately between 1880 to 1890 m.a.s.l., similar to the lake itself (Clarke et. al., 1990). The zone omitted was used in the two-layer model for the purpose of having the picture of general groundwater flow direction.

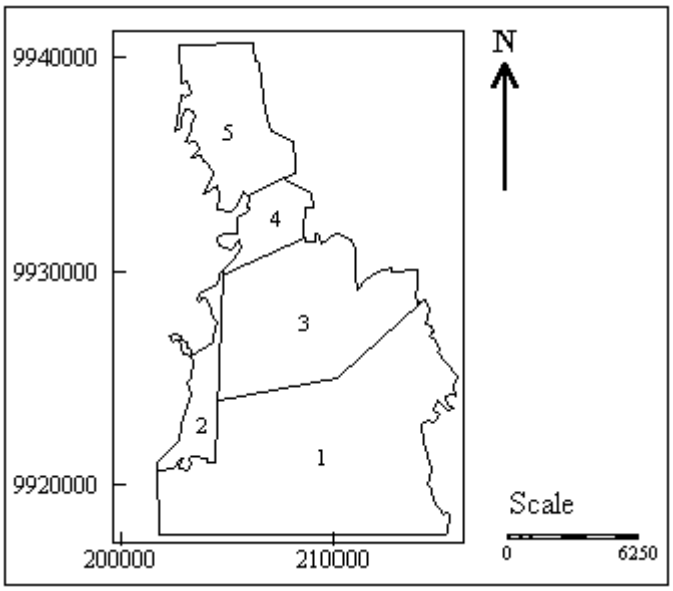


**Figure 4-17** ***Transmissivity zones***

4.4.2.1.2 Vertical Hydraulic Conductivity

The hydraulic conductivity values used in the model are 10,000 m/day for the lake, 1 m/day for the first aquifer and 100 $m^2$/year for the confined aquifer.

4.4.2.1.3 Recharge

The recharge to the model has been applied to the second layer. As in the first layer the inactive cell blocked the recharge.

### 4.4.2.2 Evapotranspiration

Evapotranspiration from acacia forest was included in a model. By trial and error different reasonable values were put with a purpose of matching the observed heads.

### 4.4.2.3 Evaporation from the lake

A value of 3 mm/day was used as average lake evaporation.

### 4.4.2.4 Groundwater Inflow and outflow

Inflow into the aquifer was estimated from the percentage of average yearly precipitation. The estimate of the amount of outflow was obtained by calculation according to Darcy's law by using the hydraulic gradient and the transmissivity which are known along the boundary.

#### 4.4.2.5 Inflow into the lake

A well package was used to put inflow in the lake the amount of inflow was estimated from the total lake inflow, as the modelled area includes only part of the lake. The amount of inflow into the lake differs according to climatic conditions, in wet years the amount of inflow is high therefore increases the lake level and the surface area. In dry years is the opposite.

#### 4.4.2.6 River Package

Rivers Malewa and Gilgil are loosing water to the aquifer. The rate of water loss is a function of the depth of the water and the hydraulic conductivity of the underlying alluvium (Fetter, 1994). The hydraulic conductivity was measured during fieldwork and was found to be in order of 0.1 to 0.38 m/day. Therefore a river package was used to model the Malewa and Gilgil Rivers.

### 4.4.3 Model Calibration

The groundwater flow model was calibrated by adjusting model-input data and model out put so that model results matched field observations within the acceptable level of accuracy. Parameters changed during the calibration process include transmissivity and evapotranspiration. After each change in one of the parameters, the simulation was run and simulated groundwater heads were compared to observed groundwater heads.

#### 4.4.3.1 Steady –state calibration

The steady-state calibration was necessary in order to obtain historical piezometric level, confirm the conceptual model of groundwater flow, and obtain approximate transmissivity, recharge, evapotranspiration and discharge values for transient calibration.

The calibration was carried by trial and error on estimated pre heavy pumping condition of the groundwater system. The collected data prior to 1970 provided an estimate of the head distribution under relatively undisturbed condition. Since before 1970 there were few drilled wells which were mainly used for domestic purposes. Heavy groundwater pumping started on early 1970's in the area, the piezometric level of before 1970's was assumed a reasonable estimate of the average undisturbed piezometric level prior to heavy pumping. The model was calibrated to reproduce observed heads by varying transmissivity and evapotranspiration.

##### 4.4.3.1.1 Model Running

During model running some of the lake cells were turning dry, therefore a wetting capability was used to prevent lake cells to become dry, as the purpose of three-layer model was to model the first layer as the lake. During modelling the *wetting factor* and *wetting threshold*, which are critical parameters, were changed for the purpose of convergence of the model.

### 4.4.4 Simulation results

#### 4.4.4.1 Wetting capability

The wetting threshold (THRESH) in the first layer was set to >0 so that the cell below a dry cell and the four horizontally adjacent cells can cause the cell to become wet, this was done in order to keep lake cells wet or dry depending on the lake level. The equation used was;

H = BOT + WETFCT(hn – BOT)

Where;
hn is the head at the neighbouring cell that causes the dry cell to wet.
WETFCT is a user-specified constant called the wetting factor.

Finally the THRESH was set to 2 and WETFCT to 0.5. The package also allows to specify the iteration interval for attempting to wet cells, this was set to 2.

#### 4.4.4.2 Transmissivity

The transmissivity values that reproduced reasonable heads were later on found to be 10 $m^2$/day for the first aquifer and for the third layer the values are as indicated in the map (figure 4-18)

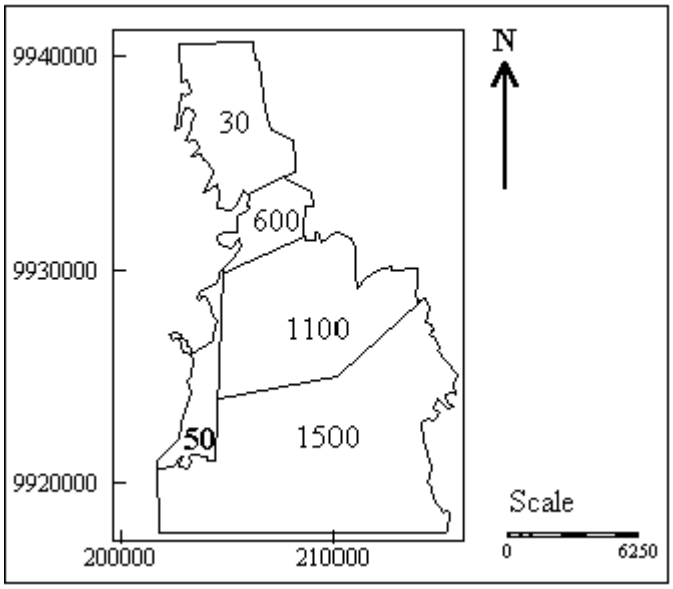


**Figure 4-18** ***Transmissivity zones with their respective transmissity values in $m^2$/day for the third layer.***

#### 4.4.4.3 Evapotranspiration

The simulated evapotranspiration that gave a reasonable fit between observed and simulated heads was 73 mm/year.

#### 4.4.4.4 Groundwater inflow and outflow

The amount of inflow and out flow that reasonable fit the observed are as indicated in the water balance of the whole model (table 4-4)

| Flow Term | In | Out | In-Out |
|---|---|---|---|
| Wells | 115785.8 | 13500 | 102285.8 |
| Recharge | 0 | 120000 | -120000 |
| Evapotranspiration | 22680 | 5000 | 17680 |
| River Leakage | 34.3464 | 0.59608 | 33.75031 |
| Sum | 138500.1 | 138500.6 | -0.47969 |

**Table 4-4** ***Simulated water balance for the modelled area. Values are in $m^3$/day.***

### 4.4.5 Calibration Evaluation

The results of the calibration were evaluated both qualitatively and quantitatively as follows;

#### 4.4.5.1 Scatter Plot

The model was considered to be calibrated when observed and simulated heads in the scatter plot showed a reasonable fit and points in the straight line were randomly distributed (Figure 4-19).

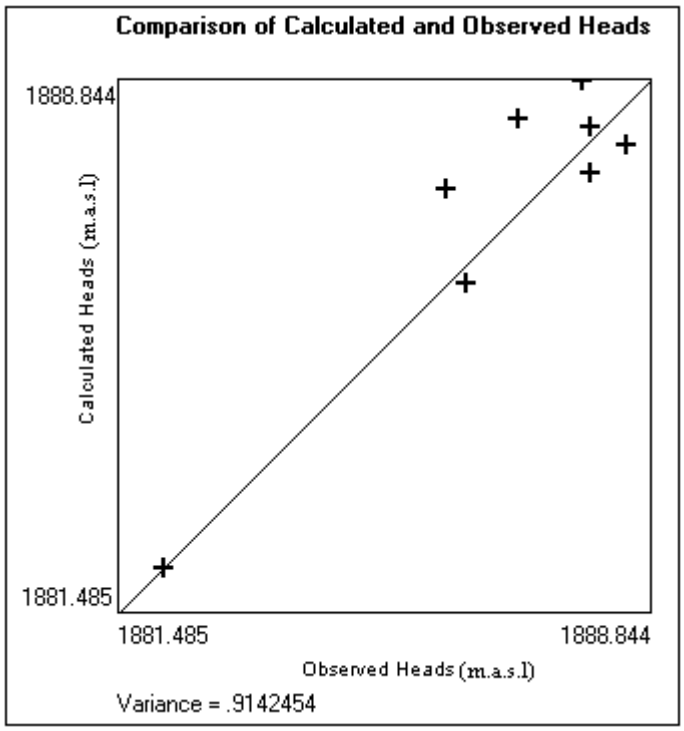


**Figure 4-19** ***A scatter plot of observed and simulated heads (m.a.s.l)***

#### 4.4.5.2 Heads

The difference between observed and simulated heads was also evaluated, when the difference between observed and simulated heads was in order of ±2 the model was considered calibrated (Table 4-5).The simulated steady-state lake level was 1888 m.a.s.l.

| ITC_number | C_Number | UTM_X | UTM_Y | Observed Heads (m.a.s.l) | Simulated Heads (m.a.s.l) | Difference Between Observed and simulated (m) |
|---|---|---|---|---|---|---|
| ITC027 | | 207680 | 9925645 | 1888 | 1887.572 | 0.428 |
| ITC042 | | 207165 | 9925364 | 1886 | 1887.356 | -1.356 |
| ITC043 | | 210769 | 9920726 | 1887 | 1888.324 | -1.324 |
| ITC045 | C54 | 208741 | 9926237 | 1889 | 1887.971 | 1.029 |
| ITC074 | | 213600 | 9921500 | 1888 | 1888.847 | -0.847 |
| ITC082 | C3929 | 206306 | 9931350 | 1886 | 1886.053 | -0.053 |
| ITC156 | | 214009 | 9917763 | 1888 | 1888.212 | -0.212 |
| N23 | | 203786 | 9925304 | 1880 | 1881.487 | -1.487 |
| N24 | | 204040 | 9925879 | 1882 | 1882.099 | -0.099 |

**Table 4-5** ***A list of observed and simulated heads together with their differences.***

### 4.4.5.3 Head residuals

Difference between observed and simulated heads were also represented in the map, positive value means simulated head is lower than observed head. Likewise negative value means simulated head is higher than observed head.

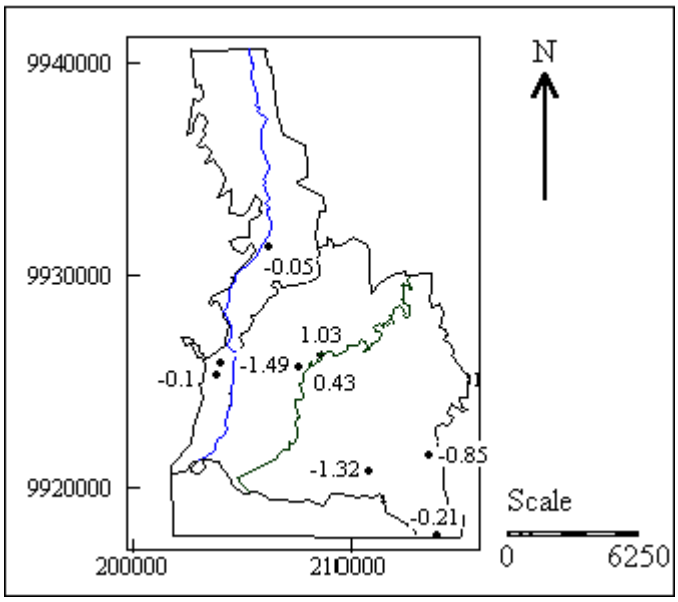


**Figure 4-20** ***Map showing head residuals.***

### 4.4.5.4 Graphical representation

Observed and simulated heads were plotted in the same graph to see how simulated heads deviate from observed heads.

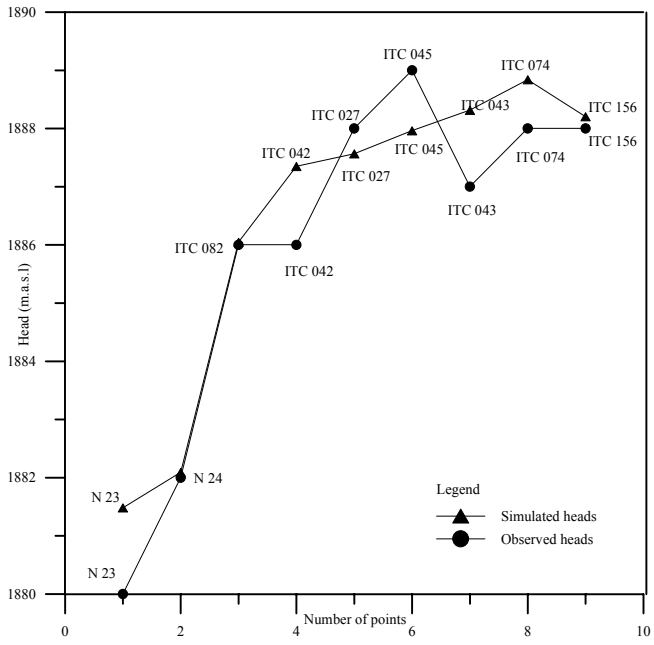


**Figure 4-21** ***Observed versus simulated heads.***

### 4.4.5.5 Contour map of simulated heads

A contour map of simulated was plotted together with the observed heads, to have an overview of the pattern (figure 4-22)

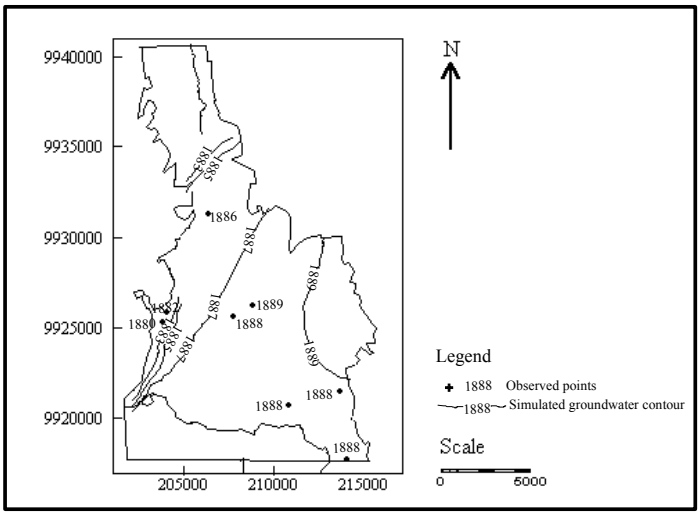


**Figure 4-22** ***Groundwater contour of simulated heads (m.a.s.l), contour interval 2 m.***

### 4.4.5.6 The root mean squared (RMS)

The average of differences was used to quantify the average error in the calibration. The RMS was used, which is the average of the squared differences in observed and simulated heads. The RMS of the simulated heads is 0.93 m calculated according to:

$$RMS = \left[ 1/n \sum_{i=1}^{n} (h_m - h_s) i^2 \right]^{0.5}$$

Where

$h_m$ = observed heads
$h_s$ = simulated heads

### 4.4.6 The difference between two and three layer model

The difference between the two-layer and three layers model is in the way the lake is modelled. In two-layer model the lake level was modelled as constant head, therefore its level was fixed to the value specified in initial head. For this study it was 1888 m.a.s.l., which is the average lake level before 1980. For that reason the level remained constant despite the changes in the water system, therefore the lake level was forced to remain constant. The situation, which is unrealistic, bearing in mind that Lake Naivasha, is fluctuating.

Also it was not possible to apply evaporation in the lake because in MODFLOW evapotranspiration flow rate has no influence on the simulation if the designated cell is either a no-flow (inactive) cell or constant head cell (Chiang and Kinzelbach, 1998)

In three-layer model the lake level changed according to the changes in the water system, like wise it was possible to apply all stresses imposed on the system.

By modelling the lake as a constant head may not provide reliable estimates of groundwater fluxes and lake level fluctuations

The three-layer model incorporates evaporation from the lake surface, inflow from runoff and rivers. These flow components affect lake levels and changes in these components lead to lake level fluctuations.

For the mentioned reasons the study concludes that a three-layer model is more reliable than a two-layer model.

## 4.5 Sensitivity analysis

A sensitivity analysis was performed to assess the response of the model simulation to changes in various input parameter values. The model is sensitive to a parameter when a change of the parameter values changes the distribution of simulated heads. When the model is sensitive to an input parameter, the value and distribution of that parameter within the model are more accurately determined during model calibration because small changes to the parameter value cause large changes in head. If a change of parameter value does not change the simulated heads distribution, the model is insensitive to that parameter. When the model is insensitive to an input parameter, the value and distribution of that parameter within the model are more difficult to accurately determine from model calibration because large changes to the parameter do not cause large changes in heads. These values of parameter may not represent actual values.

A sensitivity analysis was carried out by varying the transmissivity and recharge ±100 percent with respect to the assumed values. In the following discussion the increase in the RMS error calculated for each sensitivity analysis was with respect to the calibrated RMS of 1.17 m and 0.93 m for two and three layer model original simulation respectively.

### 4.5.1 Two-layer model

#### 4.5.1.1 Varying Transmissivity

The sensivity of the model to changes in transmissivity is greatest when the transmissivity is decreased in all layers at the same time. Decreasing the transmissivity in all layers increased the RMS and decreased the simulated heads in zones two, six and seven (Figure 4-3), in the remaining zones simulated heads increased. Increasing the transmissivity in all layers RMS also increases but the rate of increasing is relatively less than when the transmissivity are decreased. Similarly simulated head in zones two, six and seven decreased and in the remaining zones the heads increased. RMS for sensitivity analysis is presented in the table;

| Decrease in Transmissivity in Percent | RMS (m) | Increase in Transmissivity in Percent | RMS (m) |
|---|---|---|---|
| 25 | 2.02 | 25 | 2.03 |
| 50 | 7.01 | 50 | 2.9 |
| 75 | 21.24 | 75 | 3.55 |
| | | 100 | 4.06 |

**Table 4-6** ***RMS values as a result of increasing and decreasing transmissivity in two-layer model.***

Graphical Presentation

The effect of change in simulated transmissivity on simulated heads was also presented in a graph.

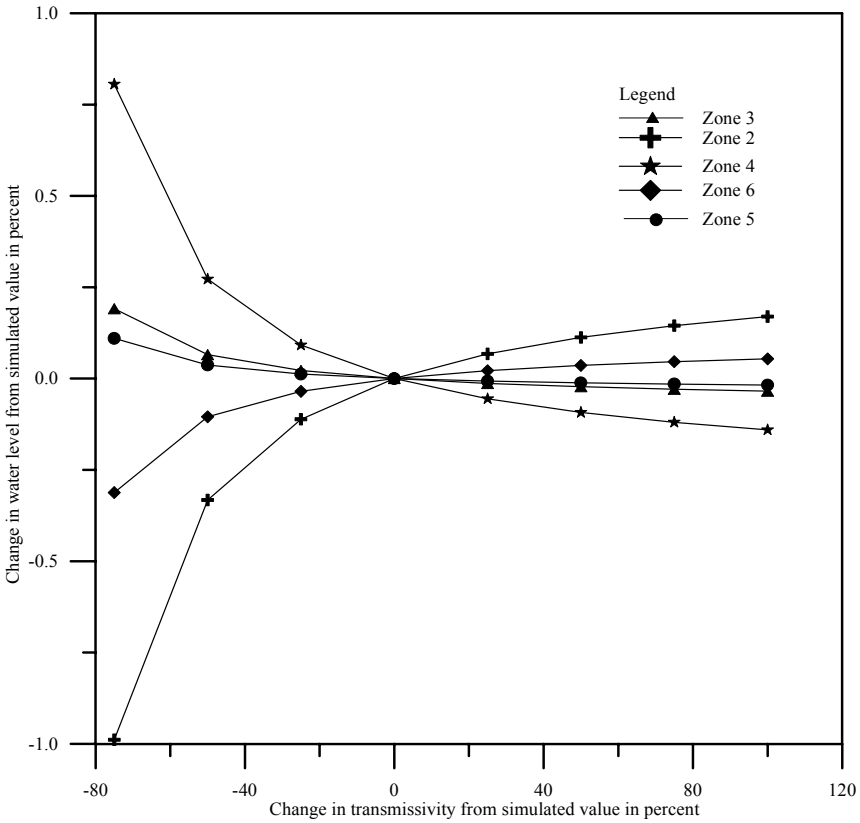


**Figure 4-23** ***Sensitivity analysis of the effect of the value of transmissivity on simulated heads in two-layer model.***

### 4.5.1.2 Varying Recharge

The sensitivity of the models to change in the recharge is also greater when the recharge is decreased than when it is increased. Increasing recharge increases the heads in all zones and decreasing recharge decreased the heads. The RMS also increased as indicated in the table;

| Decrease in Recharge in Percent | RMS (m) | Increase in Recharge in Percent | RMS (m) |
|---|---|---|---|
| 25 | 2.97 | 25 | 2.66 |
| 50 | 5.48 | 50 | 5.1 |
| 75 | 8.05 | 75 | 7.61 |
| | | 100 | 10.14 |

**Table 4-7** ***RMS values as a result of increasing and decreasing recharge in two-layer model.***

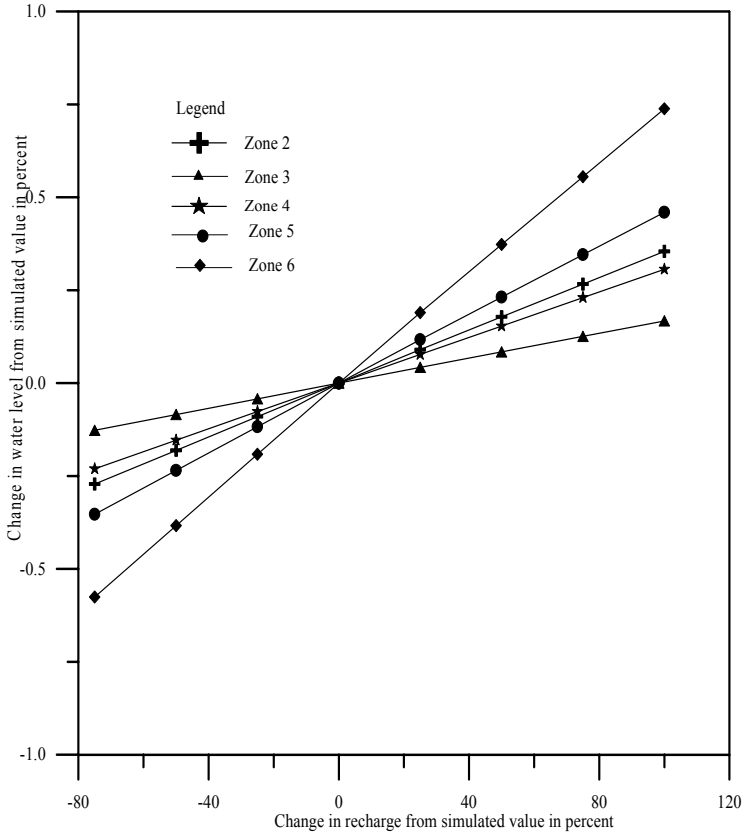


**Figure 4-24** ***Sensitivity analysis of the effect of the value of recharge on simulated heads in two-layer model.***

### 4.5.2 Three-layer model

#### 4.5.2.1 Varying Transmissivity

The sensivity of the model to changes in transmissivity is greatest when the transmissivity is decreased in all aquifers at the same time. Decreasing the transmissivity in all aquifers increased the RMS and decreased the simulated heads in all zones except zone one (figure 4-17). Increasing the transmissivity in all layers RMS also increases but the rate of increasing is relatively less than when the transmissivity are decreased. Similarly simulated heads in zone one increased and in the rest of zones the heads decreased. RMS for sensitivity analysis is presented in the table;

| Decrease in Transmissivity in Percent | RMS (m) | Increase in Transmissivity in Percent | RMS (m) |
|---|---|---|---|
| 25 | 1.07 | 25 | 1.29 |
| 50 | 2.8 | 50 | 1.61 |
| 75 | 8.77 | 75 | 1.87 |
| | | 100 | 2.06 |

**Table 4-8** ***RMS values as a result of increasing and decreasing transmissivity in three-layer model.***

Graphical representation

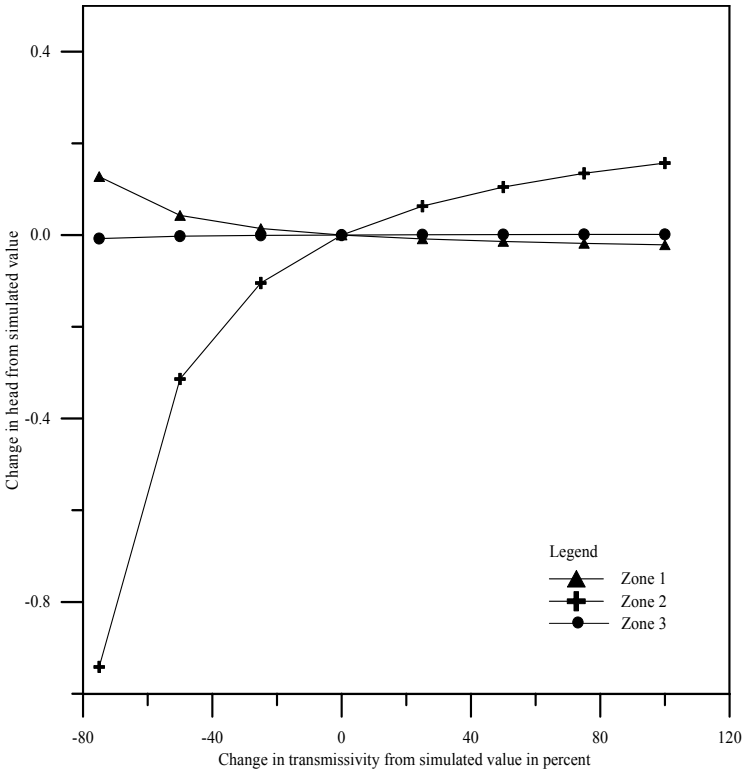


**Figure 4-25** ***Sensitivity analysis of the effect of the value of transmissivity on simulated heads in three-layer model.***

### 4.5.2.2 Varying Recharge

The sensitivity of the model to change in the recharge is greatest when the recharge is increased than when it is decreased. Increasing recharge increased RMS as well as the heads in all zones. Reducing recharge reduced the heads in all zones. RMS values are indicated in the table;

| Decrease Recharge in Percent | RMS (m) | Increase Recharge in Percent | RMS (m) |
|---|---|---|---|
| 25 | 1.07 | 25 | 1.44 |
| 50 | 1.7 | 50 | 2.18 |
| 75 | 2.48 | 75 | 2.99 |
| | | 100 | 3.81 |

**Table 4-9** ***RMS values as a result of increasing and decreasing recharge in three-layer model.***

The graphical presentation is shown in figure below;

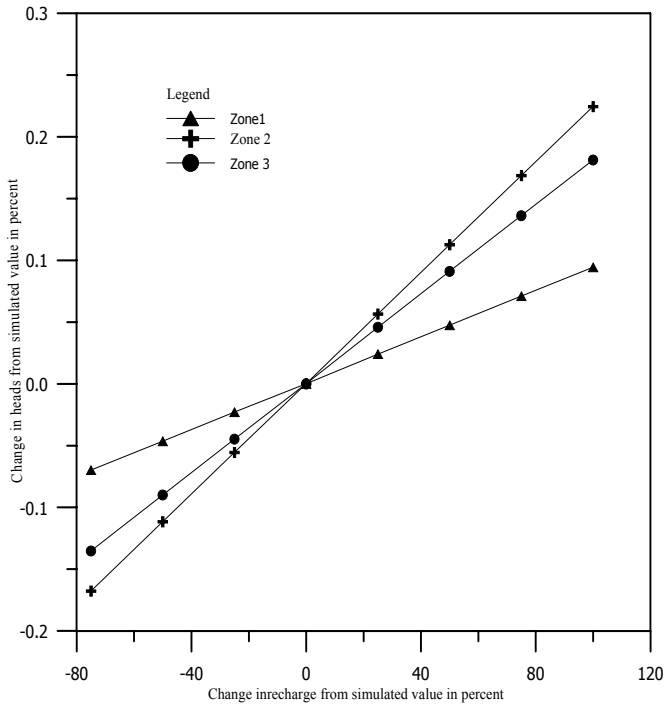


**Figure 4-26** ***Sensitivity analysis of the effect of the value of recharge on simulated heads in three-layer model.***

### 4.5.3 Conclusion

The steady-state simulations of the groundwater flow in the study area achieved satisfactory results using transmissivity, recharge and evapotranspiration (for three-layer model) as the fitting parameters.

Both models are sensitive to overall changes in the transmissivity and recharge, when the transmissivity and recharge are separately changed in all layers, as indicated by the large change of RMS error compared to 1.17 m and 0.93 m for two and three layer models original simulation respectively. In both models varying transmissivity gave

RMS in the same order of magnitude while changing recharge the RMS returned were slightly different in magnitude.

Systematic variation of parameters allowed easy visualization of what occurs when parameters are varied one at time. The more detailed examination of parameter ranges is useful to make sure the sensitivity analysis doesnot lump sensitivity ranges with nonsensitive ranges and therefore miss the effect.

## 4.6 THREE- LAYER MODEL TRANSIENT SIMULATION

The transient conditions were meant to be from 1980 when heavy pumping started in the study area. Transient simulation was made to predict the hydrogeological effects of increased pumping in the study area. For that reason the simulated heads from steady-state were applied to transient model as initial heads.

### 4.6.1.1 Aquifer Parameters

Specific storage was set to $10^{-5}$ for the second and third layer.

Specific yield for the lake was set to 1 and second layer was given 0.25. The rest of parameters remained the same as in steady-state model.

### 4.6.1.2 Model run

The model was run for one year after steady-state condition by using initial heads from steady-state, there was no change in the simulated heads as shown in the graph. Indicating that the steady state solution is reliable.

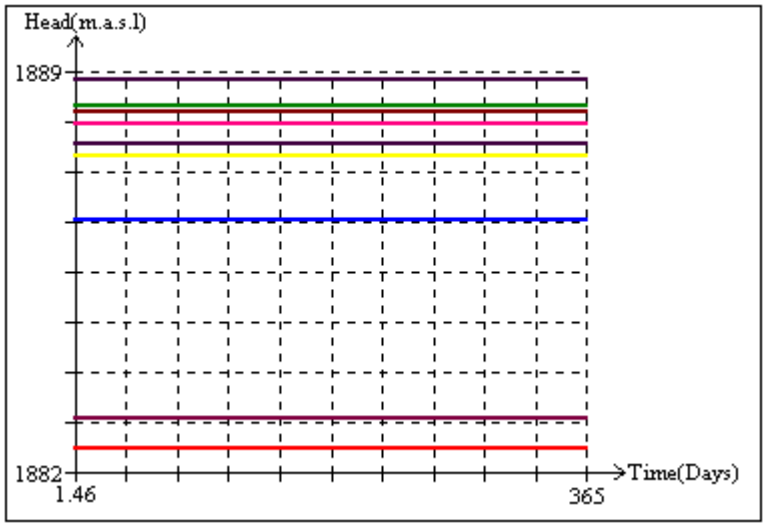


**Figure 4-27** ***Response of simulated heads in transient condition without pumping.***

### 4.6.1.3 Response after pumping in the aquifer

In the study area as for October 1999 the amount of groundwater abstracted for irrigation was about 14,000 m3/day. Basing on steady-state condition the value was put in the model to see how the aquifer will respond after 40 years. In this area intensive groundwater abstraction started recently (1998). The results indicate that the water level in the well field went down up to 8 m and in the lake 1 m, as indicated in table 4-10 and figure 4-28. The plot of drawdown versus time (figure 4-29) clearly shows that the water levels continue to decline until it reached steady-state after 17 years.

| Observation Point | UTM_X | UTM_Y | Maximum water level drop in the points |
|---|---|---|---|
| P1 | 213675 | 9925238 | 8.1 |
| P2 | 213692 | 9924759 | 8 |
| P3 | 211668 | 9924266 | 6.5 |
| P4 | 211688 | 9923803 | 6.2 |
| P5 | 211147 | 9922763 | 4.7 |
| ITC045 | 208741 | 9926237 | 5.1 |
| ITC074 | 213600 | 9921500 | 3.9 |
| ITC082 | 206306 | 9931350 | 5.3 |
| N24 | 204040 | 9925879 | 3.8 |

**Table 4-10** ***Water level drop in observation points.***

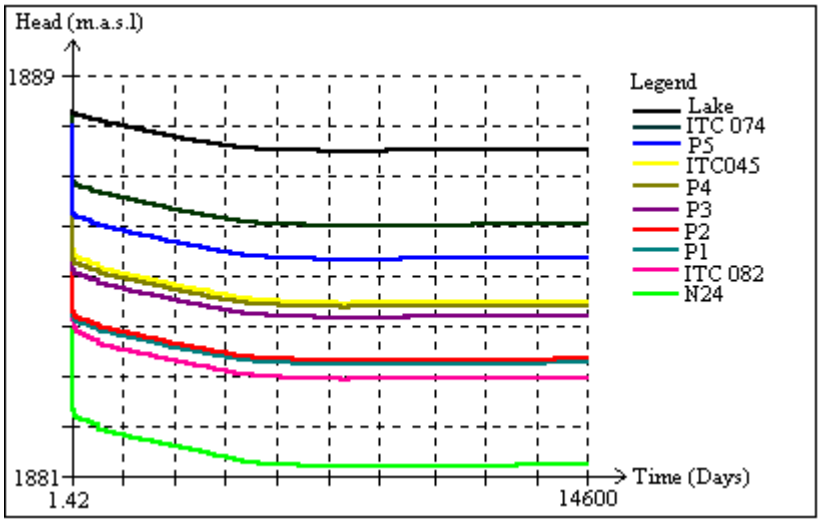


**Figure 4-28** ***Responses of the lake and aquifer due to pumping in the aquifer.***

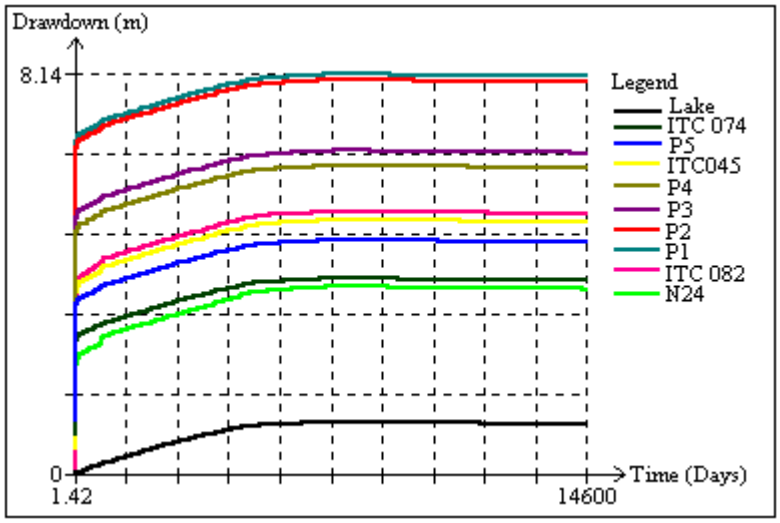


**Figure 4-29** ***Simulated drawdown after 40 years of pumping.***

#### 4.6.1.4 Drawdown contour map

The contour map of the drawdown of the area as a result of pumping for 17 years was drawn as indicated in figure 4-30. Shows an extensive cone of depression centred on the well field, which is eastern part of the study area, where maximum drawdown is 8 m.

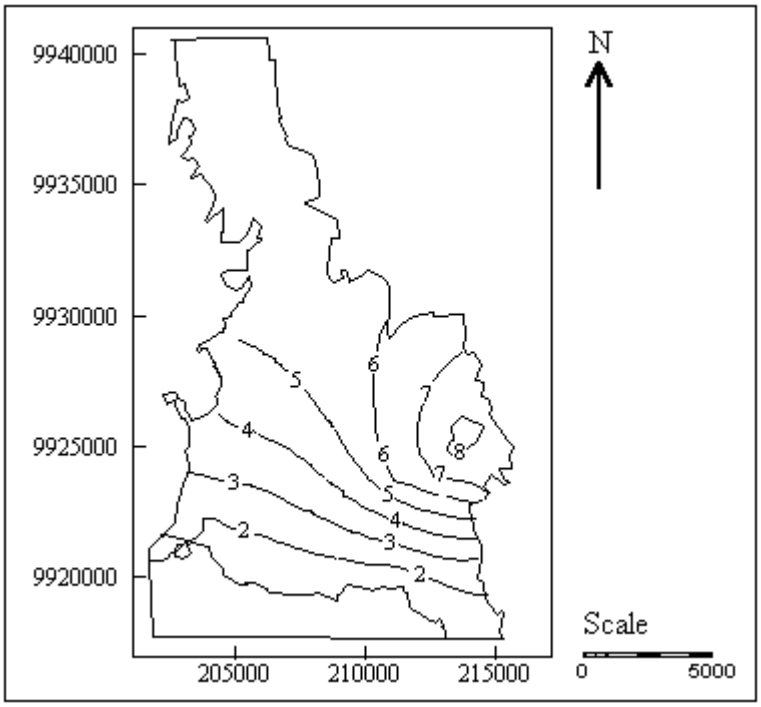


**Figure 4-30** ***Simulated contour map of drawdown after 17 years of pumping in m contour interval 1.5 m.***

#### 4.6.1.5 Groundwater contour map

Groundwater Contour map after 17 years of pumping was also drawn (figure 4-31). The map shows that locally water flows from the lake towards the well field, while basing on the steady-state condition water flows from the well field towards the lake.

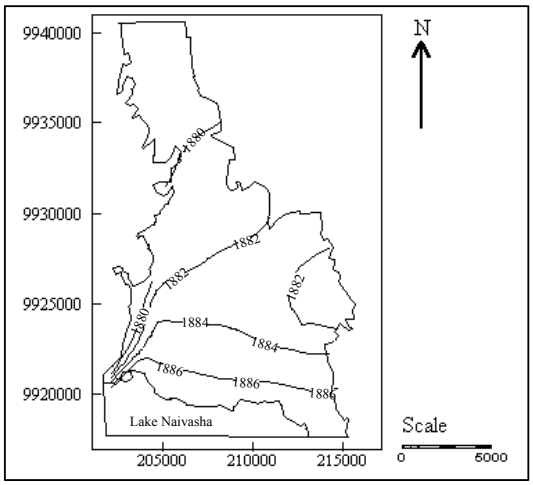


**Figure 4-31** ***Contour map after 17 years of pumping*** **in (m.a.s.l), contour interval 2 m**

A map of points used for the analysis.

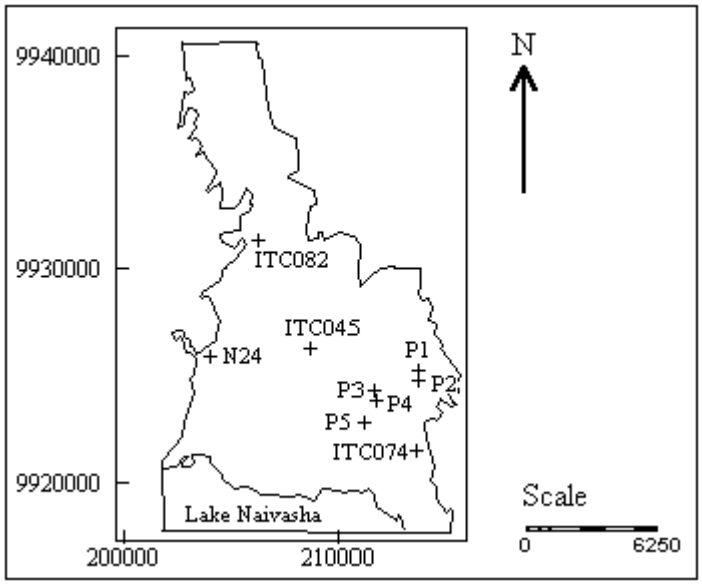


**Figure 4-32** ***Position of the points used in the analysis.***

#### 4.6.1.6 Water abstraction from the Lake Naivasha

The amount abstracted in the aquifer was also abstracted in the lake to see how the aquifer and the lake will respond. The water level in the lake as well as in the aquifer

went down by 1 m after 40 years of pumping. The equilibrium was reached after 15 years (Figure 4-32).

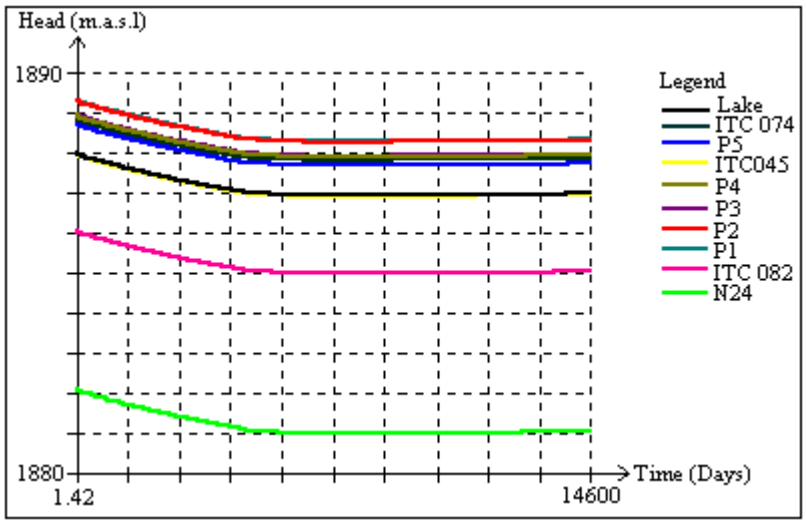


**Figure 4-33** ***Responses of the lake and aquifer due to pumping in the lake.***

### 4.6.2 Conclusion

Although the model was not calibrated, nonetheless the transient simulation was made to show how increasing pumping could affect the water system in the area. From the graphs it clearly indicates that, the groundwater abstraction of 14,000 $m^3$/day in the study area, for the period of 40 years will cause the water level to go down as much as 8 m as indicated in the figures above. The equilibrium will be reached after 17 years if the water system conditions will remain the same.

A clear picture can be seen how groundwater and lake water abstraction lowers the water level in the aquifer as well as in the lake. Moreover from simulated results it shows that, direction of water flow will change locally.

## 4.7 MODEL LIMITATIONS

- As is in all finite-difference groundwater flow models, a single, unique mathematical solution cannot be obtained to solve the system of equations that represent groundwater flow. Therefore different input values (transmissivity, recharge etc.) than those used in the model could be input to the model, from which corresponding values for the other inputs could be obtained during calibration, resulting in the same simulated water levels in the model layers as were produced. The results of the model simulations are dependant on the assumption that input to the model and are representative of the groundwater flow system in the study area.

- Data that are input to the model to represent the entire extents of the aquifer are based on properties and conditions that are interpolated across large areas between wells and other locations.

- Homogeneity and isotropy is assumed for the model, which may or may not be valid.

- The boundaries between sediments and volcanics are not accurately known makes setting boundary conditions likely to error.

# 5 CHAPTER FIVE

## 5.1 SUMMARY AND CONCLUSION

A groundwater flow model was constructed for the purpose of constructing the historic piezometric level, which represent the water level before commencement of heavy pumping, to obtain the approximate transmissivity and recharge. Moreover to find the effect of acacia xanthophloea trees to groundwater and assessing the impact of water level depletion from increased pumping for irrigation.

The simulations include initial conditions (steady-state), the 1930's-1970's historical period.

At first a two-layer model was constructed simulating the lake as a constant head, but by modelling the lake as a constant head may not provide reliable estimates of groundwater fluxes and lake level fluctuations. For this reason a three-layer test model was created in order to see if it is possible to model the lake the way it behaves. The three-layer test model worked perfectly. Then on the basis of the three-layer test model a two-layer model of the study area was changed to three-layer model. The three layers model was not able to converge, then a decision was made to change the grid size of the model where by 500 m by 500 m grid size was used.

The steady-state simulation of the groundwater flow in the study area achieved satisfactory results using transmissivity, recharge and evapotranspiration (in three-layer model) as fitting parameters. To do so, seven and five transmissivity zones were defined for two and three layer model respectively, on the basis of calculated transmissivity from different researchers where possible. The zone on the southeast has been omitted in three-layer model in order to model only the aquifers around lake Naivasha.

The assigned values of transmmisivity are low for fine material (clays, diatomite, silts and fine-grained sands) and high for reworked volcanics or weathered contacts between different lithological units). Also low transmissivity were assigned where the second aquifer is wedging out to volcanics. The simulated values are in order of magnitude like those calculated in different points. Final transmissivity in the clays, diatomite, silts and fine-grained sands units was not more than 10 $m^2$/day and in the second aquifer (reworked volcanics or weathered contacts between different lithological units), ranges from 10 to 1500 $m^2$/day.

Four recharge zones were defined on the basis of sediments thickness, where by higher recharge was given to thick sediments (thickness > 10 m) and lower recharge to thin sediments. The recharge values simulated by the model are 25 mm/year and 52 mm/year for thin and thick sediments respectively, they are in order of magnitude as that calculated by Graham 1998 (49 to 65 for sediments). In the north of the study area sediments thickness is less than ten metres therefore it was considered to have less recharge comparing to the southern part. For that reason half of the amount of recharge in the south was assumed as recharge value in the north. McCann 1974, calculated recharge in the catchment area and found that the mean annual total

recharge represent about 9.2 percent of total precipitation. The simulated recharge values are 4 to 8 percent of mean annual rainfall of 650 mm.

Water flows into the model area on the southeast, the amount of flow has been estimated to be 5 percent of the average annual rainfall. Outflow from the aquifer has been calculated using Darcy's law by using the hydraulic gradient and transmissivity that are known.

The amount of water abstracted by acacia trees was taken as 3 mm/day and put in the two-layer model, but the model returned simulated water levels in order of 30 m lower than the observed levels. The values showed that evapotranspiration cannot be so high or rather transmissivity value must be high. Therefore the values was not used instead no recharge was put in the acacia forest. In the three-layer model a value of 0.0002 mm/day was used to simulate the abstraction by acacia trees.

In both models simulated heads satisfactorily match observed heads.

The RMS error for two and three-layer steady-state calibrations were 1.17 m and 0.93 m respectively. Sensitivity analysis indicates that the models are most sensitive to decrease in transmissivity and recharge, are least sensitive to increase in transmissivity and recharge. A sensitivity analysis on the transmissivity and recharge values reinforces the result of the simulation presented.

A three-layer model was used to simulate transient condition where by the simulated heads from steady-state model were used as initial heads. The amount of water pumped as for 1999 was put in the model that is 14,000$m^3$/day. After 40 years of pumping the model showed that water level in the aquifer has gone down maximum up to 8 m and in the lake by 1 m, the equilibrium was reached after 17 years. The same amount when abstracted from the lake, both lake and groundwater level went down by 1 m, the equilibrium was reached after 15 years. Because the model was not calibrated this was just to show how the system will behave.

By modelling the lake as a constant head may not provide reliable estimates of groundwater fluxes and lake level fluctuations, as it was done in two-layer model. Considering this reason the study concludes that, a three-layer model is reliable than a two-layer model, because the three-layer model incorporates evaporation from the lake surface, inflow from runoff and rivers. These flow components affect lake levels and changes in these components lead to lake level fluctuations. Also the effect of groundwater and lake pumping was possible to be observed in the lake because the lake level changed.

Differences between Lake Package and Method used to model the lake are;

Lake package contains routines to calculate water budgets for a lake that overlies many groundwater cells, and the package can subsequently update the lake water level (stage), volume and area as a result of the computed water budget.

While the method used in the study, do not provide a way to automatically update the lake water level as a result of changing water fluxes to and from a lake.

Further more groundwater flow models are numerical representations that simplify and aggregate natural systems. Models are not unique; different combinations of aquifer characteristics may produce similar results. Therefore, values of transmissivity and recharge used in the model are not precise, but are within a reasonable range when compared to independently collected data.

The model solution represents only one of many plausible and reasonable solutions.

## 5.2 RECOMMENDATIONS

The study recommends the following;

A three-layer model transient calibration to be carried by using observed heads from 1980 to recent and future prediction should be done by using the calibrated model.

A finer mesh is recommended, for a three-layer model especially in areas with strong groundwater extraction. The grid size used for a three-layer model in this study was for the easiest of convergence, therefore it is recommended to use another code, which provide flexibility of changing grid size. As in MODFLOW it is not possible to change grid size after you have saved, it only allows to refine the existing model grid.

A study on evapotranspiration from acacia forest should be carried out so as to know exactly how much the trees abstract from groundwater.

More data collection through groundwater level monitoring and periodic well discharge should be done to facilitate future improvements in the model. Continuous water-levels measurements are important in order to monitor changes.

# 6 REFERENCES

**Abiya I. O.,** 1996. *Towards sustainable utilization of Lake Naivasha, Kenya*. Paper Presented at the sixth International Conference on the Conservation and management of Lakes, Kasumigaura's 1995. Lakes and Reservoirs: Research and Management 1996.

**Anderson, M.P., and W.W. Woessner**, 1992. *Applied Groundwater modeling; Simulation of flow and Advective Transport*. Academic Press, San Diego.

**Behar H. A.,** 1999. *Surface water - Groundwater Interaction.Lake Naivasha, Kenya.* M.Sc. Thesis, International Institute for Aerospace Survey and Earth Sciences (ITC), Enschede, The Netherlands.

**Chiang W. and Kinzelbach W.** 1996. *Processing Modflow (for Windows). A simulation system for Modelling Groundwater Flow and Pollution.* Version 5.0.

**Chelemisinoff, P.N., K.A. Gigliello, T.K.O'Neill,** 1984. *Ground-water-Leachate: Modeling/Monitoring/Sampling.* Technomic Publishing Company, Inc.Pennsylvania

**Clarke A.C.G., D. Allen, G. Darling**. 1990. *Geological, Volcanological and Hydrogeological Controls on the Occurrence of the Geothermal Activity in the Area Sorrounding Lake Naivasha*, Kenya. Ministry of Energy, Republic of Kenya.

**Fetter, C.W.,** 1994. *Applied Hydrogeology.* Prentice Hall, Upper Saddle River, New Jersey.

**Freeze, R. A., and J.A. Cherry.** 1979. *Groundwater*. Prentice Hall, Englewood Cliffs, NJ.

**Graham, A.,** 1998. *Groundwater Recharge Estimation of the Malewa Catchment, Naivasha, Kenya*. M.Sc. Thesis, International Institute for Aerospace Survey and Earth Sciences (ITC), Enschede, The Netherlands.

**Groundwater Survey (Kenya) LTD.** 1998. *Borehole Site Investigations Naibor Ajijik,* Report No. 98/547, Nairobi.

**ITC, Water Resources Surveys.** 1996. Water Resources Assessment Project Phase v, Mission Report, (WRAP**).** *Water Resources modelling of the Rift valley lake Basins and Laikipia (Groundwater Component).*

**ITC** 1997. *The Itergrated Land and Water Information System 2.1. User's Guide Manual.* ITC, Enschede, The Nertherlands.

**Kresic, N.,** 1997. *Quantitative Solutions in Hydrogeology and Groundwater Modeling.* CRC Press LLC, Frolida.

**Kruseman, G.P., and De Ridder, N.A,** 1994. *Analysis and Evaluation of Pumping Test Data,* ILRI Publication 47, The Netherlands.

**Lake Naivasha Riparian owners Association.** 1993. *A Three Phase Environmental Impact Study of the Recent Developments Around Lake Naivasha.* Phase I, Executive summarry. John Goldson Associates, P. O. Box 70560, Nairobi Kenya.

**Landon J.R.,** 1991. *Booker Tropical Soil Manual, A handbook for soil survey and agricultural land evaluation in tropics and subtropics*. John Wiley & Sons, Inc., 605 Third Avenue New York, NY 10158, United States

**Meijerink, A.M.J., de Brouwer, H.A.M., Mannaerts,C.M. and Valenzuela,C.R**. 1994. *Introduction to the use of Information Systems for Practical Hydrology.* ITC Publication Number 23, ITC, Enschede, The Netherlands.

**Mmbui, S.G.,** 1999. *Long Term Water Balance of Lake Naivasha, Kenya*, M.Sc. Thesis, International Institute for Aerospace Survey and Earth Sciences (ITC), Enschede, The Netherlands.

**Ojiambo, B.S.,** 1996. *Characterization of Subsurface Outflow from a Closed-basin Freshwater Tropical Lake, Rift Valley, Kenya.* Ph. D Thesis, University of Nevada, Reno.

**Ojiambo, B.S.,** 1992. *Hydrogeologic, Hydrogeochemical and Stable Isotopic Study of Possible Interaction between Lake Naivasha, Shallow subsarface and Olkaria Geothermal,* **M.Sc.** Thesis, University of Nevada, Reno.

**Ramirez, R.H.,** 1999. *Groundwater Flow Modeling of Naivasha Basin, Kenya*, M.Sc. Thesis, International Institute for Aerospace Survey and Earth Sciences (ITC), Enschede, The Netherlands.

**Röhrich, T.** *User's Manual for Aquifer Test, waterloo Hydrogeology Inc*, Ontario, Canada.

**Salah, A. 1999.** *Productive and Sustainable Use of Water Among Competitive Sectors, A Study in the Naivasha Catchments, Kenya*. M.Sc. Thesis, International Institute for Aerospace Survey and Earth Sciences (ITC), Enschede, The Netherlands.

**Seeber G.** 1993**.** *Satellite Geodesy, Foundations, Methods and Application.* Water de Gruyter & Co., D-1000 Berlin 30.

**Spitz, K. and J. Moreno.** 1996. *A Practical Guide to Groundwater and Solute Transport Modeling*. John Wiley & sons, Inc.

**Stuttard, M.J., J. Hayball, G. Narcos, M. Suppo, R. Catani, L.Isavwa, J. Baraza and**
**A. Oroda.** 1995. *Monitoring Lakes in Kenya: An Environmental Analysis Methodology for Developing Countries*, Final Report to European Commission, Contract No. TS3*-CT92-0016.

**Thompson, A.O. and R. G. Dodson.** 1963. *Geology of the Naivasha Area*. Geological Survey of Kenya, Report. No. 55.

**Trottman, D. K**., 1998. *Modeling Groundwater Storage change in Response to Fluctuating Levels of Lake Naivasha, Kenya*, M.Sc. Thesis, International Institute for Aerospace Survey and Earth Sciences (ITC), Enschede, The Netherlands.

**Wiberg,I. 1976.** *Naivasha Water Supply Project, Groundwater Investigation*, VIAK EA Ltd., Consulting Engineering and Mapping Services.

# 7 Appendices

## 7.1 Appendix 2-A

Long term mean monthly rainfall data

| Month | Naivash D.O. | Naivasha K.C.C Ltd | Naivasha Vet. Experimental Stn. | Naivasha Marula | Thome Farmers No.2 | Naivasha W. D. D. | Olarogwai Farm Naivasha |
|---|---|---|---|---|---|---|---|
| | (214315, 9920714) | (208743, 9926243) | (212455, 9928088) | (208742, 9928088) | (197602, 9929925) | (216173, 9918872) | (216168, 9928090) |
| Elevation (m) | 1900 | 1951 | 1829 | 2042 | 2350 | 1936 | 1981 |
| Record Length (Years) | 77 (1916-1993) | 57(1936-1993) | 54(1939-1993) | 50(1943-1993) | 22(1971-1993) | 21 (1972-1993) | 26 (1967-1993) |
| Total Yearly (Rainfall) (mm) | 669 | 598 | 711 | 655 | 929 | 681 | 770 |
| | (mm) | (mm) | (mm) | (mm) | (mm) | (mm) | (mm) |
| Maximum | 113 | 102 | 117 | 113 | 170 | 116 | 124 |
| Minimum | 25 | 28 | 33 | 32 | 28 | 37 | 31 |
| January | 25 | 28 | 33 | 32 | 28 | 39 | 31 |
| February | 36 | 35 | 39 | 33 | 51 | 44 | 47 |
| March | 58 | 48 | 55 | 51 | 44 | 60 | 57 |
| April | 113 | 102 | 117 | 113 | 170 | 116 | 124 |
| may | 84 | 83 | 96 | 84 | 112 | 79 | 80 |
| June | 82 | 51 | 55 | 50 | 68 | 51 | 51 |
| July | 34 | 40 | 43 | 47 | 55 | 37 | 45 |
| August | 45 | 50 | 55 | 59 | 86 | 45 | 60 |
| September | 43 | 31 | 42 | 38 | 53 | 44 | 98 |
| October | 49 | 39 | 62 | 40 | 64 | 56 | 61 |
| November | 61 | 53 | 68 | 62 | 118 | 62 | 71 |
| December | 40 | 38 | 46 | 44 | 83 | 48 | 45 |

Source: Behar 1999

## 7.2 Appendix 2-B

### Section A-A

### Geological Profile

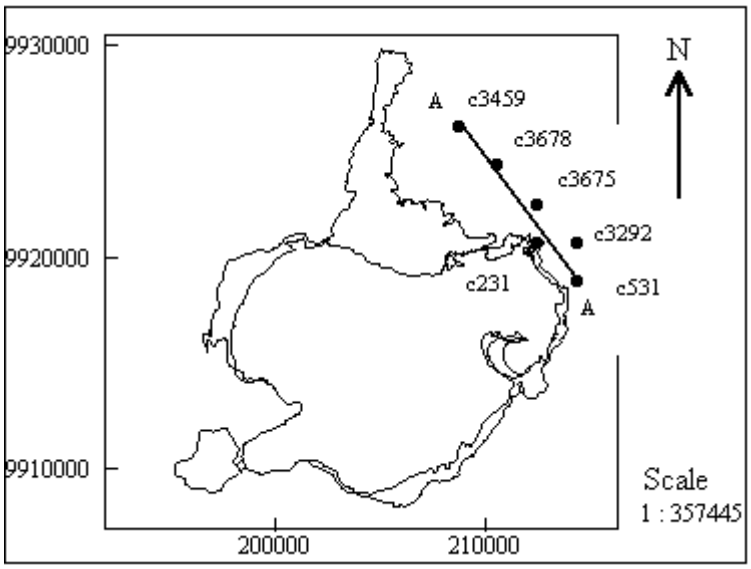


### Legend

- **Borehole**

## 7.3 Appendix 2-C

**Profile for Section A-A**

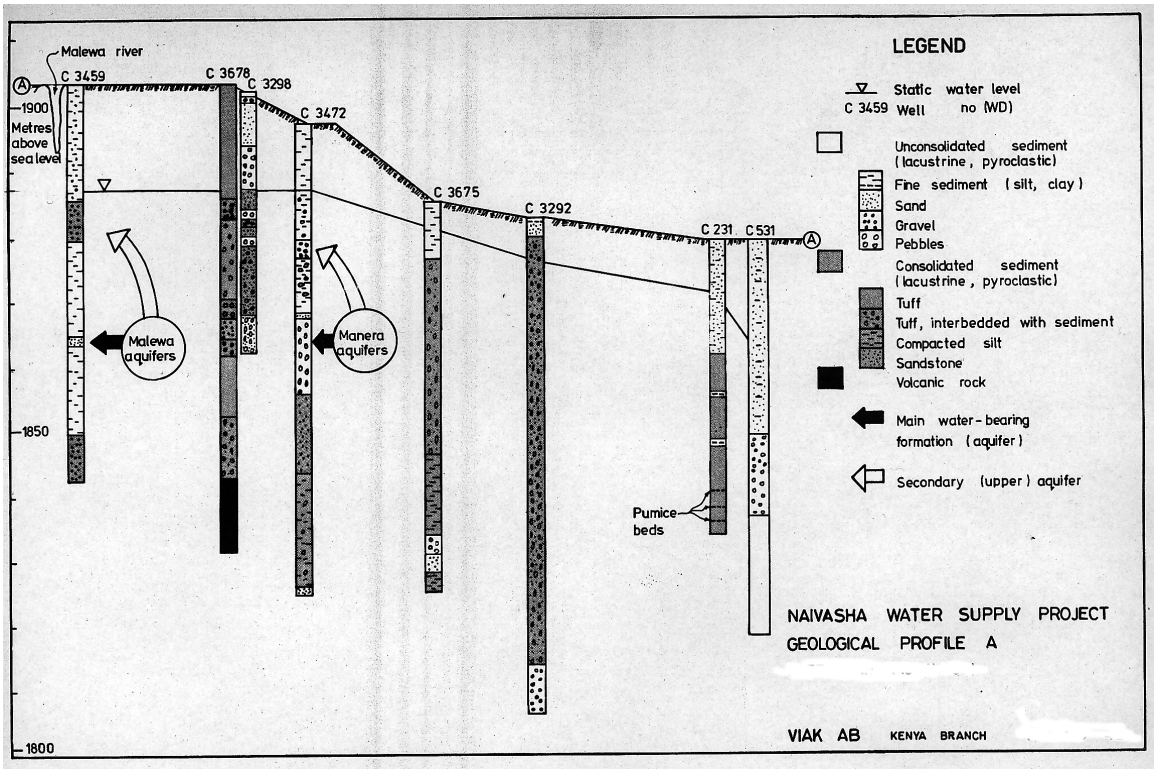


**Source: VIAK AB Kenya Branch**

## 7.4 Appendix 3-A

**All wells in the database**

| ITC_Number | C_Number | UTM_X | UTM_Y | Construction Static Water level (m) | Piezometric Level (m.a.s.l) | Elevation (m.a.s.l) |
|---|---|---|---|---|---|---|
| ITC001 | c11527 | 213518 | 9924527 | 26.05 | 1883.95 | 1910 |
| ITC002 | BH A | 213735 | 9925528 | 29.46 | 1885.54 | 1915 |
| ITC003 | BH B | 213713 | 9924977 | 25.18 | 1884.82 | 1910 |
| ITC004 | BH C | 213459 | 9924929 | 26.69 | 1881.31 | 1908 |
| ITC005 | BH D | 213384 | 9924777 | 26.64 | 1882.06 | 1908.7 |
| ITC006 | BH E | 213058 | 9924642 | 23.86 | 1882.14 | 1906 |
| ITC007 | BH green house | 214004 | 9925600 | 33.65 | 1884.35 | 1918 |
| ITC008 | TANINI | 213544 | 9925720 | 33.21 | 1883.79 | 1917 |
| ITC009 | | 211437 | 9921386 | 5.29 | 1885.71 | 1891 |
| ITC010 | | 211914 | 9924455 | 12.45 | 1890.55 | 1903 |
| ITC011 | C2883 | 213101 | 9928951 | 60.00 | 1880.00 | 1940 |
| ITC012 | C4155 | 214504 | 9926572 | 27.00 | 1920.90 | 1947.9 |
| ITC013 | | 212603 | 9923764 | 19.05 | 1882.95 | 1902 |
| ITC045 | | 209462 | 9928455 | 18.00 | 1905.01 | 1923 |
| ITC015 | | 210473 | 9928944 | 27.11 | 1904.89 | 1932 |
| ITC016 | C4161 | 212958 | 9923304 | 16.71 | 1884.29 | 1901 |
| ITC017 | C11691 | 203842 | 9924134 | 4.20 | 1885.80 | 1890 |
| ITC018 | | 202866 | 9921790 | 7.04 | 1887.96 | 1895 |
| ITC019 | | 202662 | 9921507 | 3.57 | 1894.63 | 1898.2 |
| ITC020 | BH 7 | 211230 | 9924941 | 20.13 | 1882.87 | 1903 |
| ITC021 | C3366 | 211822 | 9923166 | 15.63 | 1879.97 | 1895.6 |
| ITC022 | C3365 | 212334 | 9922728 | 10.80 | 1885.40 | 1896.2 |
| ITC023 | C3676 | 212267 | 9923041 | 13.50 | 1883.90 | 1897.4 |
| ITC024 | | 213126 | 9921647 | 4.80 | 1889.50 | 1894.3 |
| ITC025 | | 212267 | 9923041 | 14.18 | 1883.23 | 1897.4 |
| ITC026 | | 208752 | 9928952 | 11.31 | 1885.89 | 1897.2 |
| ITC027 | w16(M6) | 207935 | 9925786 | 9.10 | 1887.90 | 1897 |
| ITC028 | | 207705 | 9925654 | 12.22 | 1884.78 | 1897 |
| ITC029 | | 204034 | 9928849 | 28.95 | 1886.05 | 1915 |
| ITC030 | | 205375 | 9924689 | 27.11 | 1862.29 | 1889.4 |
| ITC031 | C3677 | 211769 | 9924324 | 20.44 | 1882.26 | 1902.7 |
| ITC032 | C3678 | 211300 | 9924682 | 18.00 | 1885.50 | 1903.5 |
| ITC033 | C2536 | 202866 | 9922388 | 4.20 | 1896.40 | 1900.6 |
| ITC034 | C2539 | 202342 | 9920746 | 4.50 | 1885.30 | 1889.8 |
| ITC035 | | 215467 | 9917087 | 37.07 | 1902.73 | 1939.8 |
| ITC036 | | 214224 | 9919179 | 6.72 | 1886.08 | 1892.8 |
| ITC037 | | 214078 | 9920423 | 10.05 | 1884.25 | 1894.3 |
| ITC038 | | 203516 | 9924230 | 5.17 | 1885.83 | 1891 |
| ITC040 | C11494 | 201591 | 9926461 | 191.00 | 1879.40 | 2070.4 |
| ITC041 | | 203634 | 9925042 | 3.69 | 1887.11 | 1890.8 |
| ITC042 | | 207165 | 9925364 | 8.16 | 1885.84 | 1894 |
| ITC043 | | 210769 | 9920726 | 1.77 | 1887.23 | 1889 |

| | | | | | | |
|---|---|---|---|---|---|---|
| ITC046 | C231 | 214220 | 9919875 | 9.00 | 1883.80 | 1892.8 |
| ITC047 | C465 | 208988 | 9937384 | 41.00 | 1933.60 | 1974.6 |
| ITC048 | C457 | 212459 | 9931771 | 26.00 | 1957.50 | 1983.5 |
| ITC049 | C468 | 208741 | 9926237 | 17.00 | 1886.50 | 1903.5 |
| ITC050 | C531 | 214314 | 9918872 | 16.00 | 1877.60 | 1893.6 |
| ITC051 | C631 | 197605 | 9920698 | 27.00 | 1875.80 | 1902.8 |
| ITC052 | C632 | 214316 | 9917024 | 11.00 | 1883.30 | 1894.3 |
| ITC053 | C1062 | 197600 | 9929926 | 11.00 | 2332.50 | 2343.5 |
| ITC054 | C1063 | 197600 | 9929926 | 11.00 | 2332.50 | 2343.5 |
| ITC055 | C1481 | 214375 | 9916225 | 17.00 | 1888.60 | 1905.6 |
| ITC056 | C1482 | 213900 | 9916550 | 11.00 | 1882.40 | 1893.4 |
| ITC057 | C1483 | 216171 | 9926241 | 31.00 | 2037.20 | 2068.2 |
| ITC058 | C1488 | 218032 | 9922558 | 75.00 | 1999.00 | 2074 |
| ITC059 | C1898 | 216171 | 9924404 | 58.00 | 2005.50 | 2063.5 |
| ITC060 | C1947 | 216175 | 9918873 | 16.00 | 1984.00 | 2000 |
| ITC061 | C2222 | 214316 | 9917024 | 15.00 | 1879.30 | 1894.3 |
| ITC062 | C2224 | 214316 | 9917024 | 15.00 | 1879.30 | 1894.3 |
| ITC063 | C2246 | 210602 | 9924401 | 14.00 | 1882.70 | 1896.7 |
| ITC064 | C2304 | 197608 | 9917014 | 5.00 | 1881.50 | 1886.5 |
| ITC065 | C2430 | 212466 | 9918870 | 6.00 | 1881.00 | 1887 |
| ITC066 | C2523 | 199466 | 9920700 | 30.00 | 1877.10 | 1907.1 |
| ITC067 | C2535 | 203174 | 9922549 | 7.00 | 1888.90 | 1895.9 |
| ITC068 | C2537 | 205035 | 9920703 | 3.00 | 1883.60 | 1886.6 |
| ITC069 | C2538 | 201326 | 9920701 | 10.00 | 1876.40 | 1886.4 |
| ITC070 | C2701 | 195752 | 9928078 | 7.00 | 2523.20 | 2530.2 |
| ITC071 | C2703 | 205035 | 9920703 | 3.00 | 1883.60 | 1886.6 |
| ITC072 | C2705 | 197605 | 9920698 | 17.00 | 1885.80 | 1902.8 |
| ITC073 | C2706 | 199465 | 9922547 | 38.00 | 1902.90 | 1940.9 |
| ITC074 | C3292 | 213600 | 9921500 | 8.00 | 1887.90 | 1895.9 |
| ITC075 | C3298 | 210602 | 9924401 | 5.00 | 1891.70 | 1896.7 |
| ITC076 | C3299 | 212463 | 9922555 | 2.00 | 1894.10 | 1896.1 |
| ITC077 | C3459 | 208741 | 9926237 | 17.00 | 1886.50 | 1903.5 |
| ITC078 | C3674 | 203173 | 9924397 | 6.00 | 1937.50 | 1943.5 |
| ITC079 | C3675 | 212463 | 9922555 | 5.00 | 1891.10 | 1896.1 |
| ITC080 | C3740 | 212469 | 9913339 | 15.00 | 1877.20 | 1892.2 |
| ITC081 | C3767 | 195762 | 9911480 | 27.00 | 1886.30 | 1913.3 |
| ITC082 | C3929 | 206306 | 9931350 | 16.00 | 1886.30 | 1902.3 |
| ITC083 | C4155 | 214310 | 9926240 | 34.00 | 1910.00 | 1944 |
| ITC084 | C4157 | 214313 | 9920708 | 11.00 | 1895.00 | 1906 |
| ITC085 | BH 3 | 212995 | 9923310 | 16.00 | 1884.70 | 1900.7 |
| ITC086 | BH 4 | 212936 | 9923318 | 16.00 | 1885.00 | 1901 |
| ITC087 | C4301 | 211625 | 9927400 | 33.00 | 1905.80 | 1938.8 |
| ITC088 | C4302 | 213350 | 9921550 | 10.00 | 1884.80 | 1894.8 |
| ITC089 | C4504 | 203600 | 9925900 | 12.00 | 1887.80 | 1899.8 |
| ITC090 | C4610 | 213100 | 9923300 | 16.00 | 1884.60 | 1900.6 |
| ITC092 | C210 | 219888 | 9911496 | 15.24 | 2134.46 | 2149.7 |

| | | | | | | |
|---|---|---|---|---|---|---|
| ITC093 | C467 | 195763 | 9909632 | 82.91 | 1885.09 | 1968 |
| ITC097 | C578 | 195762 | 9911480 | 19.81 | 1893.49 | 1913.3 |
| ITC098 | C579 | 214320 | 9909645 | 22.25 | 1951.65 | 1973.9 |
| ITC099 | C580 | 203182 | 9909637 | 45.72 | 1899.28 | 1945 |
| ITC100 | C581 | 201332 | 9911484 | 23.16 | 1859.04 | 1882.2 |
| ITC101 | C582 | 214318 | 9913340 | 13.72 | 1930.68 | 1944.4 |
| ITC102 | C594 | 199473 | 9909635 | 15.85 | 1878.45 | 1894.3 |
| ITC103 | C628 | 212469 | 9913339 | 33.53 | 1858.67 | 1892.2 |
| ITC104 | C629 | 205043 | 9907802 | 57.91 | 1843.89 | 1901.8 |
| ITC105 | C630 | 210608 | 9915174 | 99.67 | 1800.73 | 1900.4 |
| ITC106 | C667 | 212469 | 9913339 | 21.95 | 1870.25 | 1892.2 |
| ITC107 | C729 | 212412 | 9903826 | 160.02 | 1899.18 | 2059.2 |
| ITC110 | C1068 | 210612 | 9907806 | 45.11 | 1935.69 | 1980.8 |
| ITC114 | C1359 | 208751 | 9909641 | 12.50 | 1878.80 | 1891.3 |
| ITC121 | C1927 | 210619 | 9898578 | 18.29 | 2070.41 | 2088.7 |
| ITC124 | C2058 | 203182 | 9909637 | 15.24 | 1929.76 | 1945 |
| ITC125 | C2069 | 208751 | 9909641 | 45.72 | 1845.58 | 1891.3 |
| ITC128 | C2220 | 203182 | 9909637 | 30.48 | 1914.52 | 1945 |
| ITC129 | C2221 | 212468 | 9915175 | 12.50 | 1874.50 | 1887 |
| ITC130 | C2223 | 214317 | 9915176 | 12.50 | 1907.50 | 1920 |
| ITC131 | C2534 | 212468 | 9915175 | 17.09 | 1869.91 | 1887 |
| ITC132 | C2636 | 212468 | 9915175 | 4.57 | 1882.43 | 1887 |
| ITC133 | C2659 | 208751 | 9909641 | 17.36 | 1873.94 | 1891.3 |
| ITC134 | C2660 | 210610 | 9911490 | 19.81 | 1920.19 | 1940 |
| ITC135 | C2661 | 197610 | 9913329 | 21.03 | 1922.47 | 1943.5 |
| ITC136 | C2823 | 197610 | 9913329 | 260.30 | 1683.20 | 1943.5 |
| ITC139 | C11093 | 214338 | 9913285 | 59.86 | 1885.14 | 1945 |
| ITC140 | C11841 | 213885 | 9912005 | 60.15 | 1883.85 | 1944 |
| ITC141 | | 194855 | 9909913 | 7.16 | 1894.54 | 1901.7 |
| ITC142 | | 208383 | 9909763 | 1.33 | 1887.58 | 1888.9 |
| ITC143 | | 208923 | 9909870 | 13.15 | 1887.96 | 1901.1 |
| ITC144 | | 213038 | 9914522 | 15.14 | 1890.86 | 1906 |
| ITC145 | | 212664 | 9915091 | 1.66 | 1886.55 | 1888.2 |
| ITC146 | C8994 | 212469 | 9926230 | 15.24 | 1913.96 | 1929.2 |
| ITC147 | C11351 | 213850 | 9921800 | 15.00 | 1885.00 | 1900 |
| ITC148 | C11548 | 214925 | 9916700 | 27.00 | 1885.30 | 1912.3 |
| ITC149 | C11600 | 217150 | 9918100 | 94.50 | 1929.00 | 2023.5 |
| ITC151 | C11688 | 212675 | 9918025 | 8.00 | 1878.90 | 1886.9 |
| ITC152 | C11889 | 201200 | 9910050 | 23.83 | 1909.17 | 1933 |
| ITC153 | C12287 | 218100 | 9930525 | 139.00 | 2164.50 | 2303.5 |
| ITC154 | | 211200 | 9912475 | 8.70 | 1885.60 | 1894.3 |
| ITC155 | C11906 | 213700 | 9920950 | 23.00 | 1872.00 | 1895 |
| ITC156 | | 214009 | 9917763 | 2.33 | 1887.67 | 1890 |
| ITC157 | | 213271 | 9914310 | 24.07 | 1885.93 | 1910 |
| ITC158 | | 202435 | 9909675 | 6.09 | 1889.81 | 1895.9 |
| ITC159 | | 195974 | 9908951 | 5.85 | 1887.15 | 1893 |

| | | | | | | |
|---|---|---|---|---|---|---|
| ITC160 | | 196851 | 9915861 | 1.88 | 1888.13 | 1890 |
| ITC161 | | 197660 | 9918954 | 2.40 | 1887.60 | 1890 |
| ITC162 | | 215784 | 9912357 | 96.00 | 1884.00 | 1980 |
| ITC163 | | 215884 | 9913478 | 81.00 | 1898.00 | 1979 |
| ITC164 | | 210644 | 9920323 | 2.06 | 1887.14 | 1889.2 |
| ITC165 | | 210713 | 9920651 | 3.13 | 1886.27 | 1889.4 |
| ITC166 | | 210884 | 9920823 | 18.06 | 1871.54 | 1889.6 |
| ITC167 | | 210973 | 9921029 | 3.80 | 1885.80 | 1889.6 |
| ITC168 | | 211194 | 9921180 | 3.34 | 1886.27 | 1889.6 |
| ITC169 | | 213725 | 9918128 | 3.01 | 1886.79 | 1889.8 |
| ITC170 | | 213751 | 9918121 | 3.32 | 1886.48 | 1889.8 |
| ITC171 | | 213884 | 9918174 | 6.87 | 1883.03 | 1889.9 |
| ITC172 | | 214014 | 9918202 | 4.90 | 1885.10 | 1890 |
| ITC173 | | 214151 | 9918303 | 5.43 | 1888.57 | 1894 |
| ITC174 | | 214271 | 9918436 | 8.31 | 1884.09 | 1892.4 |
| ITC175 | | 214309 | 9918588 | 11.95 | 1881.45 | 1893.4 |
| ITC176 | | 214340 | 9918801 | 13.45 | 1880.35 | 1893.8 |
| ITC177 | | 213608 | 9918087 | 1.30 | 1886.70 | 1888 |
| ITC178 | | 213721 | 9918148 | 3.24 | 1886.56 | 1889.8 |
| ITC179 | | 213989 | 9918187 | 6.76 | 1883.24 | 1890 |
| ITC180 | | 203360 | 9925256 | 52.00 | 1848.40 | 1900.4 |

**More details of the wells can be found in well database file, in the folder Kibona.**

## 7.5 Appendix 3-B

Observation during pumping
Pumping was done in borehole D and borehole C was used as an observation well.

Distance between borehole C and D: 65 m
Borehole Number: C
Location: Three Point Ostrich Farm
Coordinates: (213459,9924929)
Radius of the Borehole: 0.15 m
Depth: 60 m
Date: 13/10/1999. Time start:7.00 am. Time stop: 3.00 pm
Static Water Level: 26.69 m
Final Water Level: 28.22 m
Method of Measuring Water Level: Electric Dipper
Discharge: 4905.36 $m^3$/d (Measured at the pump)
Pumping duration: 480 minutes

| Time (hr) | Time(min) | Water Level (m) | Drawdown (m) | Time (hr) | Time(min) | Water Level (m) | Drawdown (m) |
|---|---|---|---|---|---|---|---|
| 7:00 | 0.00 | 26.69 | 0.00 | 7:00 | 170.00 | 28.02 | 1.33 |
| 7:47 | 47.00 | 27.01 | 0.32 | 7:47 | 175.00 | 28.03 | 1.34 |
| 7:53 | 53.00 | 27.30 | 0.61 | 7:53 | 180.00 | 28.04 | 1.35 |
| 7:55 | 55.00 | 27.35 | 0.65 | 7:55 | 190.00 | 28.05 | 1.36 |
| 7:57 | 57.00 | 27.39 | 0.70 | 7:57 | 200.00 | 28.07 | 1.38 |
| 7:59 | 59.00 | 27.43 | 0.74 | 7:59 | 210.00 | 28.08 | 1.39 |
| 8:00 | 60.00 | 27.45 | 0.76 | 8:00 | 220.00 | 28.08 | 1.39 |
| 8:05 | 65.00 | 27.54 | 0.85 | 8:05 | 230.00 | 28.10 | 1.41 |
| 8:10 | 70.00 | 27.60 | 0.90 | 8:10 | 240.00 | 28.11 | 1.42 |
| 8:15 | 75.00 | 27.64 | 0.95 | 8:15 | 250.00 | 28.12 | 1.43 |
| 8:20 | 80.00 | 27.69 | 0.99 | 8:20 | 260.00 | 28.13 | 1.44 |
| 8:25 | 85.00 | 27.72 | 1.03 | 8:25 | 270.00 | 28.14 | 1.45 |
| 8:40 | 100.00 | 27.77 | 1.08 | 8:40 | 280.00 | 28.14 | 1.45 |
| 8:48 | 108.00 | 27.84 | 1.15 | 8:48 | 290.00 | 28.14 | 1.45 |
| 8:55 | 115.00 | 27.87 | 1.18 | 8:55 | 300.00 | 28.14 | 1.45 |
| 9:00 | 120.00 | 27.89 | 1.20 | 9:00 | 315.00 | 28.15 | 1.46 |
| 9:05 | 125.00 | 27.89 | 1.20 | 9:05 | 330.00 | 28.16 | 1.47 |
| 9:10 | 130.00 | 27.93 | 1.24 | 9:10 | 345.00 | 28.15 | 1.46 |
| 9:15 | 135.00 | 27.94 | 1.25 | 9:15 | 385.00 | 28.19 | 1.50 |
| 9:20 | 140.00 | 27.95 | 1.26 | 9:20 | 410.00 | 28.21 | 1.52 |
| 15:25 | 145.00 | 27.96 | 1.27 | 15:25 | 420.00 | 28.22 | 1.53 |
| 9:30 | 150.00 | 27.97 | 1.28 | 9:30 | 450.00 | 28.22 | 1.53 |
| 9:35 | 155.00 | 27.98 | 1.29 | 9:35 | 455.00 | 28.23 | 1.54 |
| 9:45 | 165.00 | 27.99 | 1.30 | 9:45 | 480.00 | 28.22 | 1.53 |

## 7.6 Appendix 3-C

Graphs and tables from Aquitest

## 7.7 Appendix 3-D

Nomograph

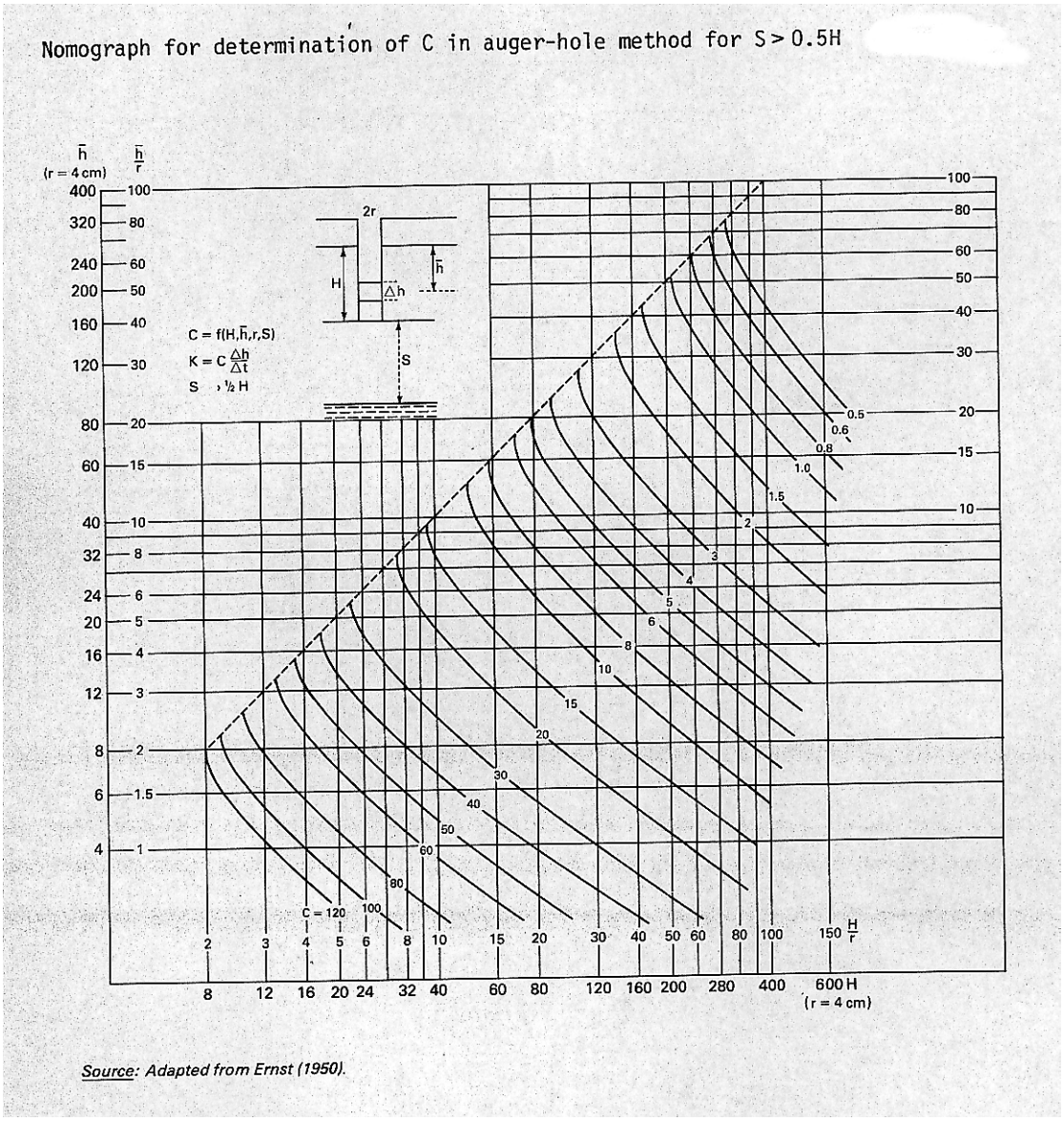


*Source: Adapted from Ernst (1950).*

**Source: Landon 1991**

## 7.8 Appendix 3-E

**Auger hole method field data sheet**

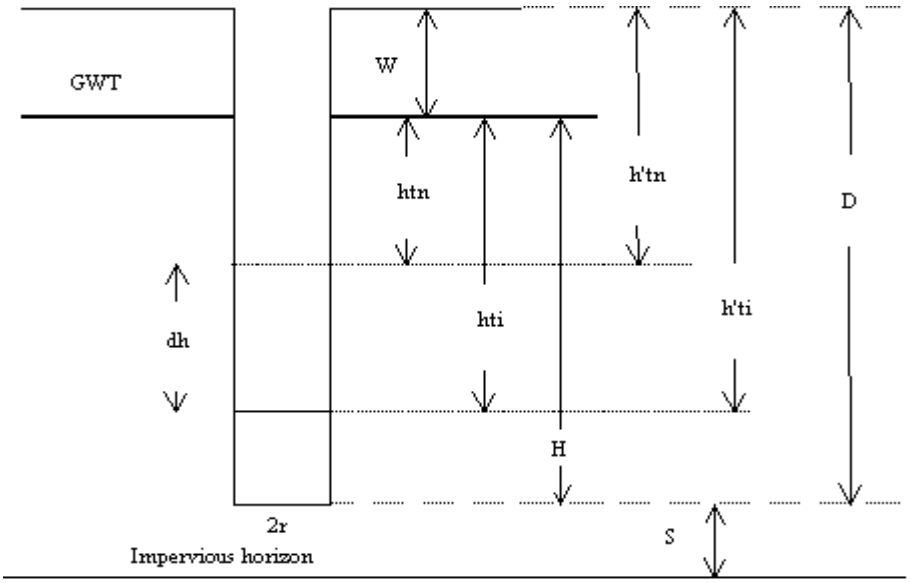


Auger hole A

**Distance from Malewa River to the auger-hole is 175 cm**
Date: 18/10/1999
Soil Type: Silt
Position: (211900, 9927739)
Depth of the hole: 186.5 cm
Depth of groundwater: 68.5 cm

| Radius of hole, r (cm) 4 | Depth of hole, D (cm) 186.5 |
|---|---|
| Depth of GWT,W (cm) 68.5 | |
| H = D-W (cm) 118 | S (cm) > 1/2H |
| Hydraulic conductivity, k (m/day) 0.102 | |

| ti (sec) | h'ti (cm) | h'ti-h'tn (cm) |
|---|---|---|
| 0 | 101 | - |
| 80 | 100 | 1 |
| 145 | 99 | 1 |
| 213 | 98 | 1 |
| 265 | 97 | 1 |

| | | |
|---|---|---|
| 311 | 96 | 1 |
| 348 | 95 | 1 |
| Total | | 6 |

**Check: dh = h'ti – h'tn < 1/4hti**
dh = 6 < 1/4 (101-68.5) = 1/4*32.5 = 8.125 cm
*h* = hti – ½ dh
*h* = 32.5-(1/2*8.125) = 28.44 cm
H = 186.5-68.5 =118
H/r =118/4 = 29.5
h/r = 28.44/4 = 7.11
dh = 6 cm
dt = 348
**dh/dt = 6/348 = 0.017**

**c = 6 is the reading from nomograph**
k = cdh/dt m/day
k = 6*0.017

**k = 0.102 m/d**

**Auger hole B**

**Distance from Malewa River to the auger-hole is 110 cm**

Date: 18/10/1999
Soil Type: Silt
Position: (211900, 9927739)
Depth of the hole: 186.5 cm
Depth of groundwater: 68.5 cm

| Radius of hole, r (cm) | Depth of hole, D (cm) |
|---|---|
| 4 | 174 |

| Depth of GWT,W (cm) 99 | |
|---|---|
| H = D-W (cm) 75 | S (cm) > 1/2H |
| Hydraulic conductivity, k (m/day) 0.42 | |

| ti (sec) | h'ti (cm) | h'ti-h'tn (cm) |
|---|---|---|
| 0 | 160 | - |
| 44 | 159 | 1 |
| 54 | 158 | 1 |
| 73 | 156 | 2 |
| 85 | 155 | 1 |
| 98 | 154 | 1 |
| 106 | 153 | 1 |
| 116 | 152 | 1 |
| 128 | 151 | 1 |
| 153 | 150 | 1 |
| 166 | 149 | 1 |
| 177 | 148 | 1 |
| 190 | 147 | 1 |
| 201 | 146 | 1 |
| Total | | 14 |

**Check: dh = h'ti - h'tn < 1/4hti**
dh = 14 < 1/4 (160 - 99) = 1/4*61 = 15.25 cm
*h* = hti – ½ dh
*h* = 174 - (1/2*15.25) = 53.375 cm
H = 174-99 =75
H/r =75/4 = 18.75
*h*/r = 53.375/4 = 13.34
dh = 14
dt = 201
**dh/dt = 14/201 = 0.07**

**c = 6 is the reading from nomograph**
**k = cdh/dt m/day**
**k = 6*0.07**
**k = 0.42 m/d**

## 7.9 Appendix 3-F

**Inverse auger-hole method**

**Point C**

Distance from Malewa River to the auger-hole is 330 cm
Date: 18/10/1999
Position: (212717, 9928025)
Depth of the hole: 330 cm
Source of Water: River Malewa
Radius of the Hole: 5 cm

**Data for the graph**

| time( sec) | Depth to ground water (cm) | Depth of hole-depth to GW(hti) (cm) | (hti + r/2) (cm) |
|---|---|---|---|
| 0 | 75 | 255 | 257.5 |
| 60 | 75.5 | 254.5 | 257 |

| time( sec) | (hti + r/2) (cm) |
|---|---|
| 0 | 257.5 |
| 60 | 257 |

| | | | |
|---|---|---|---|
| 120 | 75.5 | 254.5 | 257 |
| 180 | 75.5 | 254.5 | 257 |
| 240 | 76 | 254 | 256.5 |
| 300 | 76 | 254 | 256.5 |
| 360 | 76 | 254 | 256.5 |
| 420 | 76 | 254 | 256.5 |
| 480 | 76.5 | 253.5 | 256 |
| 540 | 76.5 | 253.5 | 256 |
| 660 | 77 | 253 | 255.5 |
| 720 | 77.3 | 252.7 | 255.2 |
| 900 | 77.5 | 252.5 | 255 |
| 960 | 77.5 | 252.5 | 255 |
| 1020 | 78 | 252 | 254.5 |
| 1140 | 78.5 | 251.5 | 254 |
| 1260 | 78.5 | 251.5 | 254 |

| | |
|---|---|
| 120 | 257 |
| 180 | 257 |
| 240 | 256.5 |
| 300 | 256.5 |
| 360 | 256.5 |
| 420 | 256.5 |
| 480 | 256 |
| 540 | 256 |
| 600 | 255.5 |
| 660 | 255.2 |
| 900 | 255 |
| 960 | 255 |
| 1020 | 254.5 |
| 1140 | 254 |
| 1260 | 254 |

k=1.15r*Tan a*864
Tan 0.0027 = 0.00004712
**k = 0.234 m/day**

**Point D**

**Distance from Malewa River to the auger-hole is 100 cm**
Date: 18/10/1999
Soil Type: Silt
Position: (212717, 9928025)
Depth of the hole: 110 cm
Source of Water: River Malewa
Radius of the Hole: 5 cm

Data for the graph

| time( sec) | Depth to groundwater (cm) | Depth of hole-depth to GW(hti) (cm) | (hti + r/2) (cm) |
|---|---|---|---|
| 0 | 30 | 80 | 82.5 |
| 60 | 30.5 | 79.5 | 82 |
| 120 | 30.5 | 79.5 | 82 |
| 300 | 31 | 79 | 81.5 |
| 360 | 31.5 | 78.5 | 81 |

| time( sec) | (hti + r/2) (cm) |
|---|---|
| 0 | 82.5 |
| 60 | 82 |
| 120 | 82 |
| 300 | 81.5 |
| 360 | 81 |

| | | | |
|---|---|---|---|
| 480 | 32 | 78 | 80.5 |
| 600 | 32.5 | 77.5 | 80 |
| 780 | 32.8 | 77.2 | 79.7 |
| 900 | 33 | 77 | 79.5 |
| 1080 | 33.5 | 76.5 | 79 |
| 1200 | 34 | 76 | 78.5 |
| 1380 | 34.5 | 75.5 | 78 |
| 1500 | 35 | 75 | 77.5 |
| 1680 | 35.8 | 74.2 | 76.7 |
| 1800 | 36 | 74 | 76.5 |

| | |
|---|---|
| 480 | 80.5 |
| 600 | 80 |
| 780 | 79.7 |
| 900 | 79.5 |
| 1080 | 79 |
| 1200 | 78.5 |
| 1380 | 78 |
| 1500 | 77.5 |
| 1680 | 76.7 |
| 1800 | 76.5 |

k =1.15r*Tan a*864
Tan 0.0032 = 0.00005585
**k = 0.277 m/day**

**Point E**

**Distance from Malewa River to the auger-hole is 270 cm**
Soil Type: Silt
Date: 19/10/1999
Position: (211489, 9927104)
Depth of the hole: 71 cm
Source of Water: River Malewa
Radius of the Hole: 4 cm

Data for the graph

| time( sec) | Depth to Groundwater (cm) | Depth of hole-depth to GW(hti)cm | (hti + r/2)cm |
|---|---|---|---|
| 0 | 46 | 25 | 27 |
| 60 | 46.5 | 24.5 | 26.5 |
| 120 | 47 | 24 | 26 |
| 180 | 48 | 23 | 25 |
| 240 | 48.5 | 22.5 | 24.5 |
| 300 | 49 | 22 | 24 |

| time( sec) | (hti + r/2)cm |
|---|---|
| 0 | 27 |
| 60 | 26.5 |
| 120 | 26 |
| 180 | 25 |
| 240 | 24.5 |
| 300 | 24 |

| | | | |
|---|---|---|---|
| 360 | 49.5 | 21.5 | 23.5 |
| 420 | 50 | 21 | 23 |
| 480 | 50.5 | 20.5 | 22.5 |
| 540 | 51 | 20 | 22 |
| 600 | 51.5 | 19.5 | 21.5 |
| 720 | 52 | 19 | 21 |
| 780 | 52.5 | 18.5 | 20.5 |
| 840 | 53 | 18 | 20 |
| 960 | 53.5 | 17.5 | 19.5 |
| 1020 | 54 | 17 | 19 |
| 1320 | 54.5 | 16.5 | 18.5 |
| 1500 | 55 | 16 | 18 |
| 1860 | 55.5 | 15.5 | 17.5 |

| | |
|---|---|
| 360 | 23.5 |
| 420 | 23 |
| 480 | 22.5 |
| 540 | 22 |
| 600 | 21.5 |
| 720 | 21 |
| 780 | 20.5 |
| 840 | 20 |
| 960 | 19.5 |
| 1020 | 19 |
| 1320 | 18.5 |
| 1500 | 18 |
| 1860 | 17.5 |

k =1.15r*Tan a*864
Tan 0.0055 = 0.00009599
k = 0.381 m/day

## 7.10 Appendix 3-G

**Water level measured during fieldwork October 1999**

| ITC_Number | X | Y | Date | Static water level | Piezometric level |
|---|---|---|---|---|---|
| ITC001 | 213518 | 9924527 | 21-Oct-99 | 28.1 | 1881.9 |
| ITC002 | 213735 | 9925528 | 14-Oct-99 | 30.385 | 1884.615 |
| ITC003 | 213713 | 9924977 | 21-Oct-99 | 25.18 | 1885.82 |
| ITC004 | 213459 | 9924929 | 13-Oct-99 | 26.69 | 1882.31 |
| ITC005 | 213384 | 9924777 | 13-Oct-99 | 26.64 | 1882.76 |
| ITC006 | 213058 | 9924642 | 20-Oct-99 | 23.86 | 1882.14 |
| ITC007 | 214004 | 9925600 | 21-Oct-99 | 33.65 | 1884.35 |
| ITC008 | 213544 | 9925720 | 21-Oct-99 | 33.21 | 1883.79 |
| ITC009 | 211437 | 9921386 | 02-Oct-99 | 5.1 | 1885.9 |
| ITC010 | 211914 | 9924455 | 02-Oct-99 | 20.07 | 1883.93 |
| ITC013 | 212603 | 9923764 | 21-Oct-99 | 19.05 | 1882.95 |
| ITC014 | 209462 | 9928455 | 21-Oct-99 | 18.69 | 1883.31 |
| ITC015 | 210473 | 9928944 | 21-Oct-99 | 27.11 | 1866.89 |
| ITC016 | 212958 | 9923304 | 05-Oct-99 | 18.91 | 1881.79 |

| | | | | | |
|---|---|---|---|---|---|
| ITC017 | 203842 | 9924134 | 02-Oct-99 | 3.95 | 1885.45 |
| ITC018 | 202866 | 9921790 | 02-Oct-99 | 6.49 | 1888.51 |
| ITC019 | 202662 | 9921507 | 02-Oct-99 | 3.69 | 1894.51 |
| ITC025 | 212267 | 9923041 | 02-Oct-99 | 14.8 | 1882.6 |
| ITC026 | 208752 | 9928952 | 02-Oct-99 | 11.29 | 1885.91 |
| ITC027 | 207680 | 9925645 | 02-Oct-99 | 12.71 | 1884.19 |
| ITC028 | 207705 | 9925654 | 21-Oct-99 | 12.22 | 1884.68 |
| ITC029 | 204034 | 9928849 | 02-Oct-99 | 28.98 | 1893.02 |
| ITC030 | 205375 | 9924689 | 21-Oct-99 | 27.11 | 1862.29 |
| ITC033 | 202866 | 9922388 | 02-Oct-99 | 6.59 | 1894.01 |
| ITC034 | 202342 | 9920746 | 02-Oct-99 | 1.44 | 1888.36 |
| ITC035 | 215467 | 9917087 | 02-Oct-99 | 37.21 | 1902.59 |
| ITC036 | 214224 | 9919179 | 02-Oct-99 | 6.81 | 1885.99 |
| ITC038 | 203516 | 9924230 | 02-Oct-99 | 5.76 | 1887.04 |
| ITC133 | 208751 | 9909641 | 02-Oct-99 | 17.54 | 1873.76 |
| ITC142 | 208383 | 9909763 | 02-Oct-99 | 1.5 | 1887.4 |
| ITC143 | 208923 | 9909870 | 04-Oct-99 | 13.38 | 1887.72 |
| ITC144 | 213038 | 9914522 | 04-Oct-99 | 15.38 | 1890.62 |
| ITC164 | 210644 | 9920323 | 11-Oct-99 | 2.78 | 1886.42 |
| ITC165 | 210713 | 9920651 | 11-Oct-99 | 4.1 | 1885.3 |
| ITC166 | 210884 | 9920823 | 11-Oct-99 | 4.24 | 1885.36 |
| ITC167 | 210973 | 9921029 | 11-Oct-99 | 4.37 | 1885.23 |
| ITC168 | 211194 | 9921180 | 11-Oct-99 | 3.8 | 1885.8 |
| ITC173 | 214151 | 9918303 | 09-Oct-99 | 4.12 | 1887.48 |
| ITC176 | 214340 | 9918801 | 09-Oct-99 | 13.45 | 1880.35 |
| ITC177 | 213608 | 9918087 | 1888 | 1.3 | 1887.7 |
| ITC178 | 213721 | 9918148 | 1889.8 | 3.24 | 1886.56 |
| ITC179 | 213989 | 9918187 | 1890 | 6.76 | 1884.04 |

## 7.11 Appendix 3-H

### Points used for creating the DEM

| Station number | Well Number or Name | Name | UTM_X | UTM_Y | Elevation | Correction Applied | Final Elevation | Source of Data |
|---|---|---|---|---|---|---|---|---|
| ITC001 | c11527 | 3PAUSHAND | 213518 | 9924527 | 1910.3 | 0 | 1910.3 | GEODETIC SURVEY 1999 |
| ITC002 | BH A | BH2 | 213735 | 9925528 | 1915.1 | 0 | 1915.1 | GEODETIC SURVEY 1999 |
| ITC003 | BH B | BHB | 213713 | 9924977 | 1910.5 | 0 | 1910.5 | GEODETIC SURVEY 1999 |
| ITC004 | BH C | 3P (3PHOU | 213459 | 9924929 | 1908.8 | 0 | 1908.8 | GEODETIC SURVEY 1999 |
| ITC006 | BH E | delapivot | 213058 | 9924642 | 1906 | 0 | 1906 | GEODETIC SURVEY 1999 |
| ITC007 | BH greenhouse | OSTRICHBH | 214004 | 9925600 | 1918.5 | 0 | 1918.5 | GEODETIC SURVEY 1999 |
| ITC008 | TANINI | TANINI | 213544 | 9925720 | 1917.4 | 0 | 1917.4 | GEODETIC SURVEY 1999 |
| ITC009 | M2 | manera9(M2) | 211437 | 9921386 | 1891 | 0 | 1891.1 | GEODETIC SURVEY 1999 |
| ITC010 | M4 | milkfactory | 211914 | 9924455 | 1903 | 0 | 1903.8 | GEODETIC SURVEY 1999 |
| ITC011 | C2883 | C2883 | 213101 | 9928951 | 1946.5 | 0 | 1946.5 | GEODETIC SURVEY 1999 |
| ITC013 | Kobil | Kobil Petrol Station | 212603 | 9923764 | 1902 | 0 | 1902.2 | GEODETIC SURVEY 1999 |
| ITC014 | | Marula Homegrown | 209462 | 9928455 | 1923 | 0 | 1923 | GEODETIC SURVEY 1999 |
| ITC015 | | Marula Artist | 210473 | 9928944 | 1932 | 0 | 1932 | GEODETIC SURVEY 1999 |

| | | | | | | | | |
|---|---|---|---|---|---|---|---|---|
| ITC016 | C4161 | VIAK | 212958 | 9923304 | 1898.7 | 2 | 1900.7 | Levelled by VIAK 1975 |
| ITC017 | C11691 | M8 | 203842 | 9924134 | 1890 | 0 | 1890 | GEODETIC SURVEY 1999 |
| ITC020 | BH7 Manera Farm | delapiv2 | 211230 | 9924941 | 1903 | 0 | 1903 | GEODETIC SURVEY 1999 |
| ITC027 | | Behar well | 207680 | 9925645 | 1897 | 0 | 1901 | GEODETIC SURVEY 1999 |
| ITC029 | M7 | M7 | 204034 | 9928849 | 1915 | 0 | 1915 | GEODETIC SURVEY 1999 |
| ITC038 | M9 | M9 | 203516 | 9924230 | 1891 | 0 | 1891 | GEODETIC SURVEY 1999 |
| ITC042 | | Behar well | 207165 | 9925364 | 1894 | 0 | 1894 | GEODETIC SURVEY 1999 |
| ITC043 | | Behar well | 210769 | 9920726 | 1889 | 0 | 1889 | GEODETIC SURVEY 1999 |
| ITC136 | C2823 | C2823 | 219659 | 9902553 | 2132 | 0 | 2132 | GEODETIC SURVEY 1999 |
| ITC139 | C11093 | C11093 | 214338 | 9913285 | 1945 | 0 | 1945 | GEODETIC SURVEY 1999 |
| ITC140 | C11841 | C11841 | 213885 | 9912005 | 1944 | 0 | 1944 | GEODETIC SURVEY 1999 |
| ITC156 | w2 | Behar well | 214009 | 9917763 | 1890 | 0 | 1890 | Survey of Kenya (Lake Naivasha contour in 1959) |
| ITC157 | w3 | Behar well | 213271 | 9914310 | 1910 | 0 | 1910 | Survey of Kenya (Lake Naivasha contour in 1959) |
| ITC159 | w9 | Behar well | 195974 | 9908951 | 1893 | 0 | 1893 | Survey of Kenya (Lake Naivasha contour in 1959) |
| ITC160 | w11 | Behar well | 196851 | 9915861 | 1890 | 0 | 1890 | Survey of Kenya (Lake Naivasha contour in 1959) |
| ITC161 | w12 | Behar well | 197660 | 9918954 | 1890 | 0 | 1890 | Survey of Kenya (Lake Naivasha contour in 1959) |
| ITC163 | w66 | w66 | 215884 | 9913478 | 1979 | 0 | 1979 | GEODETIC SURVEY 1999 |
| ITC169 | kws1 | owor | 213608 | 9918087 | 1888 | 0 | 1888 | GEODETIC SURVEY 1999 |
| ITC170 | kws2 | owor | 213608 | 9918148 | 1890 | 0 | 1890 | GEODETIC SURVEY 1999 |
| ITC171 | kws3 | owor | 213986 | 9918176 | 1890 | 0 | 1890 | GEODETIC SURVEY 1999 |
| ITC180 | C11954 | C1154 | 202947 | 9925208 | 1939 | 0 | 1939 | GEODETIC SURVEY 1999 |
| ITC182 | | Crater well | 194443 | 9914874 | 1910 | 0 | 1910 | GEODETIC SURVEY 1999 |

**For more information see file points for DEM in folder DEM in main folder Kibona**

## 7.12 Appendix 3-I

Points used to create piezometric map (For more details see file well database)

| Well Number | UTM_X | UTM_Y | HEAD (m.a.s.l) |
|---|---|---|---|
| C2709 | 186474 | 9907789 | 2114 |
| C0466 | 190189 | 9917009 | 1907 |
| C1404 | 190190 | 9915161 | 1894 |
| C2300 | 190500 | 9909750 | 1914 |
| N41 | 190925 | 9909573 | 1912 |
| 301 | 193940 | 9902400 | 1774 |
| C2557 | 195300 | 9912500 | 1892 |
| ITC097 | 195762 | 9911480 | 1893 |
| ITC159 | 195974 | 9908951 | 1887 |
| ITC160 | 196851 | 9915861 | 1888 |
| EW1 | 196900 | 9930575 | 1852 |
| ITC072 | 197605 | 9920698 | 1886 |
| ITC161 | 197660 | 9918954 | 1888 |

| | | | |
|---|---|---|---|
| C2586X | 198500 | 9905140 | 1842 |
| 701 | 199340 | 9903960 | 1734 |
| ITC102 | 199473 | 9909635 | 1878 |
| 26 | 200130 | 9902275 | 1594 |
| 30 | 200480 | 9902580 | 1643 |
| C733 | 202750 | 9940250 | 1819 |
| N24 | 204040 | 9925879 | 1882 |
| ITC082 | 206306 | 9931350 | 1886 |
| ITC042 | 207165 | 9925364 | 1886 |
| ITC027 | 207680 | 9925645 | 1888 |
| ITC133 | 208751 | 9909641 | 1883 |
| ITC047 | 208988 | 9937384 | 1934 |
| C1926 | 209700 | 9905700 | 1889 |
| ITC043 | 210769 | 9920726 | 1887 |
| ITC107 | 212412 | 9903826 | 1899 |
| ITC048 | 212459 | 9931771 | 1958 |
| ITC157 | 213271 | 9914310 | 1886 |
| ITC074 | 213600 | 9921500 | 1888 |
| ITC056 | 213900 | 9916550 | 1882 |
| ITC156 | 214009 | 9917763 | 1888 |
| ITC083 | 214310 | 9926240 | 1910 |
| ITC055 | 214375 | 9916225 | 1889 |
| N12 | 215200 | 9913100 | 1907 |
| ITC057 | 216171 | 9926241 | 2037 |
| ITC059 | 216171 | 9924404 | 2006 |
| N40 | 216441 | 9913361 | 1910 |
| ITC058 | 218032 | 9922558 | 1999 |
| N57 | 219112 | 9923847 | 1995 |
| N52 | 219411 | 9926765 | 2064 |
| ITC136 | 219659 | 9902553 | 1872 |
| N54 | 219848 | 9929261 | 2168 |
| ITC092 | 219888 | 9911496 | 2135 |

## 7.13 Appendix 3-J

### Soil Description of Auger holes in Acacia Forest for depth of root zone.

### Auger hole 1

**Marula farm**
Position (02071, 9922475)
Depth to groundwater 8.00 m

| Soil depth (m) | Color | Soil Description |
|---|---|---|
| 0.00 – 3.00 | Light brown | Silty clay loam |
| 3.00 – 3.50 | Dark brown | Silty clay |
| 3.50 – 4.20 | Brown | Fine sandy (Iron stained) |
| 4.20 – 6.00 | Brown | Fine gravely sandy (Iron stained) |
| 6.00 – 8.00 | Brown | Fine gravely sandy |

### Auger hole 2

**Marula Farm**
Position (208350, 9925943)
The auger-hole is 2000 m from the lake Naivasha

Depth to grounwater 8.00 m

| Soil depth (m) | Color | Soil Description |
|---|---|---|
| 0.00 – 2.50 | Dark brown | Silty clay loam |
| 2.50 – 3.50 | Brown | Gravely sandy with subround pebbles |
| 3.50 – 4.00 | Brown | Fine sandy (Iron stained) |
| 4.00 – 8.00 | Brown | Gravely sand |

## Auger hole 3

**Marula farm**
Position (205159, 992191)
The auger-hole is 1500 m from the lake Naivasha
Depth to groundwater 3.00 mm

| Soil depth (m) | Color | Soil Description |
|---|---|---|
| 0.00 – 0.50 | Dark brown | Silty clay loam |
| 0.50 – 1.50 | Brown | Silty clay |
| 1.50 – 3.00 | Grayish brown | Fine Gravely sandy |

## Auger hole 4

Position (208952, 9926664**)**
**The auger-hole is 150 m from the Malewa river**

| Soil depth (m) | Color | Soil Description |
|---|---|---|
| 0.00 – 1.20 | Fine grayish | Silty clay loam |
| 1.20 – 2.00 | Fine grayish brow | Silty (iron stained) |
| 2.00 – 12.00 | Dark brown | Silty (iron stained) |